PIK3IP1/TRIP RESTRICTS ACTIVATION OF T CELLS THROUGH INHIBITION OF THE PI3K/AKT PATHWAY

by

Uzodinma Nnaemeka Uche

BS, Warren Wilson College, 2002

MS, The Pennsylvania State University, 2007

MS, The Pennsylvania State University, 2008

Submitted to the Graduate Faculty of

the School of Medicine in partial fulfillment

of the requirements for the degree of

Doctor of Philosophy

University of Pittsburgh

2018

UNIVERSITY OF PITTSBURGH

SCHOOL OF MEDICINE

This thesis was presented

by

Uzodinma Nnaemeka Uche

It was defended on

November 13, 2018

and approved by

Marie C. DeFrances, Professor, Department of Pathology

Adrian E. Morelli, Associate Professor, Department of Immunology

Penelope A. Morel, Professor, Department of Immunology

Binfeng Lu, Associate Professor, Department of Immunology

Dissertation Director: Lawrence P. Kane, Professor, Department of Immunology

PIK3IP1/TRIP RESTRICTS ACTIVATION OF T CELLS THROUGH INHIBITION OF THE PI3K/AKT PATHWAY

Uzodinma Nnaemeka Uche, PhD

University of Pittsburgh, 2018

Phosphatidylinositide-3-Kinases (PI3Ks) are a family of lipid kinases that play important intracellular signaling roles in cellular functions such as cell proliferation, motility, growth, intracellular trafficking, differentiation and survival. PI3K produces PIP3 which further facilitates the activation of downstream effectors such as Akt and PDK1. These effectors facilitate the cellular processes associated with PI3K activity. Conversely, because of the nature of PI3Ks roles, dysregulation of PI3K, leading to over-activity of the PI3K pathway is implicated in many cancers. PTEN, SHIP and INPP4B are negative regulators of PI3K activity that function downstream of PI3K and have been shown to act as tumor suppressors. Recently, PI3K Interacting Protein 1 (PIK3IP1) or TrIP (Transmembrane Inhibitor of PI3K), a novel negative regulator that functions upstream and proximal to PI3K, has been identified. TrIP, is a transmembrane protein and has been shown to down regulate PI3K activity leading to reduction of phosphorylation on Akt in carcinoma cell lines. Our lab was the first to show that TrIP can inhibit TCR signaling and TCR activation, in T cell lines. Here I have shown that both the extracellular kringle domain and intracellular p85-like domain are required for TrIP to inhibit PI3K and T cell activation. Interestingly, I have also found that cell surface expression of TrIP is acutely down-regulated during T cell activation. Furthermore, my results indicate that TrIP oligomerizes in order to inhibit

PI3K signaling. Using knockout mice lacking expression of TrIP in T-cell compartments, I have been able to better define the requirements for TrIP in primary T cells upon TCR activation and in response to infection. Finally, I have developed a TrIP ecto-domain hIgG1 Fc fusion protein. This fusion protein has been used as an immunogen for the development of antibodies against TrIP in mice. This fusion protein has also been used to evaluate a possible ligand for TrIP.

TABLE OF CONTENTS

LIST OF FIGURES

PREFACE

I would like to thank my mentor Dr. Lawrence Kane for the opportunity and guidance provided in my development as a scientist. I would also like to thank all the members of my thesis committee- Dr. Marie DeFrances, Dr. Adrian Morelli, Dr. Penelope Morel and Dr. Binfeng Lu who have provided me with immeasurable assistance and advice throughout the course of my project. I would also like to thank all members of the Kane lab for their support and advice.

I would like to give a special thanks to my family- My parents (Prof. Luke Uka Uche and Mrs. Joyce Chibuzo Uche), my siblings (Ugochukwu Uchenna Uche, Adaku Nwadiuto Uche-Ekpo and Nnanenyem Eziudo Uche). They have been a strong and lasting source of encouragement, support, love, patience and guidance throughout graduate school.

1.0 INTRODUCTION

1.1 T CELL ACTIVATION AND THE PI3K PATHWAY

1.1.1 T cell activation and signaling pathways

Ligand binding by the T cell receptor leads to the activation, growth and translation of function in T cells. Upon ligand binding, the protein tyrosine kinases (PTKs) located close to the TCR are phosphorylated. These PTKs in turn phosphorylate other downstream cellular proteins. The biochemical reactions that proceed from these events connect the TCR to multiple pathways that lead to varying degrees of protein expression that eventually allow the T cell to respond to external stimuli in a variety of ways. In this section, I will discuss some known TCR pathways and highlight their relevance to T cell development and/or function.

The Mitogen-activated protein kinase (MAP) pathway is activated when MAP-kinase kinases (such as MEK1/2)) are phosphorylated on threonine and tyrosine residues in processes regulated by G proteins associated with the membrane. These in turn phosphorylate MAP-kinases such as Extracellular signal related kinase (ERK) and Jun kinase (JNK) (which all also bear threonine and tyrosine motifs that are phosphorylated) [1, 2]. During T cell development in the thymus, activation of the ERK pathway has been found to be necessary for positive selection and lineage commitment [2-5] while JNK signaling has been implicated in negative selection [2, 6].

Downstream of the signaling cascade, MAPKs activate transcription factors in the nucleus. For example, ERK phosphorylates Elk-1 which forms a complex with serum response factor to transcribe the Fos gene. Jun which is produced by JNK then forms a heterodimer with fos. This heterodimer AP-1 acts with NFAT as transcription factor that regulates expression of cytokines such as IL-2, IL-4 and TNFα [1, 7].

The activation of PLC-γ during T cell activation leads to the breakdown of PIP2 into diacylglycerol (DAG) and inositol 1,4,5-triphosphate (IP3). IP3 binds to calcium channels on the endoplasmic reticulum (ER) membrane and causes the release of calcium from the ER into the cytosol. The high concentration of calcium on the cytosol side of the cell leads to the opeining of calcium channels on the cell membrane which allow the flow of calcium from the extracellular area into the cell. Increased concentration of calcium in the cell leads to the dephosphorylation of nuclear factor of activated T cells (NFAT). This dephosphorylation event allows NFAT to translocate from the cytosol to the nucleus [1, 7]. The importance of NFAT in T cell activation is highlighted in early immunosuppressive drugs cyclosporin A and FK506 which are sometimes used in preventing rejection of a transplant. These drugs inhibit T cell activity by inhibiting the NFAT activator, calcineurin [8].

Another pathway that can be activated during T cell activation is the Phosphatidylinositol 3-kinase or Phosphoinositide 3 -kinase (PI3K)/Akt pathway. The PI3K/Akt pathway is particularly interesting because its dysregulation has been highlighted as the culprit in a number of autoimmune and cancerous conditions. This pathway can be activated by a host of signals such as growth factors and RTKs and is ubiquitous in cells. It is known as the PI3K/Akt pathway because of the significant involvement of the kinase, Akt, in downstream signaling events. PI3K catalyzes the phosphorylation of the 3’ hydroxyl group of the inositol ring of phosphoinsotides. In T cells, PI3K

phosphorylates phosphatidylinositol 4,5-bisphosphate (PIP2) and produces phosphatidylinositol 3, 4, 5-triphosphate (PIP3). This product acts a second messenger which recruits and activates other enzymes leading to the activation of Akt. Activation of Akt leads to activation of the mTOR pathway which translates into protein production, an increase in cell survival signals and cell proliferation among other functions [9-12]. The functions associated with this pathway are an indication as to why dysregulation of this pathway results in severe health diagnosis in patients. The central aim of this thesis is to show how the novel protein discovered by Dr. Marie DeFrances- PI3K interacting protein 1 (PIK3IP1) plays a role in the regulation of the PI3K pathway. For ease of communication, we have renamed the protein- Transmembrane inhibitor of PI3K (TrIP).

1.1.2 The PI3K Superfamily

Phosphatidylinositide-3-Kinases (PI3Ks) are a ubiquitous family of intracellular lipid kinases that phosphorylate the 3' hydroxyl group of the inositol ring of phosphatidylinositols (PtdIns) and phosphoinositides. The second messengers produced by this activity play a major role in many cellular functions such as metabolism, cellular motility, cell proliferation, intracellular trafficking, and survival. There are three main classes of PI3K and some classes have different isoforms. Class IA and Class IB PI3Ks comprise the Class I PI3Ks. The Class I PI3Ks contain both regulatory and catalytic subunits and are activated by G-Protein Coupled Receptors (GPCRs) or Receptor Tyrosine Kinases (RTKs). Class Ia PI3Ks are activated by RTKs while Class Ib PI3Ks are activated by GPCRs. Apart from being subject to different types of activation, the two subtypes of Class I PI3Ks are also composed of different heterodimers that make up the regulatory and catalytic subunits. Class Ia consists of a regulatory subunit that has different isoforms that are of three different sizes, 85kDa, 55kDa or 50kDa. These isoforms are generally called the p85

regulatory subunit. The catalytic subunit of Class Ia is composed of a 110kDa protein of which there are three isoforms (p110α, p110β and p110δ). The main structure of the p85 subunit consists of a p110 binding domain, also known as the inter-SH2 domain because this domain is flanked by two SH2 domains. The longer p85 isoforms also have a Src-homology 3 (SH3) domain and a BH domain flanked by proline residues. The catalytic subunits consist of a p85 binding domain on the N-terminal, followed by a Ras-binding domain, a C2 domain, a phosphatidylinositol kinase homology domain and a C-terminal catalytic domain [9, 10, 13].

The Class IB PI3Ks also consist of a regulatory subunit that is of different isoforms. A longer 101kDa subunit (p101) and two other subunits (p84 and p87) [14, 15]. The catalytic subunit of Class IB is p110γ and is highly homologous with the Class IA p110 isoforms. The regulatory subunits of Class IB possess a p110γ binding domain as well as a Gβγ binding domain. It is via this latter domain that Class IB PI3Ks bind the Gβγ subunits of G proteins and p110γ is activated. Class I PI3Ks phosphorylate phosphatidylinositol-4,5-bisphosphate (PIP2) and produce phosphatidylinositol-3,4,5-trisphosphate [13, 16].

The Class II PI3Ks consist of only a catalytic subunit, of which there are three isoforms (PIK3C2α, PIK3C2β and PIK3C2γ). Class II PI3Ks can be activated by cytokine receptors, receptor kinases and integrins. The preferred substrates for this class are phosphatidylinositol and phosphatidylinositol-4-phosphate [13, 16]. Recent work on Class II PI3Ks has suggested critical in vivo roles. Deletion of the PI3KC2α gene in mice resulted in embryonic lethality, suggesting that the kinase is important for embryonic development [17-19]. Furthermore, PI3KC2γ deletion resulted in insulin resistance as mice aged [20]. These data suggest that there are a wide variety of cellular functions regulated by the Class II PI3Ks that are as yet unknown. The Class III PI3K consists of only the vacuolar protein-sorting defective 34 (Vps34) enzyme which, like the Class II

PI3Ks, is composed of only a catalytic subunit. The main substrate of Vps34 is phosphatidylinositol. This enzyme has been shown to be required for efficient autophagy in cells as well as endocytic trafficking [21]. Due to the range of isoforms within the PI3K family, a host of substrates within different pathways can be activated to achieve different functions [9, 13, 22].

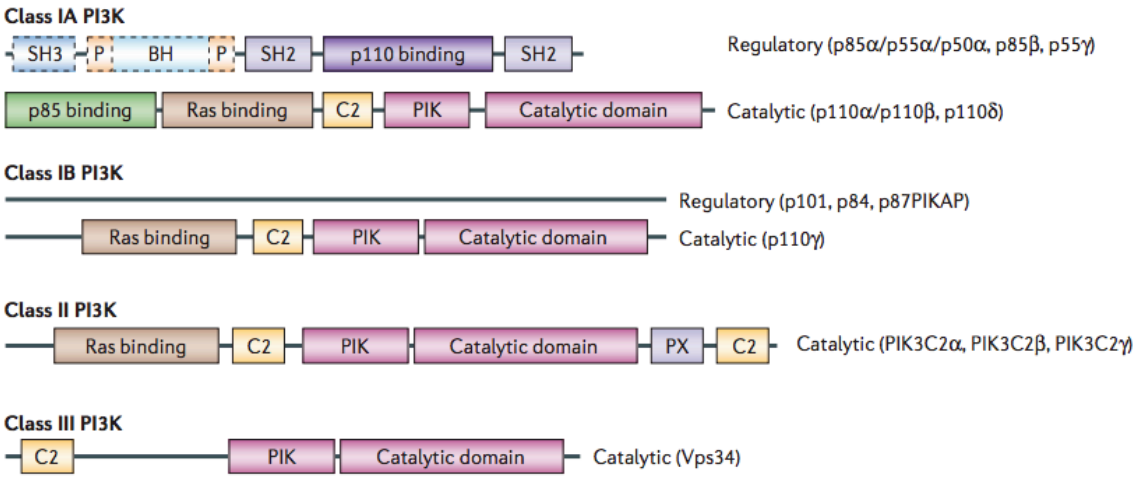

Figure 1 Domain structures of various PI3K isoforms

Nat Rev Genet, 2006. **7**(8): p. 606-19.

1.1.3 The Class IA PI3K subfamily in T cells

Due to the dysregulation of the Class IA PI3Ks in a host of ailments ranging from cancer to autoimmunity, many studies have focused on this class and subfamily [11, 13, 22-24]. These PI3Ks are composed of a 110kDa catalytic subunit (of which there are three isoforms: α, β, and δ) and a regulatory subunit which may be p85α, p55α, p50α, p85β or p55γ. The p85α subunit as well as p110δ are highly expressed in T lymphocytes [13, 22]. The regulatory subunit contains a p110 binding domain (otherwise known as the inter-SH2 domain) through which the p110 catalytic

subunit is bound and maintained in an inactive state in the cell. Upon T cell activation, class IA PI3K is recruited to the plasma membrane by binding to tyrosine-phosphorylated proteins via the SH2 domains of p85. Binding of the p85-SH2 domains to phosphotyrosines triggers a conformational change in the regulatory subunit that results in the release of the catalytic subunit. The catalytic subunit is then free to phosphorylate PtdIns via the lipid kinase domain located on its C-terminus [25, 26].

1.1.4 TCR activation of the PI3K pathway

On a physiological level, binding of the TCR to peptide and MHC complexes on antigen presenting cells results in the activation of several intracellular signaling cascades, ultimately leading to T-cell activation. First, LCK is activated and phosphorylates CD3 immunoreceptor tyrosine-based activation motifs (ITAMs). Phosphorylated ITAMs recruit zeta-chain associated protein of 70kD (zap70) which in turn phosphorylates a variety of downstream proteins including adaptor proteins LAT, SLP76 and PLCγ1 [27, 28]. This cascade results in the activation of transcription factors leading to T cell responses such as cytokine secretion, down regulation of adhesion markers, cell proliferation etc. After high avidity/affinity peptide:TCR interactions, the TCR is capable of producing a potent signal cascade to generate a response. Often times however, a co-stimulatory signal is required to generate a significant signal in order to avoid producing a non-responsive state (anergy) that may even result in T cell death. CD28 is the most prominent co-stimulatory signaling molecule expressed on the T cell. Upon TCR activation, CD28, via LCK phosphorylated tyrosine and proline motifs, bind to SH2 and SH3 domains of intracellular signaling proteins. For the PI3K/Akt pathway to get underway, PI3K is recruited to the membrane via the SH2 domain of the p85 subunit. The SH2 domain of the p85 subunit of PI3K binds to a phosphorylated tyrosine motif

in the tail of CD28. As mentioned above, p110, the catalytic subunit then converts PIP2 to PIP3 by phosphorylating the 3' hydroxyl subunit of the PtdIn. The PIP3 lipid acts as a second messenger, binding to and activating pleckstrin homology (PH) domain proteins such as PDK1 and AKT. Interaction of AKT, via its PH domain, with PIP3, causes a conformational change in AKT which allows PDK1 to partially activate AKT by phosphorylation at T308. Full activation of AKT is achieved by mTORC2 mediated phosphorylation at S473. Activated AKT goes on to phosphorylate FOXO, pro-caspase 9, Bad, IKK and CREB. These phosphorylation events promote cell survival by blocking transcription of pro-apoptotic proteins [13, 22, 29]. In addition, AKT regulates cytoplasmic and nuclear localization of proteins like B-catenin, which are known to activate transcription factors that facilitate functions such as cell cycle progression. This signaling cascade continues, leading to protein synthesis, cell proliferation and cell survival, among other events.

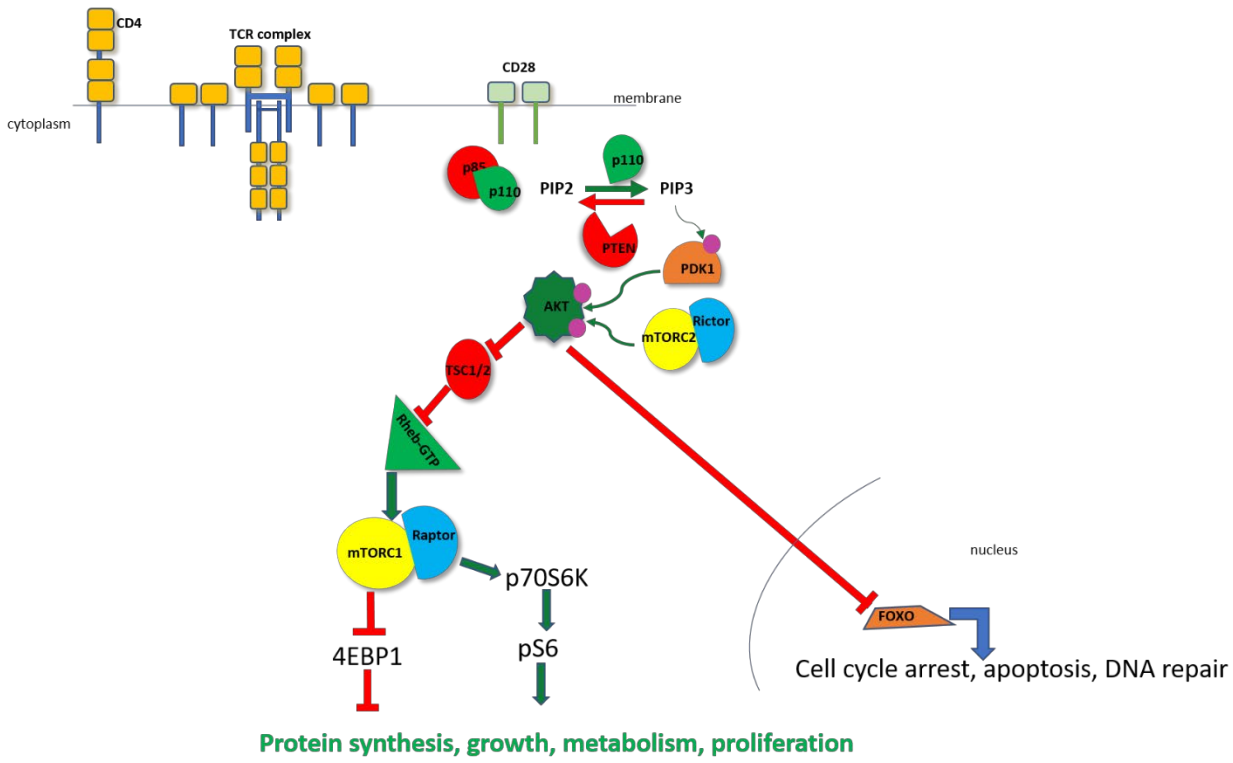

Figure 2 Schematic of TCR activation of the PI3K pathway

1.1.5 Regulators of the PI3K/Akt Pathway

PTEN was discovered when groups working on various forms of cancer discovered a region of chromosome 10 (10q23) was frequently deleted [30, 31]. PTEN (phosphatase and tensin homolog deleted on chromosome 10) was thus identified as a tumour suppressor gene. The PTEN gene encodes a phosphatase that in earlier experiments was found to deplete phosphate groups from both proteins [31, 32] and lipids [33]. However, conclusive evidence on PTEN substrate specificity was observed on phosphatidylinositols (PtdIns) wherein overexpression of PTEN reduced PtdIn phosphorylation and an accumulation of phosphorylated PtdIns was observed when an inactive mutant PTEN was overexpressed [33].

PTEN structure consists of an N-terminal phosphatase domain (which contains the active site), a C2 domain (which aids in binding to the phospholipid), a tail region with phosphorylation sites (which promote stability and activity of PTEN) and a PDZ-B domain (for anchoring the protein to cytoskeletal components)[34-36]. PTEN is also considered as a member of the protein tyrosine phosphatase (PTP) superfamily as it bears the active site sequence Cys-X5-Arg [$C(X)_5R$] (an active site motif present in other PTPs). Within this motif in PTEN, the cysteine attacks and breaks the bond between the hydroxyl group and the phosphate group on the inositol ring of the lipid [35]. It is via this mechanism that PTEN dephosphorylates phosphatidylinositol 3, 4, 5-triphosphate (PIP3). As previously discussed, PIP3 is an important second messenger in the PI3K/AKT pathway which activates pathway components such as PDK1 and AKT, eventually leading to such processes as cell protein synthesis, cell proliferation and cell survival. Due to the important role PTEN plays in the regulation of the PI3K pathway, mutation or dysregulation of PTEN function has been shown to be a major factor in several forms of cancer and autoimmunity [29, 36-38].

Other regulators of the PI3K/Akt Pathway include SH2-containing Inositol 5'-Phosphatase (SHIP). The motifs within the structure of SHIP allow for several types of protein-protein interactions. As the name suggests, there is a Src homology 2 (SH2) domain present on the N-terminus. The SH2 domain allows for interaction of SHIP with phosphorylated tyrosines on other intracellular proteins. The phosphatase domain (inositol 5' phosphatase domain) located in the middle of the protein catalyzes the dephosphorylation of inositol rings at the 5' position. Thus, SHIP acts on PIP3 by removing the phosphate group from the 5' position and converts PIP3 to phosphatidylinositol (3,4)-bisphosphate [39]. On the carboxy-terminal end are an NPXY motif and a PxxP motif. The NPXY motifs serve as an interaction site for phosphotyrosine binding domains

and other SH2 proteins. The PxxP motif contains proline and serves as binding sites for SH3 domain containing proteins [40].

Compared to PTEN, the dephosphorylation of PIP3 by SHIP has been observed to not be critical to PI3K activation of most downstream processes. In both cell lines and null mice, deletion of PTEN resulted in embryonic lethality (mice) and inhibition of Akt phosphorylation and thus cell growth, and SHIP overexpression could not rescue these conditions [41, 42]. Furthermore, the phosphatidylinositol 3,4-bisphosphate, the initial product of SHIP dephosphorylation of PIP3 was found to be a substrate capable of binding and activating PDK1 and Akt [9]. The discovery of inositol polyphosphate 4-phosphatase type II (INPP4B) suggested a mechanism by which SHIP could be important for regulation of the PI3K pathway. While INPP4B was also found to be unable to act on PIP3, INPP4B dephosphorylates the 4'position and converts phosphatidylinositol (3,4)-bisphosphate into phosphatidylinositol 3-phosphate [43, 44]. Thus a pathway was proposed wherein the actions of first SHIP on PIP3 and then INPP4B on the product of SHIP dephosphorylation of PIP3, leads to the production of a monophosphate substrate: phosphatidylinositol 3-phosphate and the regulation of PI3K through the turnover of a viable second messenger in PIP3 [45].

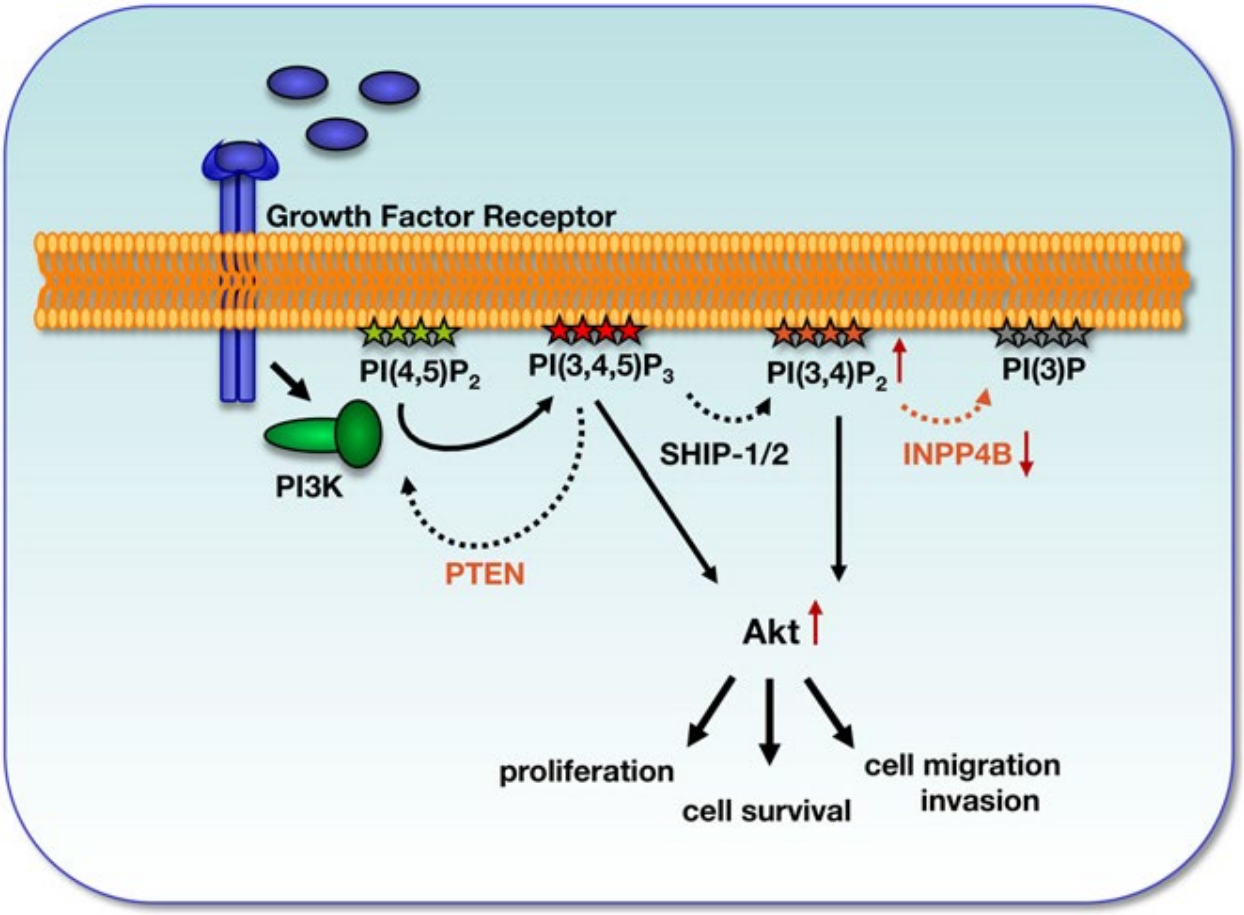

Figure 3 Model of regulation of Class IA PI3K signaling

Cancer Cell, 2009. **16**(2): p. 115-25.

1.1.6 Effects of PI3K on T cell development

The role of PI3K in immune cell development has been highlighted in several studies. Deletion of the gene encoding p85α and the isoforms p55α and p50α (by injection of ES cells containing these deletions into a RAG 2 deficient background) has been shown to lead to a reduction in mature B cell numbers as well as reduced antibody production. However, in the same studies, T cell development appeared unaffected [46, 47]. Studying the role of PI3K in T cell development has

been complicated due to the various isoforms of both the regulatory and catalytic subunits. Deletion of one isoform has been observed to bring about compensatory function and over-experession by other isoforms [48, 49]. Researchers have attempted to avoid this complication by evaluating PI3K through mutation or deletion of PTEN, a master regulator of PI3K. In studies focused on the regulation of PI3K, PTEN null mice ($PTEN^{-/-}$) have been found to be embryonically lethal. Interestingly, even though they survive longer than PTEN-/- mice, $PTEN^{+/-}$ mice eventually develop lethal autoimmune disorders [50, 51]. These observations hint at the important role PI3K plays in various cells as well as in immune cells (and further complicates studying the role of PI3K in T cell development).

T cell development occurs in the thymus and is characterized by lineage determination (through the expression of the TCR and lineage markers) and thymic education (negative and positive selection that bring about self-tolerance). This development requires appropriate integration of signals throughout the different stages of thymocyte development. Since activation of the PI3K pathway results in cell survival and proliferation, researchers have been interested in the role of PI3K in T cell development. Indeed, Ciofani and colleagues have shown that the relevance of Notch to pre-T cell survival depends on the PI3K/Akt pathway [52]. Akt promotes cell survival by inhibiting proapoptotic factors such as Bad, caspase 9 and the Foxo transcription factors. They found that in DN3 cells, Akt phosphorylation was significantly reduced in the absence of Notch signaling and cells deprived of Notch signaling underwent significant apoptosis. This cell death was rescued when an active Akt construct was transfected into the cells [52]. In the absence of PTEN, PI3K activity is higher and PIP3 production is increased [53]. This leads to higher Akt activation, reduced apoptosis and higher proliferation in T cells. Supporting these

findings, in studies targeting Akt to the membrane in mice (in order to bypass second messenger requirements), mature T cells were found to be more resistant to apoptosis [54-56].

Even more conclusive evidence for the role PI3K plays in T cell development was found when the Cantrell lab manipulated phosphoinositide dependent kinase 1 (PDK1) expression in mice. PDK1 is located upstream in the PI3K pathway and upon recruitment and activation by PIP3, activates Akt at T308. Mice lacking PDK1 show reduced numbers of cells in the thymus. These PDK1 null mice were also observed to have an inhibited progression from the DN to DP stage during T cell development [57].

These data suggest that PI3K plays a major role in T cell development and function as well as cell homeostasis. In deciphering how TrIP regulates PI3K activity, it is important to consider how T cell development may be affected by manipulation of TrIP expression.

1.1.7 Effects of PI3K on T cell differentiation

In order to further understand how expression of TrIP affects the PI3K pathway in T cells, it is important to consider the various subsets of T cells and how PI3K activity affects differentiation into these subsets. CD4 T cells have been extensively studied due to their role in many immune responses such as adaptive immunity to pathogens as well as allergic response and autoimmunity. These studies have uncovered several lineages T cells may differentiate into in order to function in varying microenvironments. The T cell subsets have to be specialized for particular situations in order to bring about appropriate responses. In addition, these cells have to recognize targets and be specific so as not to cause severe injury to the surrounding “bystander” areas of the

environment. Finally, there has to be a mechanism of "shut off" after generation of an appropriate response and elimination of an immune threat.

T cell subset differentiation is characterized by the expression of unique transcription factors along with the secretion of specific cytokines. Th1 cells express Tbet and secrete IFNγ; Th2 cells express GATA3 and secrete IL-4 and IL-13; Th17 cells express RORγT and secrete IL-17 and Tregs express Foxp3 and secrete IL-10 and TGFβ. The significant evidence for the role of PI3K in T cell development and lineage determination, coupled with this pathways involvement in T cell lymphomas, researchers have also looked at the possible role this pathway plays in T cell differentiation. In order to understand how TrIP regulates PI3K activity in T cells, it is important to elaborate on how regulation of PI3K activity in naïve and lineage differentiated cells, may affect subset differentiation. As previously stated, p110δ is highly studied in T cells due to the prevalent expression profile of Class I PI3Ks and the disease relevance associated with Class IA. For example, an overactive p110δ gene can result in T cell senescence and immunodeficiency which leads to chronic viral infections [58]. Studies focused on p110δ, have shed light on how PI3K affects T cell function but as previously mentioned, deletion studies are complicated due to the possibility of catalytic subunit isoform substitutions. The conserved DFG motif which is located in the catalytic domain of PI3Ks helps to determine lipid substrate specificity [59]. By carrying out a point mutation whereby the DFG motif was mutated to AFG, Okkenhaug and colleagues were able to disrupt p110δ function without deletion of the gene [49]. Here, I have termed these mice "D910A mice".

The advent of the D910A mice has allowed for more specific evaluation of p110. While T cells from D910A mice do not exhibit any apparent differences in development (CD4 and CD8 ratios were similar in lymph node compartments), it was found that phosphorylation of both Akt

and Foxo were reduced upon activation. Okkenhaug and colleagues also found that D910A T cells proliferated at a lower rate than WT mice. Furthermore, while IL-2 production was not severely affected, secretion of IFNg and IL-4 by antigen stimulated cells was greatly reduced compared to WT. These results suggested that activation of the PI3K pathway may be necessary for Th1 and Th2 differentiation and function [49, 60].

The use of PI3K inhibitors has also helped to shed more light on the requirements for PI3K signaling with respect to Treg and Th effector differentiation. For example, work by Soond et al supported the theory that PI3K signaling was responsible for Th1 and Th2 phenotypes. By employing the use of IC87114, the p110δ specific chemical inhibitor, release of a host of cytokines including IFNg and IL-17 in stimulated T cells was blocked [61]. In other work, Rapamycin was found to block the formation of the mTORC1 complex by preventing Raptor and mTOR from binding. This prevents activation of S6 kinase and results in reduced proliferation [62]. Rapamycin inhibition experiments also found that T cell differentiation was affected by attenuating mTOR. Naïve T cells activated in the presence of rapamycin were observed to upregulate Foxp3 and were functional in *in vivo* allograft suppression assays [63]. It is important to note that in these rapamycin experiments, the PI3K pathway was only partially inhibited as rapamycin does not affect phosphorylation of PDK1 or T308 of Akt. Thus, these experiments had begun to define the requirements of PI3K signaling for Treg differentiation compared to Teff differentiation.

Supporting evidence was provided by Delgoffe and colleagues who utilized mice with conditional deletion of mTOR (via a CD4-Cre flox system). They observed that stimulation of naïve T cells lacking mTOR resulted in a reduction of Th1, Th2 and Th17 differentiation potential. Interestingly, the absence of mTOR also led to an increase in Treg differentiating potential. These latter results whilst helping to explain the rapamycin data, suggested that different degrees of PI3K

signals corresponded with cytokine and transcription factors to dictate T cell subset determination [64]. In fact, Faeder et al have shown that this theory is accurate. Via a logic circuit model and experiments to validate the model, they show that a low TCR signal strength favours Foxp3 Treg cell induction and high TCR signal favours mTOR activation which leads to inhibition of Foxp3 and T effector phenotypes [65].

In order to follow up on these findings, I have evaluated how the absence of TrIP affects T cell differentiation both in *in vitro* differentiation assays and in the generation of an immune response to an infection.

1.1.8 The PI3K pathway in human disease

The PI3K pathway is present in all tissue types studied so far. Dysregulation of the PI3K pathway can lead to several ailments such as cancer, autoimmune disorders, pathogen response disorders, neurological disorders and cardiovascular disease. Thus, this pathway has been one of the main focuses of medicinal research. Several tools have been developed, targeting different aspects of the pathway. There are PI3K inhibitors such as rapamycin (sirolimus an mTOR pathway inhibitor) and Cal-101/IC87114 (a specific p110δ inhibitor) which have been used in both basic research and clinical studies [66, 67]. There are also several elegant mouse models- for example, mouse models featuring a loss of PTEN heterozygous knockouts (PTEN +/-) show the development of tumours in several tissues [68]. But there are several types of PI3Ks and though substrate specificity appears to define the functions of the different classes (see section 1.1.2), most classes have several isoforms. These factors combined make it particularly challenging to use inhibitors against the pathway due to the possibility of non-specific inhibition in "un-erring" cells. Targeting mutations is one way to get around this. Also, increasing knowledge of the different classes and isoforms can

allow for more specific targeting. Here I will briefly highlight the impact of PI3K dysregulation on human disease and advances made in the field in dealing with these conditions.

Genomic studies have revealed that mutations, which lead to increased PI3K signaling is one of the hallmarks of cancer [69]. These mutations can either be inactivating regulatory factors or leading to gain of function in catalytic factors that favour progression of the pathwat. For example, loss of PTEN function is associated with high degrees of metastases [30]. While activating mutations in the class IA PI3K have been identified in several types of cancer (e.g. epithelial, breast, colon, prostate). The loss of PI3K regulatory factor functions or gain of function mutations in the pathway lead to an increase in lipid kinase activity, maintenance of signaling and stimulation of growth and proliferation of cancerous cells. In fact, clinical studies show that hyperactivation of Akt is an indicator of poor prognosis [70].

Basic research also strongly supports this assertion. Clues for the effects of overeactive PI3K signaling on T cell development and function have come from deletion/mutation experiments. Mice lacking PTEN develop T cell lymphoma and are also characterized by highly active T cells which secrete inflammatory cytokines that result in significant autoimmunity [71]. This phenotype is replicated in mice with a p85a mutation that renders the regulatory subunit unable to bind the p110 catalytic subunit [72]. In evaluating effector T cell response to infection, researchers have also found that loss of the transcription factor Foxo1, leads to a loss of secondary response to Listeria infection [73]. These latter findings further highlight the relevance of the PI3K pathway in autoimmunity and infectious diseases.

Activated phosphoinositide 3-kinase-d syndrome (APDS) is a recently identified primary immunodeficiency resulting from dysregulation of the p110d catalytic subunit. Clinical features of APDS include: persistent infections of viruses such as CMV, EBV and HSV, defective killing

of mycobacteria, juvenile arthritis and lymphomas [74]. APDS is caused by a gain of function mutation in the gene encoding p110d (PIK3CD) or a mutation that leads to a dysfunctional regulatory subunit p85a, unable to bind p110d [58, 75, 76]. This leads to increased activity of p110d resulting in hyper-phosphorylation of Akt and hyperactivation of the mTOR pathway. The result appears to be that initially responsive T cells end up exhausted and patients are then subject to infections and immunodeficiencies [58]. Loss of function mutations in humans also lead to severe immune consequences. Patients have been reported with recurrent pneumonia and development of colitis. These latter conditions have been suggested to be due to stunted B cell development and low T reg cell numbers [77]. These observations are also in line with mouse model data and further highlight the relevance of such models.

For over two decades, several studies and developments have been targeting the PI3K pathway as a means of alleviating immune and cancerous ailments. Below are some of the methods employed.

LY294002 a pan PI3K inhibitor developed by the Eli Lilly company has been used as a research tool to further understanding of this pathway in basic sciences as well as a potential inhibitor in cancer and inflammatory disease studies. But as a small molecule inhibitor, LY294002 carries high potential for non-specific effects. Thus, there has been limited use of this compound in clinical treatment [70].

Physicians have employed the use of popular PI3K/mTOR inhibitors in treating patients. Sirolimus, also known as Rapamycin is an mTOR inhibitor that has shown some promise in immunodeficiency treatments [78, 79]. However, the various feedback loops associated with the mTOR pathway appear to prevent complete inhibition by sirolimus. Thus, sirolimus is often applied in combination therapy whereby multiple targets associated with cell survival and cell

growth as well as the mTOR pathway are targeted. In some circles however, the use of rapamycin is cautioned and its long-term use is still under evaluation considering the role of the mTOR pathway in efficient immune cell development and function as well as its various roles in other cell types.

Targeting specific PI3K isoforms that are implicated in cell type lymphomas and autoimmune conditions is also an option that is being evaluated [80]. For example, Idealisib, developed by Gilead, is a more specific inhibitor targeting PI3Kd and has been licensed for use in chronic leukemia and in certain lymphomas (e.g. non-hodgkins lymphoma). It works by inhibiting the catalytic domain of p110d and thereby inducing apoptosis and preventing proliferation in tumor cells. This drug comes with significant side-effects however. After treatment, patients have presented with conditions suggesting immune deficiency. Indicating that the specificity of the drug renders other would be "good cells" ineffective towards invading pathogens and normal homeostasis. This highlights one of the greatest difficulties researchers have faced in tackling PI3K pathway dysregulation. More clinical trials are underway investigating dosage with respect to severity of disease.

In some cases, experimental treatment involving haematopoeietic stem cell transplants have been attempted as it carries the added benefit of treating malignancies[74, 81, 82].

Finally, research has suggested that targeting receptor tyrosine kinase activity as well as factors within the PI3K pathway will result in more efficient anti-tumour medication and therapy [10, 83-88]. But cancer cells have proven to be effective at resisting PI3K inhibition. Most cancers drive PI3K activation in cells through multiple RTKs, thus cancer cells are resistant to single RTK or signaling factor targeting. Cancer cells have also been observed to undergo genomic evolution whereby loss of regulatory factors in the cell help to create resistance in the face of inhibitors [89].

Upregulation of pro-survival mechanisms in cancer cells also leads to drug resistance [90]. Thus, combination therapy whereby clinicians use a combination of drugs so as to prevent development of resistance is presently being employed.

In light of these studies, it is indeed exciting to be part of the pioneering team that has begun to elucidate the role of TrIP in PI3K regulation. Especially as TrIP presents a new avenue, upstream of the PI3K/Akt pathway that can be targeted for the development of new treatment regimen.

1.2 PI3K INTERACTING PROTEIN 1 (PIK3IP1): A NOVEL PI3K REGULATOR

In a search for kringle-bearing transmembrane proteins, De Frances and colleagues identified a transmembrane protein, PI3K interacting protein 1 (PIK3IP1) (which we have renamed Transmembrane Inhibitor of PI3K (TrIP)), with a motif similar to the inter-SH2 (iSH2) domain of PI3K regulatory subunit- p85 [91]. This motif was located in the cytoplasmic portion of the protein. In T cells, the SH2 domains of p85 are known to bind the adaptor binding domain (ABD) of p110δ. Whilst the iSH2 domain binds p110δ, the nSH2 and cSH2 stabilize p110δ. Only after phosphorylation of the nSH2 and cSH2 is p110δ activated [26, 92, 93]. Thus, the presence of this iSH2 domain on the newfound PIK3IP1 protein piqued interest. In further experiments, the DeFrances lab found that not only was the expression of PIK3IP1 associated with attenuated PI3K activity, but knock-down of PIK3IP1 led to enhanced PI3K activity in fibroblasts [94]. Furthermore, the p85-like domain of PIK3IP1 was shown to bind to p110δ [91]. Not only did the early work of DeFrances et al demonstrate a role for PIK3IP1 in regulation of PI3K signaling in fibroblasts, but they also showed that PIK3IP1 can act as a tumour suppressor. Mice transgenic for

PIK3IP1 in hepatocytes were able to reduce hepatocyte proliferation and showed significant survival compared with controls [94]. However, nothing was yet known about a possible role of this novel protein in the immune system. In work done in collaboration with the DeFrances group, we showed that when PIK3IP1 is silenced by siRNA, PI3K downstream activity is increased. Conversely, overexpression of PIK3IP1 resulted in decreased downstream signaling in T cells [95]. These results strongly supported the model that PI3K can be negatively regulated by PIK3IP1. These studies also indicated that PIK3IP1 can regulate T cell activation, possibly through the inhibition of PI3K signaling. The presence of the kringle domain also implied the possibility of ligand interaction. How these findings affect T cell development and activation in different scenarios in the immune system was of interest to us. This required a better understanding of the structure of PIK3IP1.

1.2.1 Kringle Domains

Named after a Scandinavian pastry due to their secondary structure, these domains are typically about 80 amino acids in length and consist of two antiparallel β-sheets with 3 disulphide bridges. The cysteine residues that form the disulphide bonds are highly conserved and typically connected pairwise as follows: 1-80, 22-63 and 51-75 (based on 80 amino acid kringles) [96, 97]. These disulphide bridges give the kringle its characteristic fold by forming three loops that restrict the domain into the pastry like shape when viewed by planar projection [98]. Functionally, kringles are structural domains that mediate binding with other proteins and ligands. The basic kringle structure, though present on different types of proteins is mostly conserved but has evolved to bind different types of proteins or ligands as dictated by the functions of its parent protein [99-101].

Several proteins have been identified with kringle domains. The majority of these proteins are involved in blood clotting and fibrinolysis. It appears that depending on the function of the domain within a protein, kringle containing proteins can possess varying numberss of kringle domains. Some examples include: prothrombin (two kringles), plasminogen (five kringles), urokinase (one kringle) and tissue-type plasminogen activator (two kringles) [99, 101, 102].

An example of how kringle domains function in physiology outside the immune system can be seen in the blood clotting pathway. Plasmin is a fibrolytic protein that dissolves blood clots and prevents obstruction of blood flow. Plasmin levels are therefore carefully regulated, as the presence of an excess of active plasmin could lead to excessive bleeding, while a shortage of plasmin could lead to thrombosis. Plasmin circulates in the blood as the inactive precursor plasminogen. Depending on the pathway, plasminogen activation can be carried out by a host of factors including tissue-type plasminogen activator (tPA) and urokinase-type plasminogen activator (uPA) [103, 104]. Plasminogen has five kringle domains, which mediate substrate binding, membrane association and activation and inhibition [105]. Several other kringle domain-containing proteins also show substrate specificity via the kringle domain. For example, uPA has been shown to bind $\alpha_v\beta_3$ integrins, resulting in an inflammatory response to LPS in neutrophils, while tPA binds fibrin and plasminogen during the activation of plasmin [106, 107]. In fact, recent work has shown that kringle domains can be engineered to make functional agonists/antagonists [96].

Based on these observations, the presence of the kringle domain on TrIP suggests not only the possibility of homotypic or heterotypic protein:protein interactions as a means of TrIP regulation of PI3K but also as a means by which TrIP itself may be regulated during PI3K driven T-cell activation.

1.2.2 The p85-like Domain.

As previously stated, the p85 regulatory subunit of PI3K associates with p110d via the inter SH2 (iSH2) domain. DeFrances and colleagues found a region close to the C-terminus of TrIP with 70% and 65% homology to p85β and p85α iSH2 domains respectively. This iSH2-like domain was termed the p85-like region of TrIP. The presence of a transmembrane domain suggested that TrIP is a transmembrane protein with an ecto-kringle domain and a p85-like domain in the cytosol. The importance of the structure was highlighted by the finding that TrIP was able to bind p110α only when this p85-like region was present [91].

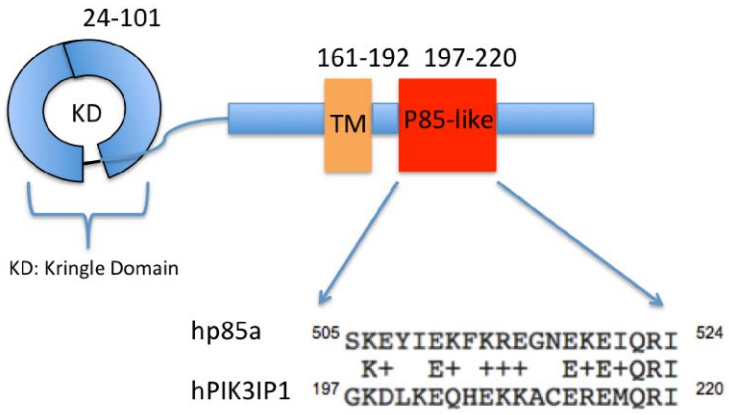

Figure 4 Schematic of PIK3IP1 highlighting homology of the p85-like domain to hp85a iSH2 domain

Biochem Biophys Res Commun, 2007. **358**(1): p. 66-72.

1.2.3 The Importance of the Transmembrane Domain in PIK3IP1

All the previously mentioned regulators of the Class Ia PI3K pathway are intracellular regulatory factors. Structural analysis indicates that TrIP contains a transmembrane domain between amino-

acids 161-192. The presence of a transmembrane in TrIP indicates that this novel protein is expressed on the cell surface. This further suggests that TrIP functions upstream of other known regulators of the PI3K pathway.

2.0 STATEMENT OF THE PROBLEM

Regulation of the PI3K signaling pathway is important for proper control of cellular activation, metabolism, survival and proliferation. Abnormal activation of this pathway can lead to the development of cancer, as observed, with activating mutations in PI3K or Akt or inactivating ones in negative regulators of PI3K such as PTEN. In a search for kringle bearing transmembrane proteins, DeFrances and colleagues identified PIK3IP1 (PI3K Interacting Protein 1), which we have renamed TrIP (Transmembrane Inhibitor of PI3K). TrIP possesses a motif similar to the inter-SH2 (iSH2) domain of PI3K subunit p85. This motif is located in the cytoplasmic portion of TrIP. These findings suggested that TrIP might represent a novel regulator of the PI3K signaling pathway. The iSH2 domain of p85 is known to bind the adaptor binding domain (ABD) of p110. Indeed, this novel protein was able to bind to p110 subunit of PI3K *in vivo* and *in vitro*. In addition, DeFrances and colleagues showed that expression of TrIP was associated with attenuated PI3K activity, while conversely knock-down of TrIP led to enhanced PI3K activity, in fibroblasts.

While the early work of the DeFrances lab demonstrated a role for TrIP in regulation of PI3K signaling in fibroblasts and in the liver, nothing was yet known about a possible role of this novel protein in the immune system. In work done in collaboration with the DeFrances lab we showed that when TrIP is silenced by siRNA in T cells, downstream signaling associated with PI3K activation (e.g. Akt) is upregulated. An increase of approximately 50% in activity was observed when an NFAT/AP-1 luciferase reporter was transfected with siRNA specific for TrIP,

in Jurkat T cells. In a similar experiment, IL-2 secretion was increased in the presence of TrIP siRNA, compared to control siRNA. Conversely, overexpression of TrIP resulted in decreased downstream signaling in T cells. These results strongly support the model that PI3K is negatively regulated by TrIP.

These previous studies showed that TrIP has the ability to regulate T cell activation, possibly through inhibition of PI3K signaling. However, it is still not known how TrIP expression is regulated during T cell development and activation. In addition, although TrIP is a transmembrane protein with a defined ecto kringle domain, it is not known whether TrIP is regulated by interaction with any corresponding ligands. Finally, the *in vivo* function of TrIP has yet to be defined by any knock-out models.

We hypothesized that both the kringle and the p85-like domains are necessary for the inhibitory function of TrIP on the PI3K/Akt pathway. In particular, our hypothesis tested if ligand binding on the kringle domain was essential for TrIP function and if the p85-like domain of TrIP interacts with p110δ in T cells. Furthermore, using a conditional knock-out mouse model, we hypothesized that the absence of TrIP in T cells would lead to early activation kinetics which would translate into a heightened immune response in the case of an infection. The studies described here begin to answer these questions regarding TrIP function in T cells and would shed more light on the PI3K/Akt pathway in conditions such as autoimmunity, cancer and infectious diseases.

Portions of the following chapters were compiled and submitted to the Journal of Experimental Medicine in the following manuscript [108]:

Uzodinma U. Uche, Ann R. Piccirillo, Shunsuke Kataoka, Stephanie J. Grebinoski, Louise M. D'Cruz and Lawrence P. Kane (2018). "PIK3IP1/TrIP restricts activation of T cells through inhibition of PI3K/Akt." *Journal of Experimental Medicine* 215 (12) 3165-3179. DOI:10.1084/jem.20172018.

3.0 TRIP INHIBITS PI3K/AKT/MTOR PATHWAY SIGNALING AND BOTH THE EXTRACELLULAR AND INTRACELLULAR DOMAINS OF TRIP ARE REQUIRED FOR INHIBITION OF PI3K/AKT PATHWAY

3.1 INTRODUCTION

In order to study the structure of TrIP with respect to T cell function, I evaluated the effect overexpression of TrIP would have on activated D10 T cells. The D10 cell line is derived from pooled lymph node T cells of chicken conalbumin-primed AKR/J mice [109] and has no apparent aberration in T cell signaling [110, 111]. Through the use of alternate readouts suitable for T cell activation, I sought to replicate previous results from both the Kane lab [95] and DeFrances [91] which showed that TrIP regulates PI3K activation.

Activation of the PI3K pathway leads to protein synthesis via Akt activation of the mTOR pathway. The phosphorylation of ribosomal S6 (pS6) is important for the translation of mRNA transcripts and is downstream of Akt in the PI3K signaling pathway. In light of the function of TrIP as an inhibitor of the PI3K/Akt pathway, reduction of S6 phosphorylation was an ideal readout for T cell activation studies.

Another method employed was evaluation of FoxO nucleus exit after T cell stimulation. Pro-survival and anti-apoptotic gene expression are ways by which the PI3K pathway induces cell proliferation. Nuclear localization of FoxO leads to cell cycle arrest and apoptosis as FoxO binds

to the promoters of pro-apoptotic factors such as Bim and BAD as well as promotes the upregulation of factors such as the cyclin dependent kinase inhibitor, p27 (a cell cycle regulator) [112-114]. In response to TCR activation, phosphorylation of FoxO by Akt can result in Foxo exclusion from the nucleus and the inactivation of these negative cell-cycle components.

I validated these assays by comparing results to the previously established T cell luciferase readout in our lab. This method requires the use of a luciferase reporter plasmid, wherein the luciferase gene is under the control of an NFAT reporter.

Once I had established viable methods for PI3K activity evaluation in the presence or absence of TrIP, I examined the role of the kringle and p85-like domains in TrIP function. This was done by making constructs containing TrIP mutants with the extracellular kringle domain deleted (Δkringle-TrIP), the cytoplasmic region deleted (Δcyto-TrIP) or only the p85-like domain deleted (Δp85-like-TrIP). These constructs were then transfected into D10 cells and evaluated in pS6 and luciferase assays.

3.2 METHODS AND MATERIALS

Cell lines, transfections and activation. The D10 Th2 T cell clone (D10.G4.1; ATCC TIB-224) was maintained in RPMI media supplemented with 10% bovine growth serum (BGS; Hyclone), penicillin, streptomycin, glutamine and 25 U/ml recombinant human IL-2. Using a BIO-RAD GenePulser Xcell, D10 cells were individually electroporated with control plasmid or flag-tagged WT TrIP constructs, along with pMaxGFP plasmid (encoding GFP from copepod *Pontellina p.*). One day after transfection, cells were evaluated by flow cytometry for GFP expression and TrIP expression (by anti-Flag staining) using anti-DYKDDDDK APC clone L5 (BioLegend #637308).

Transfected D10 cells were stimulated in RPMI with 3 μg/ml biotinylated anti-CD3 and anti-CD28 in the presence of 15 μg/ml streptavidin (anti-mCD3ε biotin, clone 145-2C11, Tonbo Biosciences #30-0031-U500; anti-mCD28 biotin, clone 37.51, BD Biosciences #553296; streptavidin, MilliporeSigma #189730). Cells were activated for 15, 30 or 60 mins. Activation was stopped with 1 ml of cold PBS, followed by centrifugation and aspiration of media.

Luciferase Assays. D10 T cells were transfected with 10μg of control or flag-tagged TrIP along with 15 ug of NFAT luciferase reporter vector by electroporation, cultured in complete medium (RPMI, 5% BGS and penicillin/ streptomycin) for 16-20 hrs. Cells were then stimulated with 3 μg/ml biotinylated anti-CD3 and anti-CD28 in the presence of 15 μg/ml streptavidin, or PMA and ionomycin for six hours. Luciferase assays were performed as previously described [115].

Flow cytometry. Before staining, cells were washed in staining buffer (1% Bovine Growth Serum-supplemented PBS). For extracellular staining, cells were stained at 4˚C with antibodies re-suspended in staining buffer. For intracellular staining, cells were washed three times to remove excess extracellular staining and then fixed and permeablized with the BD Biosciences cytofix/perm kit (#554714) for cytosol analysis. Fixed and permeablized cells were then stained at 4˚C with antibodies re-suspended in permeablization buffer from the kit.

Imaging flow cytometry. For FoxO1 assays, D10 cells were individually electroporated (as described above in "Cell lines, transfections and activation**"**) with control plasmid or flag-tagged WT TrIP constructs, along with pMaxGFP plasmid (encoding GFP from copepod *Pontellina p.*). One day after transfection, cells were evaluated by flow cytometry for GFP expression and TrIP

expression (by anti-Flag staining) using anti-DYKDDDDK APC clone L5 (BioLegend #637308). Transfected D10 cells were then sorted for GFP positive cells on a BD FACS ARIA IIu using the 70μm nozzle at 70psi. GFP was excited by the 488nm laser and read using a 530/30 filter. Sorted D10 cells were stimulated as described in "Cell lines, transfections and activation**"** **(**above). Activation was stopped with 1 ml of cold PBS, followed by centrifugation and aspiration of media. Sorted D10 cells were then fixed and intracellularly stained as described above.

For intracellular staining, cells were washed three times to remove excess extracellular staining and then fixed and permeablized with the eBioscience Foxp3/Transcription factor staining buffer set (#00-5523-00). Fixed and permeablized cells were then stained at 4˚C with antibodies re-suspended in permeablization buffer from the same eBioscience Foxp3/Transcription factor staining kit. The following intracellular stains were used: FoxO1 (C29H4) Rabbit mAb (Cell Signaling #2880S) with Alexa Fluor 594 donkey anti-rabbit IgG (clone: Poly4064; Cat#406418) as a secondary stain. DAPI dilactate (Molecular Probes Ref#D3571) was used for DNA/nuclear staining.

Imaging cytometry data on fixed and stained cells were acquired on an Amnis ImageStreamX Mark II running INSPIRE® software (Millipore). Analysis was performed using IDEAS® software (Millipore). First, focused cells, based on the gradient root mean square feature, were identified. Singlets were identified by the aspect ratio and area of bright field data. A nucleus intensity mask was made from DAPI staining. This mask was used to determine FoxO1 intensity in the nucleus. A gate of low FoxO1 nuclear signal was then set based on the unstimulated control samples. Approximately 3000-4000 cells are represented in the D10 T cell data.

3.3 RESULTS

3.3.1 TrIP inhibits PI3K/Akt/mTOR pathway signaling

We have previously shown that ectopic expression of TrIP in T cells can inhibit the phosphorylation of Akt and thus its activation [95]. A more sensitive readout of PI3K/Akt/mTOR activity is analysis of ribosomal protein S6 phosphorylation (pS6) by flow cytometry (**Fig. 5A**). In order to study the structural requirements of TrIP for modulation of T cell function, we evaluated pS6 in D10 T cells, a cell line with apparently normal PI3K signaling [116], in the context of ectopically expressed WT or mutant TrIP. The domain structure of TrIP is illustrated in **Fig. 5B**. In the absence of a suitable antibody for detecting TrIP by flow cytometry, I transfected D10 T cells with control plasmid or Flag-tagged TrIP (WT TrIP) and monitored TrIP expression using α-Flag antibody (**Fig. 5C**). One day after transfection, cells were stimulated with α-CD3/CD28 and analyzed by gating on GFP expressing cells at various time points (**Fig. 5D-E**). At all time points evaluated cells with ectopic TrIP expression displayed lower pS6, compared with empty vector-transfected cells. I also noted that, in the absence of stimulation, ectopic expression of TrIP resulted in lower basal pS6. In these experiments, and those shown below, I have focused on the percentage of pS6+ cells, as this event appears to mainly manifest as a digital response. As an additional readout for PI3K/Akt activity, I also measured the effect of ectopic TrIP on nuclear exclusion of FoxO1, which occurs after Akt-mediated phosphorylation [117]. Thus, as shown by imaging flow cytometry, while CD3/CD28 stimulation resulted in rapid nuclear exit (and apparent degradation) of FoxO1, this effect was dramatically impaired in D10 cells expressing ectopic TrIP (**Fig. 5F-G**). These results are consistent with previous data suggesting that TrIP inhibits PI3K activation in fibroblasts and with our earlier finding that TrIP inhibits Akt activation in T cells [91, 95].

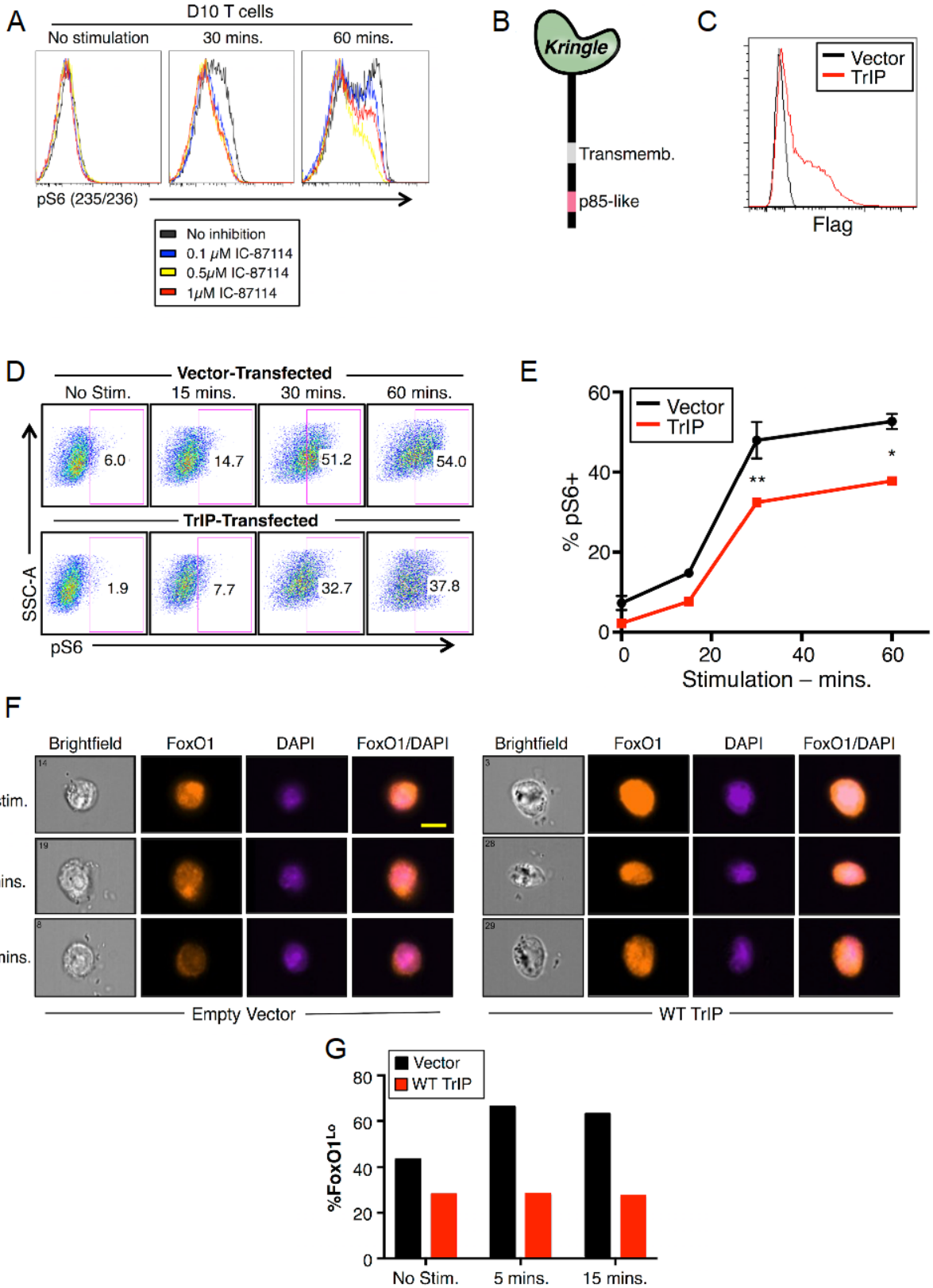
A
D10 T cells
No stimulation
30 mins.
60 mins.
pS6 (235/236)
No inhibition
0.1 μM IC-87114
0.5μM IC-87114
1μM IC-87114
B
Kringle
Transmemb.
p85-like
C
Vector
TrIP
Flag
D
Vector-Transfected
No Stim.
15 mins.
30 mins.
60 mins.
6.0
14.7
51.2
54.0
TrIP-Transfected
1.9
7.7
32.7
37.8
SSC-A
pS6
E
Vector
TrIP
% pS6+
Stimulation – mins.
F
Brightfield
FoxO1
DAPI
FoxO1/DAPI
Unstim.
5 mins.
15 mins.
Empty Vector
WT TrIP
G
Vector
WT TrIP
%FoxO1Lo
No Stim.
5 mins.
15 mins.

Figure 5 TrIP inhibits PI3K signaling.

(A) D10 T cells were stimulated with anti-CD3/CD28 Ab's for the indicated times, plus either vehicle control or indicated concentrations of the PI3Kδ inhibitor IC-87114. Cells were then permeablized, stained with mAb to pS6, and analyzed by flow cytometry. Representative of three experiments. (B) Domain structure of TrIP, indicating the kringle, transmembrane and p85-like domains. (C) Expression of Flag-tagged WT TrIP on transiently transfected D10 T cells. (D) Flow cytometric analysis of pS6 activation in control (vector) or WT TrIP-transfected D10 T cells, stimulated with anti-CD3/CD28 for the indicated times. (E) Quantitation of pS6 activation as shown in panel D. (F) D10 T cells were transfected with empty vector or TrIP and stimulated the next day with anti-CD3/CD28 Ab's for the indicated times. Cells were anayzed with an Amnis ImageStreamX MarkII imaging cytometer. Representative images are shown in panel F. Compiled data from 600-800 gated (focused singlets) cells with low FoxO1 in the nucleus are shown in panel G. The yellow scale bar in C represents 10 μM. *p* values (for TrIP vs. vector) were calculated using two-way ANOVA with Sidak's multiple comparisons test. *p* values are represented with the following symbols: *0.01-0.05, **0.001-0.01, ***<0.001.

3.3.2 The Kringle and cytoplasmic domains are required for TrIP activity

The importance of the kringle domain as a ligand-binding domain in other proteins [100, 101, 118], and the degree of homology between the p85-like domain and the inter-SH2 domain of the p85 regulatory subunit of PI3K, suggests that these two domains may play important roles in the inhibition of PI3K by TrIP. To address this, I designed Flag-tagged TrIP variants lacking either the extracellular kringle domain (Δkringle-TrIP), the entire cytoplasmic region (Δcyto-TrIP) or only the p85-like domain (Δp85-like-TrIP)**.** These constructs were transfected, along with a GFP transfection control, into D10 T cells (**Fig. 6A**) which were then stimulated with α-CD3/CD28 and analyzed by flow cytometry (after gating on GFP positive cells; see **Fig. 6B**) for S6 phosphorylation (**Fig. 6C-D**). While WT TrIP led to the attenuation of pS6, deletion of either the p85-like domain alone or the entire cytoplasmic region abolished the ability of TrIP to suppress pS6. Interestingly, expression of the kringle domain-deleted construct (which still possesses the p85-like domain) did not attenuate pS6.

To further validate this data, I transfected the Flag-tagged TrIP constructs (WT-TrIP, Δkringle-TrIP and Δcyto-TrIP) into D10 cells along with a luciferase reporter driven by the NFAT

promoter. I confirmed expression of the flag tagged constructs by flow cytometry (**Fig. 6E**). Cells were then stimulated with α-CD3/CD28 for 6 hrs and relative luciferase units were measured. I found that as observed in the pS6 assay, cells overexpressing WT-TrIP attenuated NFAT activity. Whereas, the absence of either the p85-like or kringle domains rescued the effects of TrIP on NFAT (**Fig. 6F**).

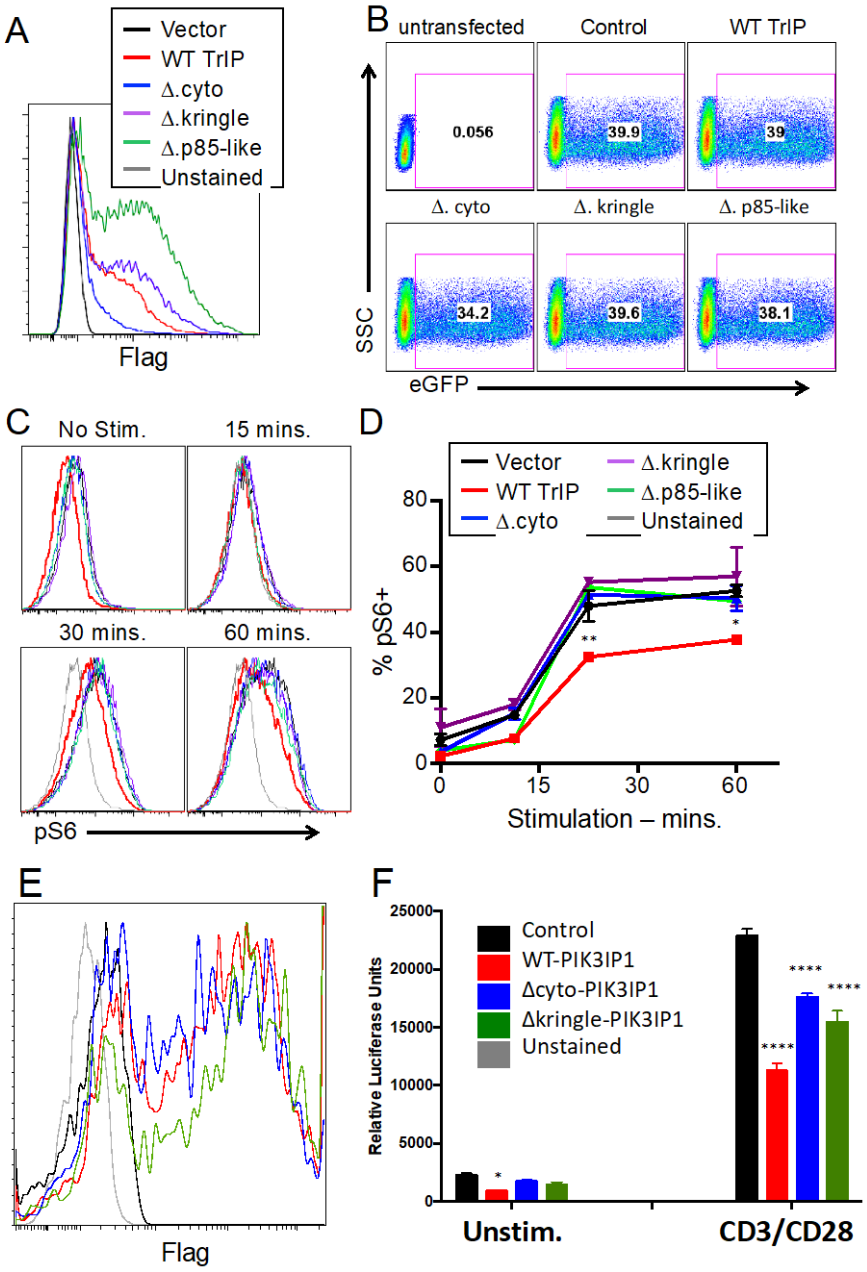

Figure 6 The Kringle and Cytoplasmic domains are required for TrIP activity.

(A) Expression of WT and mutant Flag-tagged TrIP constructs on transfected D10 cells. (B) Representative expression of a co-transfected eGFP plasmid in D10 cells transfected with control vector or TrIP constructs. GFP-positive cells were analyzed by flow cytometry for Flag and pS6 expression (C) Representative histogram of pS6 staining in D10 cells transiently transfected with Flag-tagged TrIP constructs and activated with anti-CD3/CD28. (D) Quantitation of pS6 activation obtained from flow cytometric analysis of activated

D10 cells transfected with Flag-tagged TrIP constructs, as shown in panel C. P values (for TrIP versus vector) were calculated using two-way ANOVA with Sidak's multiple comparisons test. (E) Expression of WT and mutant Flag-tagged TrIP constructs on transfected D10 cells. Cells were co-transfected with TrIP constructs along with a Luciferase plasmid,. (F) Quantitation of relative luciferase units from activated D10 cells transfected with Flag-taged TrIP constructs and luciferase plasmid, as shown in panel E. Data in each panel are representative of at least three experiments. P values (for TrIP variants versus vector) were calculated using two-way ANOVA with Dunnett's multiple comparisons test. P values are represented with the following symbols: *, P = 0.01-0.05; **, P = 0.001-0.01; ***, P = 0.0001-0.001; and ****, P < 0.0001.

3.4 DISCUSSION

TrIP is a transmembrane protein that contains two identifiable domains: an extracellular kringle domain, implicated in ligand interaction in related proteins [100, 101, 119], and an intracellular 'p85-like' domain. An initial study showed that PI3K was inhibited by TrIP through its interaction with the catalytic subunit of PI3K via the p85-like domain [91]. We also showed previously that silencing TrIP in T cells leads to upregulation of T cell signaling [95]. Here I sought to obtain a more complete understanding of TrIP structure and function in an immune context. Our results showed that overexpression of WT TrIP in D10 cells resulted in impaired phosphorylation of ribosomal S6 protein, reduced NFAT activity (via luciferase readout Fig 6F), as well as impaired nuclear exclusion of FoxO1 (a direct Akt target), further validating the model that TrIP inhibits the PI3K/Akt pathway.

In my analysis of the importance of the two domains, I hypothesized that the kringle domain might serve to modulate the activity of TrIP via protein-protein interactions as has been observed in order kringle bearing proteins[105]. Indeed, the kringle domain appears to be essential for TrIP inhibitory function. A TrIP construct in which the kringle domain was deleted led to higher induction of pS6 and NFAT activity than was observed in T cells transfected with WT TrIP.

The initial description of TrIP revealed a sequence in the cytoplasmic tail that bears homology to the inter-SH2 domain of the PI3K adaptor protein p85 (Fig. 4), which regulates

activation of catalytic p110 subunits [91]. Extending the findings of Zhu et al., I show here that deletion of the cytoplasmic tail or the p85-like domain of TrIP leads to higher induction of pS6 and NFAT activity. These results suggest that both the kringle and p85-like domains are essential for optimal TrIP inhibitory function.

4.0 TRIP IS DOWN REGULATED UPON TCR STIMULATION THROUGH CLEAVAGE OF THE KRINGLE DOMAIN

4.1 INTRODUCTION

Our data strongly support an inhibitory role for TrIP in T cells. The role of inhibitory factors in T cells is to regulate TCR activation and prevent undue or excess immune responses. In most cases, these factors antagonize T cell signaling and thus, require downregulation or a temporary "shut down" in order for the cell to generate an appropriate response to a valid stimulation. For example, Programmed cell death protein 1 (PD1) receptor is an immune checkpoint receptor expressed on activated immune cells (T cells, B cells, NK cells and Dendritic cells) that plays an important role in the maintenance of self-tolerance. Deletion of the gene encoding this protein resulted in significant autoimmune phenotypes, which included arthritis in mice [120-122]. PD1 appears to function by interacting with its ligands (PD-L1/PD-L2) which are also expressed on immune cells. This interaction leads to the recruitment and activation of phosphatase factors, eventually leading to attenuating signaling of the PI3K pathway as well as the Ras/Erk pathway [123, 124]. The result is the inhibition of cell proliferation, loss of effector functions, as well as promotion of apoptosis. In fact, one of the hallmarks of continued PD-1 expression is T cell exhaustion, a condition characterized by the inability of effector T cells to produce cytokines and kill tumor or virus loaded cells [125]. Regulation of PD-1 activity is achieved by proteolytic cleavage of the extracellelular

regions of PDL-1 and PDL-2. Recently, matrix metalloproteinase 13 (MMP-13) was observed to cleave the PD-1 binding domain on PDL-1/PDL-2 resulting in a nullification of apoptotic signals on activated T cells.

Lymphocyte activation gene-3 (LAG-3) is another inhibitory molecule that is upregulated upon T cell stimulation [126]. While the mechanism of action of LAG-3 is presently unknown, the Vignali group has shown that expression of a non-cleavable form of LAG-3 blocks cytokine production and T cell proliferation [127]. In further research, Li et al. showed that regulation of LAG-3 function on T cells is mediated by two transmembrane metalloproteases, ADAM 10 and ADAM 17 (ADAM- a disintegrin and metalloproteinases).

Given these data and the knowledge that certain other negative regulators of T cell signaling (e.g. PTEN) are actively down-regulated to promote T cell activation [128, 129], we examined how TCR activation might affect expression of TrIP protein and based on our knowledge of TrIP structure, what proteinase groups may mediate regulation of TrIP.

4.2 MATERIALS AND METHODS

Cell lines, transfections and activation. The D10 Th2 T cell clone (D10.G4.1; ATCC TIB-224) was maintained in RPMI media supplemented with 10% bovine growth serum (BGS; Hyclone), penicillin, streptomycin, glutamine and 25 U/ml recombinant human IL-2. Human embryonic kidney (HEK) 293 cells were maintained in DMEM media supplemented with 10% bovine growth serum (BGS), penicillin, streptomycin and glutamine. CH27 mouse lymphoma cells (RRID:CVCL7178) were maintained in RPMI media supplemented with 10% bovine growth serum (BGS), penicillin, streptomycin and glutamine. Using a BIO-RAD GenePulser Xcell, D10

cells were individually electroporated with control plasmid, flag-tagged WT TrIP or Flag-tagged mutant TrIP constructs, along with pMaxGFP plasmid (encoding GFP from copepod *Pontellina p.*). One day after transfection, cells were evaluated by flow cytometry for GFP expression and TrIP expression (by anti-Flag staining) using anti-DYKDDDDK APC clone L5 (BioLegend #637308).

Transfected D10 cells were stimulated in RPMI with 3 μg/ml biotinylated anti-CD3 and anti-CD28 in the presence of 15 μg/ml streptavidin (anti-mCD3ε biotin, clone 145-2C11, Tonbo Biosciences #30-0031-U500; anti-mCD28 biotin, clone 37.51, BD Biosciences #553296; streptavidin, MilliporeSigma #189730). Cells were activated for 15, 30 or 60 mins. Activation was stopped with 1 ml of cold PBS, followed by centrifugation and aspiration of media. For ADAM10/17 inhibition studies, 1 μM of a dual ADAM 10 and ADAM 17 inhibitor GW280264X (AOBIOUS #AOB3632) was incubated with cells for 30 minutes before stimulation.

T cell/APC co-cultures. CH27 cells were pulsed with 100 μg/ml chicken conalbumin (Sigma #C7786) one day before mixing with D10 cells. D10 cells were mixed in a 1:1 ratio with either pulsed or unpulsed CH27 cells for 15, 30 and 60 mins. Reactions were quenched by placing cells on ice, adding 1 ml of PBS and centrifugation to settle cells and decant activation media. Cells were then stained with anti-DYKDDDDK APC clone L5 (BioLegend #637308), anti-mouse CD19 violetFluor 450 (clone 1D3; Tonbo Biosciences #75-0193-U025) and anti-mouse CD4 Brilliant Violet 510 (clone GK1.5; BioLegend #100449). Cells were washed three times in PBS and then fixed and permeabilized with eBioscience Foxp3/transcription factor staining buffer (cat # 00-5523-00), then stained with anti-pS6 (S235/236) Alexa Fluor 647 (clone D57.2.2E; Cell Signaling #5316S).

Flow cytometry. Before staining, cells were washed in staining buffer (1% Bovine Growth Serum-supplemented PBS). For extracellular staining, cells were stained at 4˚C with antibodies re-suspended in staining buffer. For intracellular staining, cells were washed three times to remove excess extracellular staining and then fixed and permeablized with the BD Biosciences cytofix/perm kit (#554714) for cytosol analysis. Fixed and permeablized cells were then stained at 4˚C with antibodies re-suspended in permeablization buffer from the kit.

Western blotting analysis and immunoprecipitations. Cells were lysed in ice-cold NP-40 lysis buffer (1% NP-40, 1 mM EDTA, 20 mM tris-HCL pH 7.4), 150 mM NaCl) for both protein analysis and immunoprecipitation. Immunoprecipitation was performed by mixing lysate with 20 µl of M2 anti-Flag agarose beads for 3 hrs at 4^{o} C. Proteins were eluted from beads by mixing Lysate with 1X SDS (containing 5% β-mercaptoethanol) and boiling at 95 deg. C for 10 mins. For western blot analysis, proteins were resolved by 10% SDS-polyacrylamide gel electrophoresis and were transferred onto polyvinylidene difluoride membranes which were then blocked in 4% BSA. The membranes were then incubated with the primary antibodies overnight. This was followed by incubating the membrane with HRP-conjugated secondary antibodies for 2 hours before detection with the SuperSignal West Pico ECL substrate (Thermo Fisher Scientific) and imaging on a Protein Simple FluorChem M.

Western blot and CoIP reagents: Anti-HA (12CA5) (Roche #11-583-816-001); anti-Flag M2 Affinity Gel (Sigma #A2220); direct-Blot HRP anti-DYKDDDDK (Clone L5; BioLegend #637311).

4.3 RESULTS

4.3.1 Cell-surface TrIP is down-regulated upon T cell activation

In order to replicate T cell stimulation in the presence of an antigen presenting cell (APC), we used the mouse B cell lymphoma line CH27 [130] to stimulate D10 cells. CH27 cells were either pulsed with cognate antigen (chicken conalbumin) or left unpulsed, and then mixed with D10 T cells transfected with Flag-tagged TrIP. There was a notable decrease over time in Flag-TrIP expression on the surface of D10 cells (**Fig. 7A-B**). Interestingly, this decreased expression corresponded with an increase of pS6 expression (**Fig. 7C-D**). As observed when D10 T cells were stimulated with α-CD3/CD28 (**Fig. 7**), antigen-pulsed CH27 cells induced a more immediate and robust pS6 signal in T cells transfected with empty vector, compared to those transfected with WT TrIP (**Fig. 7E**). These results support the model that T cells acutely modulate the expression of TrIP to promote the activation of TCR-induced PI3K signaling.

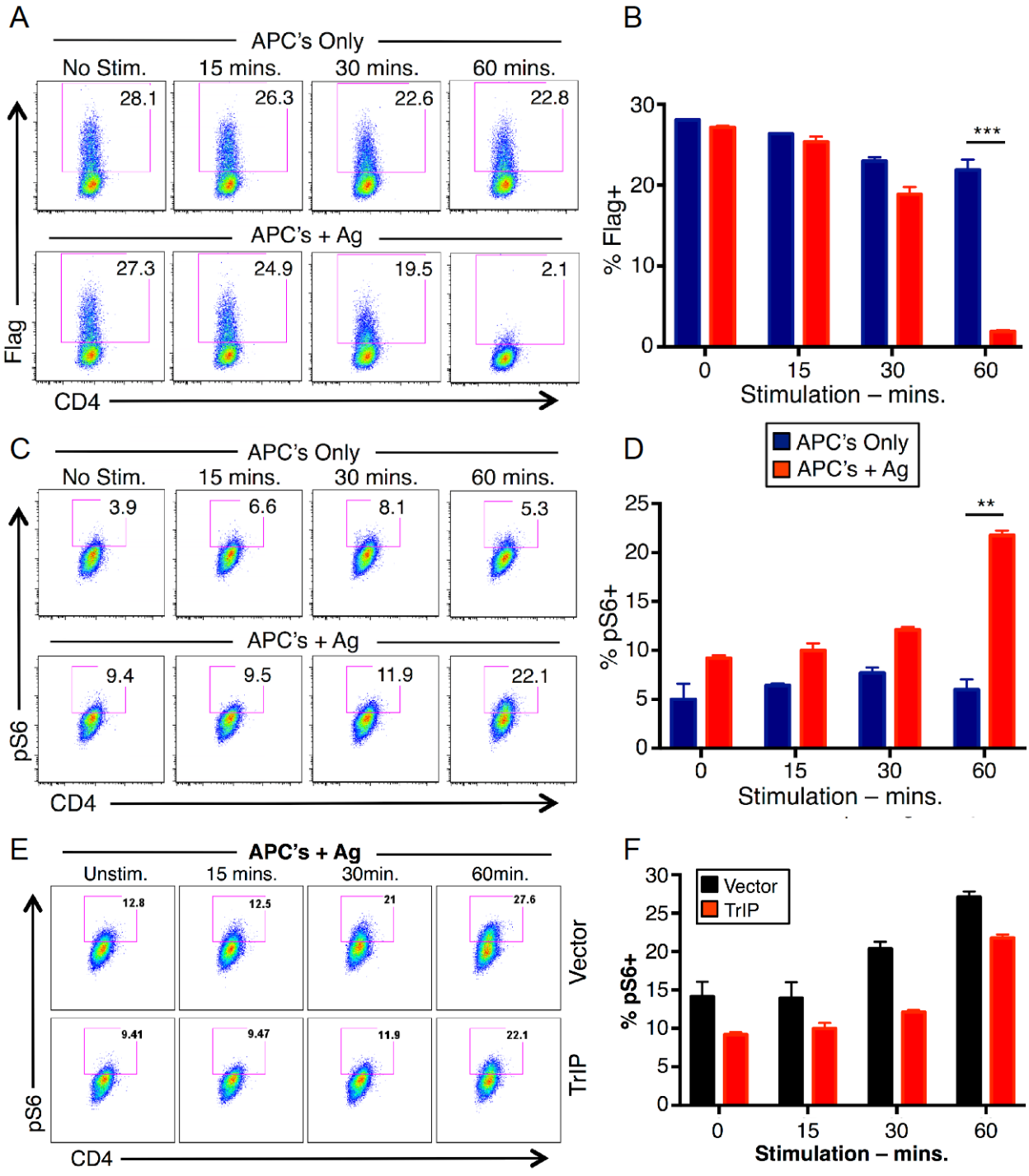
A
APC's Only
No Stim.
15 mins.
30 mins.
60 mins.
28.1
26.3
22.6
22.8
APC's + Ag
27.3
24.9
19.5
2.1
Flag
CD4
B
% Flag+
30
20
10
0
***
0
15
30
60
Stimulation – mins.
C
APC's Only
No Stim.
15 mins.
30 mins.
60 mins.
3.9
6.6
8.1
5.3
APC's + Ag
9.4
9.5
11.9
22.1
pS6
CD4
D
APC's Only
APC's + Ag
% pS6+
25
20
15
10
5
0
**
0
15
30
60
Stimulation – mins.
E
APC's + Ag
Unstim.
15 mins.
30min.
60min.
12.8
12.5
21
27.6
Vector
9.41
9.47
11.9
22.1
TrIP
pS6
CD4
F
Vector
TrIP
% pS6+
30
25
20
15
10
5
0
0
15
30
60
Stimulation – mins.

Figure 7 Cell-surface TrIP is downregulated during T cell activation

D10 cells transfected with WT TrIP were mixed with CH27 B cells as APCs (+/- conalbumin antigen) for the given time points. (**A**) Representative flow cytometry analyzing cell-surface expression of Flag-tagged WT TrIP on D10 cells stimulated with CH27 B cells alone (top row) or plus antigen (bottom row). (**B**) Quantitation of data shown in panel A. (**C**) Representative flow cytometry analyzing pS6 staining in D10 cells transfected with Flag-tagged WT TrIP and stimulated with CH27 B cells alone (top row) or plus antigen (bottom row). (**D**) Quantitation of data shown in panel C. (**E**) Representative flow cytometry of direct comparison of pS6 induction in empty vector vs. TrIP-transfected D10 T cells stimulated with APC's + Ag; (**F**) Quantitation of data shown in panel E. Data are representative of three experiments. *p* values (compared to time 0) were calculated using two-way ANOVA with Sidak's multiple comparisons test. *p* values are represented with the following symbols: *0.01-0.05, **0.001-0.01, ***<0.001.

4.3.2 The kringle domain is important for TrIP ligand/protein interaction and function

In order to probe the relevance of the kringle domain for TrIP expression and function, I used the CH27/D10 system with D10 cells expressing either Flag-tagged WT or Δkringle-TrIP T cells and monitored Flag-TrIP expression and S6 phosphorylation. Since Δkringle-TrIP transfected cells showed a recovery in TCR-dependent pS6 (**Fig. 6C-D**), I suspected that the absence of the kringle domain would lead to maintenance (and not down-regulation) of TrIP. As shown above, D10 cells transfected with WT TrIP and stimulated with CH27 B cells alone (without antigen) did not show significant loss of TrIP expression over time. However, when mixed with antigen-pulsed CH27 cells, WT TrIP-expressing D10 T cells showed a significant loss of TrIP expression (**Fig. 8A,** top row and **8B**). In contrast, D10 cells transfected with the Δkringle-TrIP mutant did not lose surface TrIP expression when stimulated with CH27 cells (with or without antigen) (**Fig. 8A,** bottom row and **8B**). Consistent with the results above, upon mixing with antigen-pulsed CH27 cells, Δkringle-TrIP-expressing D10 T cells actually showed a more rapid increase in pS6 than cells transfected with WT TrIP (**Fig. 8C-D**). These results further confirm that the kringle domain is important for the inhibitory function of TrIP and suggest the possibility that TrIP is regulated by interaction with a ligand.

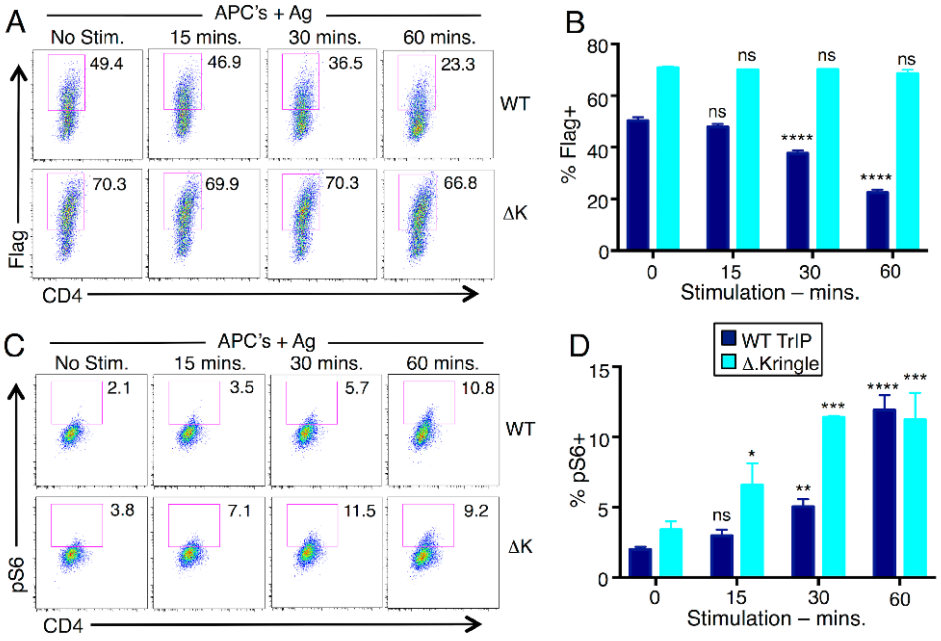

Figure 8 The Kringle domain is relevant for TrIP inhibitory function

D10 cells transiently transfected with Flag-tagged WT or Δkringle TrIP were mixed with CH27 B cells plus antigen, for the indicated times. (**A**) Representative flow cytometry analyzing cell-surface expression of Flag-tagged WT (top row) or Δkringle (bottom row) TrIP on D10 cells stimulated with CH27 B cells plus antigen. (**B**) Quantitation of data shown in panel A. (**C**) Representative flow cytometry analyzing pS6 staining in the same cells as in panel A. (**D**) Quantitation of data shown in panel C. Data are representative of three experiments. *p* values (compared to time 0) were calculated using one-way ANOVA with Dunnett's multiple comparisons test. *p* values are represented with the following symbols: *0.01-0.05, **0.001-0.01, ***<0.001

In the absence of a known ligand, I designed a hCD8-TrIP chimera to investigate possible effects of ligand engagement on TrIP function. The extracellular and transmembrane regions of human CD8 were fused with the cytoplasmic tail of TrIP, expressed in D10 T cells and detected at the cell surface with hCD8 antibody (**Fig. 9A**). Using a luciferase reporter driven by the NFAT promoter, I observed that expression of hCD8-TrIP on D10 T cells was not sufficient to inhibit TCR signaling (**Fig. 9B**). Similarly, expression of the chimera itself did not inhibit anti-CD3/CD28-induced pS6 (**Fig. 9C-D**). However, upon crosslinking of hCD8-TrIP with varying

concentrations of anti-hCD8, I observed a decrease in anti-CD3/CD28-induced pS6 (**Fig. 9C-D**). This was in contrast to the effects of a previously described CD8-ζ chimeric construct [131], which upon crosslinking with anti-hCD8, modestly enhanced the pS6 signal (**Fig. 9C-D**). These results suggest that the kringle domain of TrIP could regulate oligomerization of the protein, either after interaction with a distinct ligand or through homo-oligomerization. To investigate the latter possibility, I co-expressed Myc-tagged WT-TrIP with Flag-tagged WT-TrIP in 293T cells and used anti-Flag beads to immunoprecipitate (IP) Flag-tagged TrIP (**Fig. 9E**). Upon blotting with anti-Myc, I found that Flag-tagged WT-TrIP was able to co-IP Myc-tagged WT-TrIP (**Fig. 9E**). This suggests that TrIP oligomerizes upon expression, which promotes its ability to inhibit PI3K signaling (as evidenced by my results from **Fig. 9**). However, this finding does not rule out the possibility of a trans-interacting ligand for TrIP on the APC's.

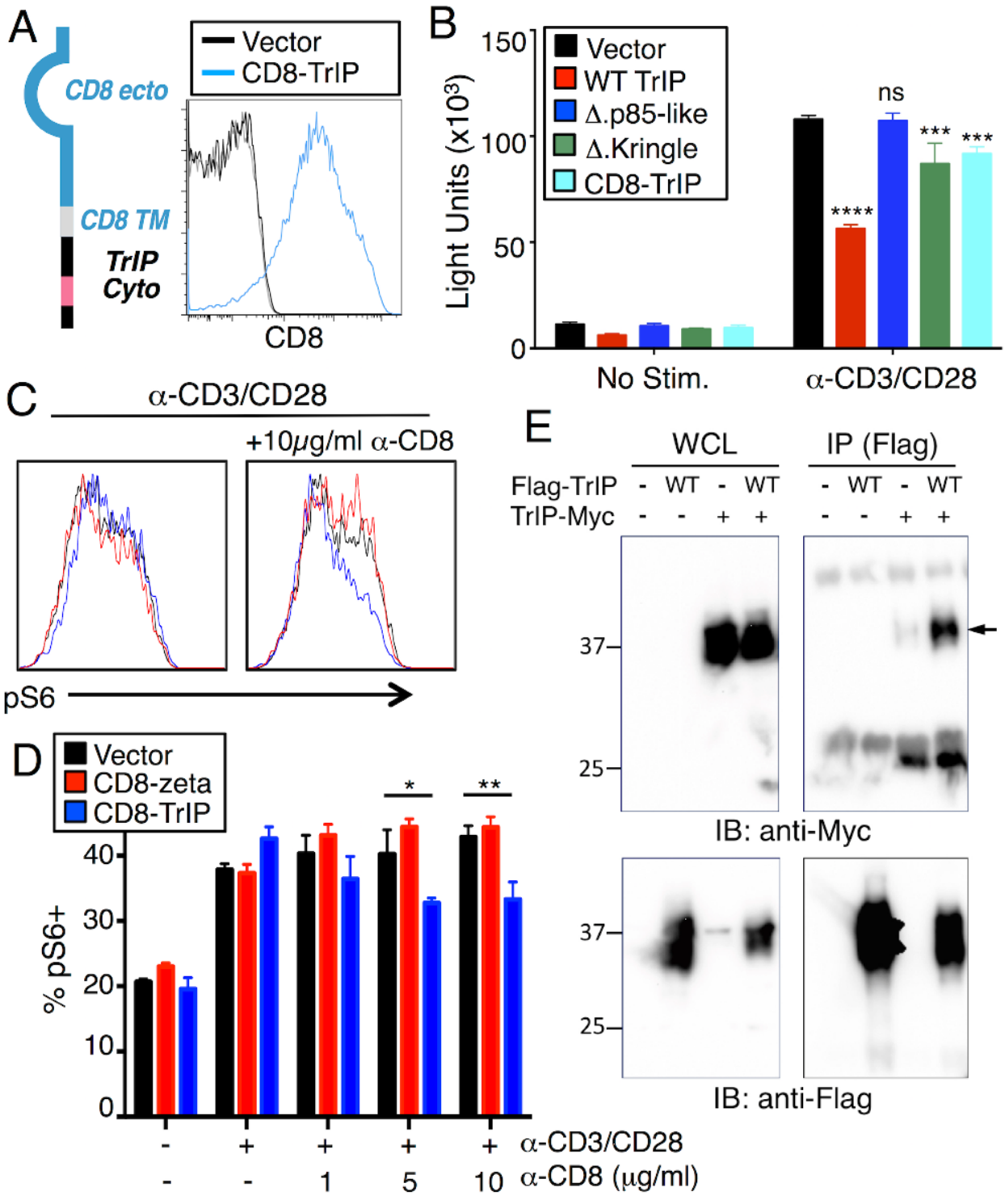
A
CD8 ecto
CD8 TM
TrIP
Cyto
Vector
CD8-TrIP
CD8
B
Vector
WT TrIP
Δ.p85-like
Δ.Kringle
CD8-TrIP
Light Units (x10³)
150
100
50
0
ns
****
***
***
No Stim.
α-CD3/CD28
C
α-CD3/CD28
+10μg/ml α-CD8
pS6
D
Vector
CD8-zeta
CD8-TrIP
% pS6+
40
30
20
10
0
*
**
- + + + + α-CD3/CD28
- - 1 5 10 α-CD8 (μg/ml)
E
WCL
IP (Flag)
Flag-TrIP - WT - WT - WT - WT
TrIP-Myc - - + + - - + +
37
25
IB: anti-Myc
37
25
IB: anti-Flag

Figure 9 TrIP oligomerizes via the kringle domain and this promotes its inhibition of PI3K signaling

A) Structure of ecto hCD8-mPIK3IP cytoplasmic chimera and its expression on transfected D10 cells. (**B**) D10 cells were transfected with the indicated TrIP constructs, plus an NFAT/AP1-luciferase construct, stimulated the next day with anti-CD3/CD28, followed by determination of luciferase activity. *p* values (compared to vector) were calculated using one-way ANOVA with Dunnett's multiple comparisons test. (**C**) Flow cytometry analysis of pS6 after stimulation of D10 cells transiently transfected with hCD8-TrIP in the presence of 10 μg/ml anti-hCD8. (**D**) Quantification of pS6 after stimulation of hCD8-TrIP transfected D10 cells in the presence of varying concentrations of anti-hCD8. *p* values (compared to vector) were calculated using one-way ANOVA with Dunnett's multiple comparisons test. (**E**) Detection of TrIP dimerization. 293T cells were transfected with Flag-tagged TrIP +/- Myc-tagged TrIP. Whole cell lysates (WCL; left panels) or anti-Flag IP's (right panels) were blotted with anti-Myc (upper panels) or with anti-Flag mAb (lower panels). *p* values (comparted to time 0) were calculated using two-way ANOVA with Tukey's multiple comparisons test. Data are representative of three experiments (A-E). *p* values are represented with the following symbols: *0.01-0.05, **0.001-0.01, ***<0.001, ****<0.0001.

4.3.3 ADAM10/17 mediate cleavage of TrIP during T cell activation

To further probe the function of the kringle domain, I next returned to the apparent down-regulation of TrIP from the surface of activated T cells. One possible mechanism that I considered for this is through metalloprotease-mediated cleavage of the ecto domain (including the kringle) of TrIP, based on past work on T cell regulators like LAG-3 and Tim-3 [127, 132, 133]. I transfected D10 T cells with Flag-tagged WT TrIP, then stimulated these cells with anti-CD3/CD28 mAb's, with or without an inhibitor of ADAM family metalloproteases 10 and 17, which were previously shown to mediate cleavage of LAG-3 and Tim-3. A constitutively expressed GFP construct was co-transfected to further track the transfected cells. As shown in the representative flow cytometry data in **Figure 10A**, stimulation of control vehicle-treated cells led to loss of cell-surface Flag staining, while the cells treated with an inhibitor of ADAM10/17 maintained Flag expression after stimulation. These results are quantified in **Figure 10B**. Thus, one mechanism for down-regulation of TrIP after T cell activation appears to be through ADAM10/17-mediated shedding of the kringle domain.

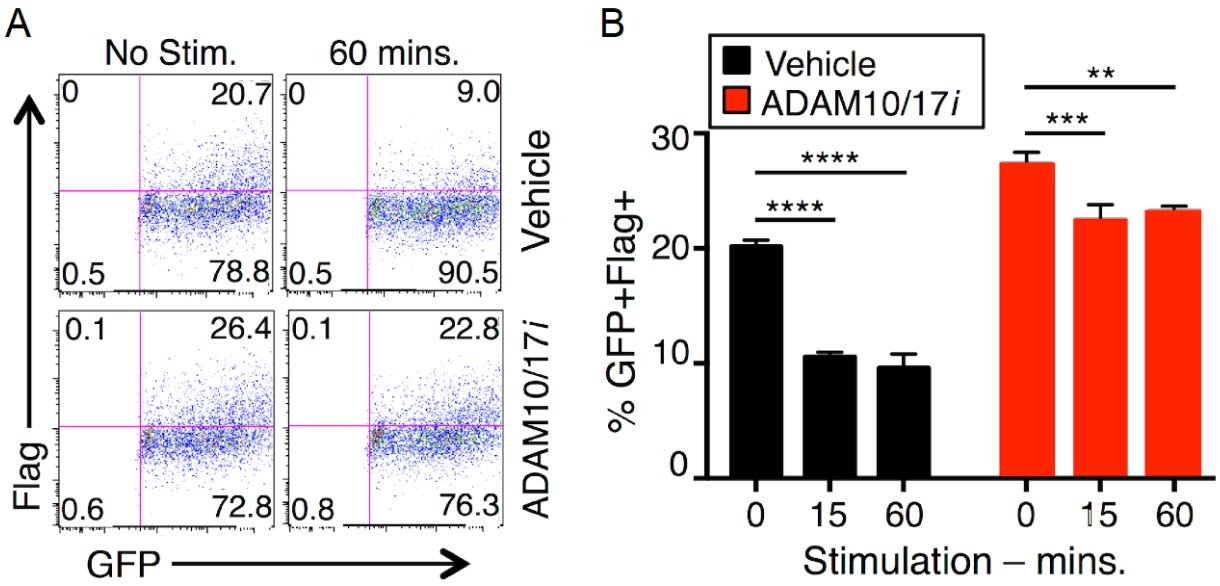

Figure 10 ADAM10/17 mediate cleavage of TrIP during T cell activation

(**A-B**) D10 T cells were transfected with Flag-TrIP plus a plasmid encoding eGFP. The next day, cells were stimulated with anti-CD3/CD28 Ab's for the indicated times, with or without 1 μM GW280264X, an inhibitor of ADAM10/17. Flag staining and GFP expression were determined by flow cytometry. Representative data are shown in panel A, and average data of quadruplicate samples are in panel B. *p* values (comparted to time 0) were calculated using two-way ANOVA with Tukey's multiple comparisons test. Data are representative of two experiments (A-B). *p* values are represented with the following symbols: *0.01-0.05, **0.001-0.01, ***<0.001, ****<0.0001.

4.3.4 Mediators of TrIP cleavage are expressed on T cells

To determine whether inducible down-regulation of TrIP only occurs in the context of stimulation by antigen and APCs (which may express a ligand for TrIP), we stimulated transfected D10 cells with α-CD3/CD28 and evaluated the surface expression of TrIP at various time points in the absence of APC and cognate antigen using the α-Flag antibody. Thus, we observed that even after CD3/CD28 stimulation, without APC's, WT TrIP expression was still down-regulated (**Fig. 11A-B**) with a concomitant upregulation of pS6 (**Fig. 11C**). In contrast, neither Δcyto-TrIP (**Fig. 11A-B**), Δkringle-TrIP or Δp85-TrIP (**Fig. 11D**) expression was down-regulated by stimulation with

CD3 and CD28 Ab's. However, despite the fact that these TrIP mutants were not down-regulated from the cell surface, they still failed to inhibit pS6 (**Fig. 11C&E**), suggesting additional levels of regulation.

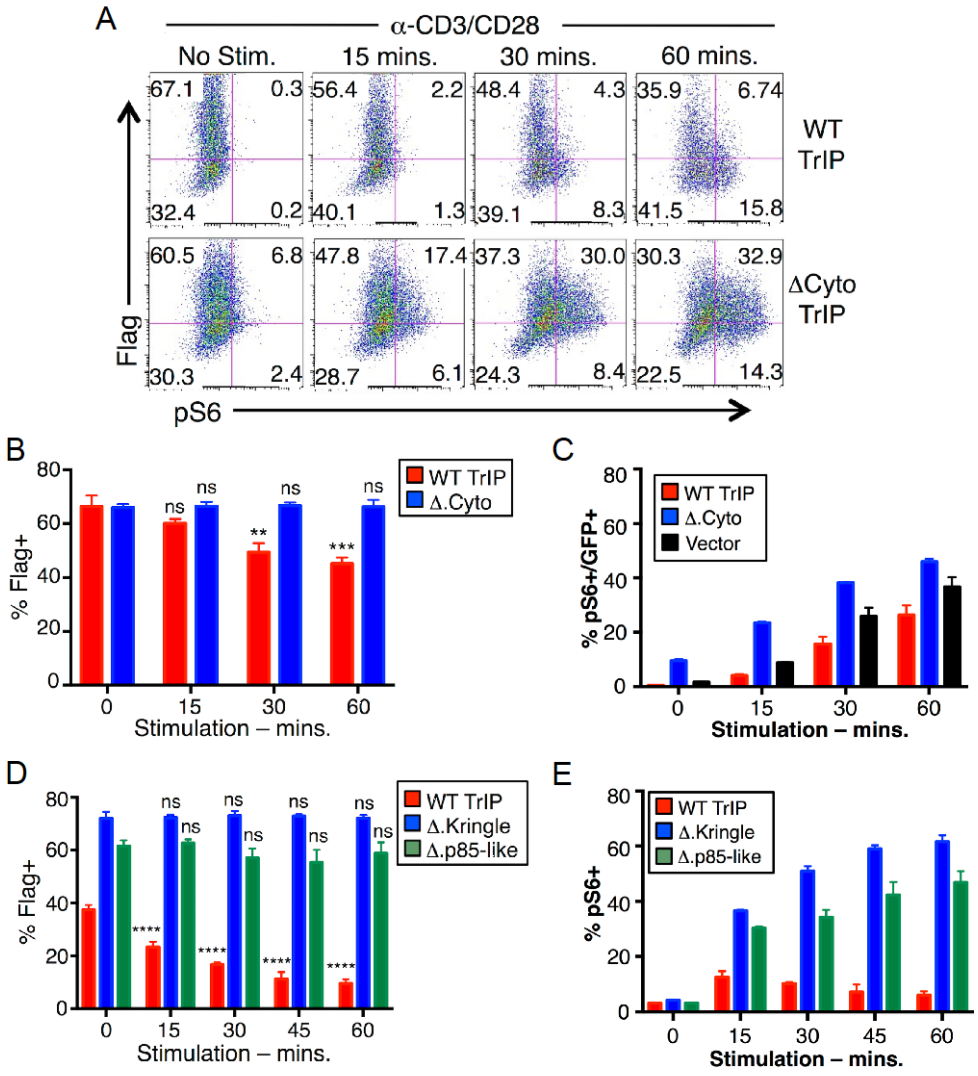

Figure 11 Mediators of TrIP cleavage are expressed on T cells

D10 cells were transfected with control, WT TrIP or Δcyto-TrIP and stimulated with anti-CD3/CD28. (**A**) Representative flow cytometric analysis of Flag-tagged TrIP and pS6 expression of cells transfected with WT TrIP (top row) or Δcyto-TrIP (bottom row). (**B**) Quantitation of Flag expression over the course of stimulation. *p* values (compared to time 0) were calculated using two-way ANOVA with Holm-Sidak's multiple comparisons test. (**C**) Corresponding pS6 data for Flag-TrIP staining in panel (B). (**D**) TrIP surface expression and (**E**) pS6 staining of cells expressing WT, Dkringle or Dp85-like TrIP, after stimulation with anti-CD3/CD28, as in panels A-C. *p* values (compared to time 0) were calculated using one-way ANOVA with Dunnett's multiple comparisons test.

4.4 DISCUSSION

In these studies, the inhibitory activity of TrIP was inversely correlated with surface expression of the protein, as I only observed significant upregulation of pS6 when TrIP expression had been mostly down-regulated, suggesting that this down-regulation is required for efficient signaling immediately following TCR activation. While the mechanisms behind this down-regulation have not been full elucidated here, I present evidence that ADAM family metallopreoteases are required for the loss of cell-surface TrIP after T cell activation. There is also precedent for acute down-regulation of other immune checkpoint molecules. For example, Lag3 and Tim-3 can be inducibly cleaved from the cell surface by metalloproteases, resulting in enhanced T cell activation [127, 133], while PTEN, an intracellular inhibitor of the PI3K pathway, is down-regulated by multiple mechanisms, including post-translational modification and degradation [128]. Thus, while I have implicated ADAM family proteases in TrIP down-regulation, I cannot rule out roles for additional mechanisms.

As previously mentioned, kringle domains in other proteins can serve regulatory functions, including acting as sites for protein-protein interactions [105, 134-136]. Further supporting my hypothesis that the kringle domain modulates the activity of TrIP, substitution of the kringle domain with the extracellular region of hCD8, and subsequent crosslinking by α-CD8, led to diminished induction of pS6 and NFAT after TCR stimulation. I show that cell-surface TrIP expression is down-regulated during the course of TCR stimulation, even in the absence of APCs, and only occurs with WT TrIP and not the truncated variants, leading me to conclude that one or more ligands that activates TrIP inhibitory activity is present on T cells. How binding of a ligand, expressed by either an APC or the T cell itself, might regulate TrIP function is not clear at this point. One possibility is that the kringle domain is required for recruitment of TrIP into proximity

of the TCR and/or CD28 during synapse formation. Another possible mechanism for which I did obtain evidence is that TrIP may undergo homotypic oligomerization, which itself could alter TrIP localization and/or activity.

5.0 THE P85-LIKE DOMAIN OF TRIP INTERACTS WITH P110δ PI3K

5.1 INTRODUCTION

My data up till this point suggests that the kringle domain and p85-like domains are important for TrIP function. Experiments earlier on (Fig 6) showed that in the absence of either the kringle or the p85-like domains in overexpressed TrIP, T cell signaling was rescued compared to when WT TrIP is overexpressed. Results from T cell-APC conjugation experiments highlighted the possibility of regulatory mechanisms whereby TrIP is cleaved extracellularly, thereby removing the kringle domain to allow the progression of signaling. These experiments have led to the discovery that the kringle domain facilitates TrIP oligomerization and this oligomerization appears to be essential for TrIP function (Fig 9). Interestingly, my data also showed that in the absence of the p85-like domain but with the kringle domain still expressed, the Δp85-TrIP does not lose flag expression. Suggesting that both domains function cooperatively in the inhibition of TrIP.

This has led me to speculate that oligomerization facilitates an increase in affinity/avidity for PI3K p110 by TrIP, via the p85-like domain located in the cytoplasmic region. The interSH2 domain of p85 is necessary for p85 to bind with p110 [137, 138]. Previous work by the DeFrances lab showed that TrIP indeed interacts with p110α in MEFs and in *in vitro* binding assays, p110α did not associate with a TrIP mutant lacking the p85-like domain [91]. Since the prevalent catalytic

subunit of PI3K in T cells is p110δ, I sought to understand if TrIP associates with p110δ in a similar fashion as observed by Zhu et al. with p110α [91].

5.2 MATERIALS AND METHODS

Cell lines, transfections and activation. For p110δ interaction assays, flag-tagged TrIP variants and HA-tagged p110δ were transfected into HEK293 cells using TransIT-LT1 (Mirus) according to the manufacturer's protocol. Cells were evaluated by western blot for expression using Roche anti-HA (clone 12CA5; #11-583-816-001) and BioLegend Direct-Blot HRP anti-DYKDDDDK (Clone L5; #637311).

Western blotting analysis and immunoprecipitations. Cells were lysed in ice-cold NP-40 lysis buffer (1% NP-40, 1 mM EDTA, 20 mM tris-HCL pH 7.4), 150 mM NaCl) for both protein analysis and immunoprecipitation. Immunoprecipitation was performed by mixing lysate with 20 µl of M2 anti-Flag agarose beads for 3 hrs at 4^{o} C. Proteins were eluted from beads by mixing Lysate with 1X SDS (containing 5% β-mercaptoethanol) and boiling at 95 deg. C for 10 mins. For western blot analysis, proteins were resolved by 10% SDS-polyacrylamide gel electrophoresis and were transferred onto polyvinylidene difluoride membranes which were then blocked in 4% BSA. The membranes were then incubated with the primary antibodies overnight. This was followed by incubating the membrane with HRP-conjugated secondary antibodies for 2 hours before detection with the SuperSignal West Pico ECL substrate (Thermo Fisher Scientific) and imaging on a Protein Simple FluorChem M.

Western blot and CoIP reagents: Anti-HA (12CA5) (Roche #11-583-816-001); anti-Flag M2 Affinity Gel (Sigma #A2220); direct-Blot HRP anti-DYKDDDDK (Clone L5; BioLegend #637311).

5.3 RESULTS

5.3.1 The p85-like domain of TrIP interacts with p110δ PI3K

TrIP has been shown to interact with the PI3K catalytic subunits p110α/β in mouse embryonic fibroblast (MEF) cells, via a 'p85-like' domain with approximately 80% homology to the inter-SH2 domain of the PI3K regulatory subunit p85 [91]. However, it is not known whether TrIP can also interact with p110δ, which is the main catalytic subunit of PI3K activated by TCR signaling [139]. To test a possible interaction of p110δ with the p85-like domain of TrIP, I transiently transfected 293 cells with Flag-tagged WT TrIP or Δp85-TrIP, along with HA-tagged p110δ, and performed co-IP and western blot analysis (**Fig. 12, top panel**). Thus, WT TrIP could co-IP p110δ-PI3K; however, there was a significant reduction in the ability of Δp85-TrIP to co-IP p110δ (**Fig. 12 top panel, last lane**). These results are consistent with a previous report that examined the interaction of TrIP with other p110 isoforms in fibroblasts [91], and suggest that TrIP may inhibit T cell activation through effects on p110δ.

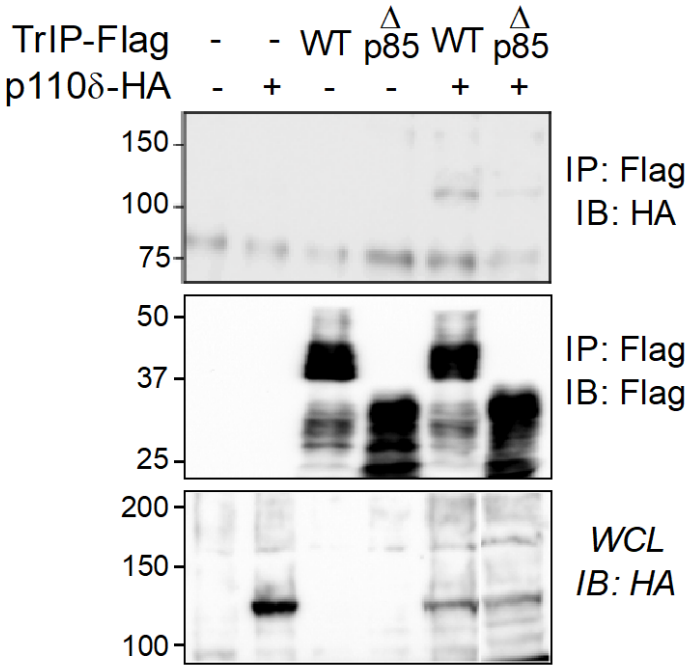

Figure 12 TrIP interacts with p110δ via the p85-like domain

The cytoplasmic p85-like domain of TrIP binds to p110δ. 293 cells were transiently transfected with Flag-tagged WT TrIP and p85Δ-TrIP along with HA-tagged p110δ, as indicated. Top: co-immunoprecipitation and western blot analysis of TrIP and p110δ; Middle: IP fractions showing IP'd Flag-tagged (TrIP) protein; Bottom: whole cell lysate (WCL) showing HA-tagged (p110δ) protein expression.

5.4 DISCUSSION

Confirming the findings of Zhu et al., I show here that TrIP can co-IP the p110δ protein, which is the dominant isoform of PI3K regulating T cell activation [140]. With this evidence and the data in Chapter 4, I can further speculate that binding of a ligand, expressed by either an APC or the T cell itself, may cause a conformational change in TrIP which promotes the binding, and inactivation, of PI3K. My operative model is that binding of TrIP interferes with the allosteric activation of p110 by p85. Although I cannot rule out the possibility that TrIP might regulate p110

stability, the kinetics with which PI3K activation recovers after TrIP downregulation suggest that this is not the dominant mechanism. Yet another possible mechanism underlying TrIP function is through effects on the subcellular localization of p110, which could impact the accessibility of p110 to either upstream activators or substrates. Although the precise mechanism by which PI3K is activated in the immune synapse have been controversial [141], such a mechanism for TrIP function could result in decreased recruitment of PI3K to CD28 and/or the TCR/CD3 complex (see model in **Fig. 13**).

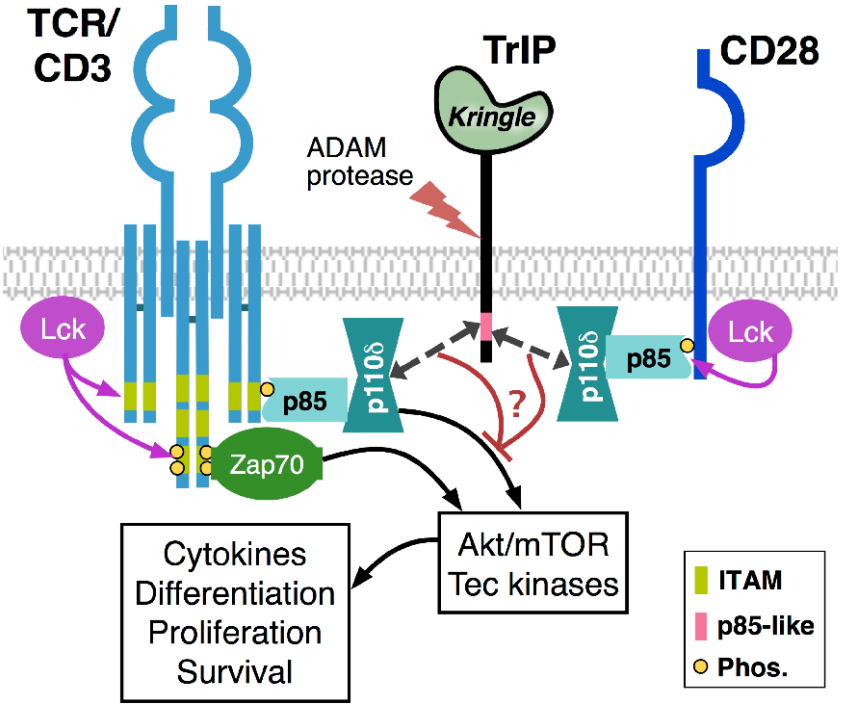

Figure 13 Model for the regulation and function of TrIP during T cell activation

6.0 DELETION OF TRIP ON PRIMARY T CELLS LEADS TO DYSREGULATION OF T CELL ACTIVATION

6.1 INTRODUCTION

While cell lines provided us with the convenient basis to evaluate how the structure of TrIP relates to its function, it was important to also ascertain the physiological relevance of TrIP in the context of a T cell. Mouse models have proven to be especially relevant to PI3K studies as most knockout models of the pathway exhibit phenotypes that are similar to clinical manifestations observed in patients. For example, mice lacking PTEN or expressing mutant forms of p85 that lack the ability to bind p110 display hyperactive T cell phenotypes are characterized by premature death due to T cell lymphomas, autoreactivity and enhanced secretion of T effector cytokines [71]. Most of these phenotypes are replicated in patients with primary immunodeficiencies such as APDS [58].

In order to assess the function of TrIP in T cells *in vivo*, we generated mice with LoxP-flanked (floxed) *Pik3ip1* alleles (Pik3ip1$^{fl/fl}$) and bred them to mice with a CD4-driven Cre recombinase transgene. Mice with CD4-Cre alone were used as controls. After confirming our breeding strategy had yielded the desired genotype, we compared tissue compartments (such as the thymus and spleen) from KO mice (CD4-Cre Pik3ip1$^{fl/fl}$) to those from control mice (CD4-Cre x *Pik3ip1*$^{wt/wt}$) to see what effects loss of TrIP may have on T cell development.

6.2 MATERIALS AND METHODS

Mice. Mice with a floxed *Pik3ip1* gene (Pik3ip1$^{fl/fl}$) were generated by inGenious Targeting Laboratory Inc., using C57BL/6 ES cells. CD4-Cre mice on a C57BL/6 background were originally purchased from Taconic (previously back-crossed for >9 generations to C57BL/6), then maintained by breeding to C57BL/6J mice (Jackson), and were used as WT controls. All control animals were either littermates of KO mice or derived from in-house breeding in the same facility and room. Mice were age-matched within experiments, with approximately equal numbers of male and female animals. Animals were maintained in facilities of the University of Pittsburgh Division of Laboratory Animal Resources. All animal studies were performed in accordance with University of Pittsburgh Institutional Animal Care and Use Committee procedures.

qPCR. RNA was extracted using the Qiagen RNeasy Mini Kit (#74106) and reverse-transcribed to generate cDNA with the Applied Biosystems High Capacity cDNA Reverse Transcription Kit (#4368813). Quantitative real-time polymerase chain reaction assays were performed with Power SYBR Green PCR Master Mix (Applied Biosystems #4367659) on a Step-One Plus Real Time PCR system. The abundance of TrIP mRNA was normalized to that of mGAPDH as calculated with the $2^{-\Delta\Delta CT}$ method. The following primers were used: forward: 5'-ATGCTGTTGGCTTTGGGTACAC-3'; reverse: 5'-CGGCAGTAGTTGTGGTTGC-3'.

T cell activation. Splenocytes and lymphocytes obtained from WT and conditional TrIP KO mice were stimulated in complete RPMI with 3 μg/ml biotinylated anti-CD3 and anti-CD28 in the presence of 15 μg/ml streptavidin (anti-mCD3ε biotin, clone 145-2C11, Tonbo Biosciences #30-

0031-U500; anti-mCD28 biotin, clone 37.51, BD Biosciences #553296; streptavidin, MilliporeSigma #189730). Cells were activated for 15, 30 or 60 mins or 4 hrs. Activation was stopped with 1 ml of cold PBS, followed by centrifugation, aspiration of media and lysis or fixation.

The following antibodies and dyes were used for flow cytometry: Anti-mCD4 Brilliant Violet 510 (clone GK1.5; BioLegend #100449); anti-mCD8α v450 (clone 53-6.7; Tonbo Biosciences #75-0081-U100); anti-pS6 (S235/236) Alexa Fluor 647 (clone D57.2.2E; Cell Signaling #5316S); anti-mCD69 FITC (clone H1.2F3; BD Biosciences #557392); Ghost Dye Red 780 (Tonbo Biosciences #13-0865-T100).

Flow cytometry. Before staining, cells were washed in staining buffer (1% Bovine Growth Serum-supplemented PBS). For extracellular staining, cells were stained at 4˚C with antibodies re-suspended in staining buffer. For intracellular staining, cells were washed three times to remove excess extracellular staining and then fixed and permeablized with the BD Biosciences cytofix/perm kit (#554714) for cytosol analysis. Fixed and permeablized cells were then stained at 4˚C with antibodies re-suspended in permeablization buffer from the kit.

Imaging flow cytometry. For FoxO1 assays, splenocytes from WT and conditional TrIP KO mice were stimulated as described in "T cell activation**"** (above) for the listed time points. Activation was stopped with 1 ml of cold PBS, followed by centrifugation, aspiration of media, staining and fixation.

For extracellular staining, cells were stained with staining buffer (1% Bovine Growth Serum-supplemented PBS) using the following antibodies: anti-mCD4 PE-Cyanine7 (clone GK

1.5; Tonbo Biosciences #60-0041-U100). For intracellular staining, cells were washed three times to remove excess extracellular staining and then fixed and permeablized with the eBioscience Foxp3/Transcription factor staining buffer set (#00-5523-00). Fixed and permeablized cells were then stained at 4˚C with antibodies re-suspended in permeablization buffer from the same eBioscience Foxp3/Transcription factor staining kit. The following intracellular stains were used: FoxO1 (C29H4) Rabbit mAb (Cell Signaling #2880S) with Alexa Fluor 594 donkey anti-rabbit IgG (clone: Poly4064; Cat#406418) as a secondary stain. DAPI dilactate (Molecular Probes Ref#D3571) was used for DNA/nuclear staining.

Imaging cytometry data on fixed and stained cells were acquired on an Amnis ImageStreamX Mark II running INSPIRE® software (Millipore). Analysis was performed using IDEAS® software (Millipore). First, focused cells, based on the gradient root mean square feature, were identified. Singlets were identified by the aspect ratio and area of bright field data. In analyzing primary T cell data, we gated on CD4 T cells via the intensity of that channel. A nucleus intensity mask was made from DAPI staining. This mask was used to determine FoxO1 intensity in the nucleus. A gate of low FoxO1 nuclear signal was then set based on the unstimulated control samples. Approximately 1000 cells are represented in the summary histograms and bar graphs of primary cells. The typical spread of the data is illustrated by the histograms in Fig. 15G.

Western blotting analysis. Cells were lysed in ice-cold NP-40 lysis buffer (1% NP-40, 1 mM EDTA, 20 mM tris-HCL pH 7.4), 150 mM NaCl) for protein analysis. For western blot analysis, proteins were resolved by 10% SDS-polyacrylamide gel electrophoresis and were transferred onto polyvinylidene difluoride membranes which were then blocked in 4% BSA. The membranes were then incubated with the primary antibodies overnight. This was followed by incubating the

membrane with HRP-conjugated secondary antibodies for 2 hours before detection with the SuperSignal West Pico ECL substrate (Thermo Fisher Scientific) and imaging on a Protein Simple FluorChem M.

6.3 RESULTS

6.3.1 No obvious T cell developmental defects in TrIP KO mice

In the absence of a suitable TrIP antibody, T cells from spleen and lymph nodes of naïve homozygous (CD4-Cre x *Pik3ip1*$^{fl/fl}$) and heterozygous (CD4-Cre x *Pik3ip1*$^{fl/wt}$) TrIP conditional knockout mice were screened by RT-PCR for TrIP mRNA expression and compared to wild type mice (CD4-Cre x *Pik3ip1*$^{wt/wt}$) (**Fig. 14A**). Analysis of thymus and spleen from these mice showed similar percentages of CD4 and CD8 T cells in all compartments as well as normal numbers of nTreg (Foxp3^{+}CD25^{+}), suggesting that T cell development was largely normal (**Fig. 14B-C**). Although we did not note any obvious signs of widespread basal inflammation, we assessed more directly whether deletion of TrIP might result in spontaneous activation of peripheral T cells, by staining for the early activation markers CD69 and CD25. As shown in **Figure 14D**, these markers were expressed at equivalent, minimal, levels in TrIP-deficient vs. WT T cells. Thus, T cell-specific deletion of TrIP does not grossly affect T cell development or homeostasis.

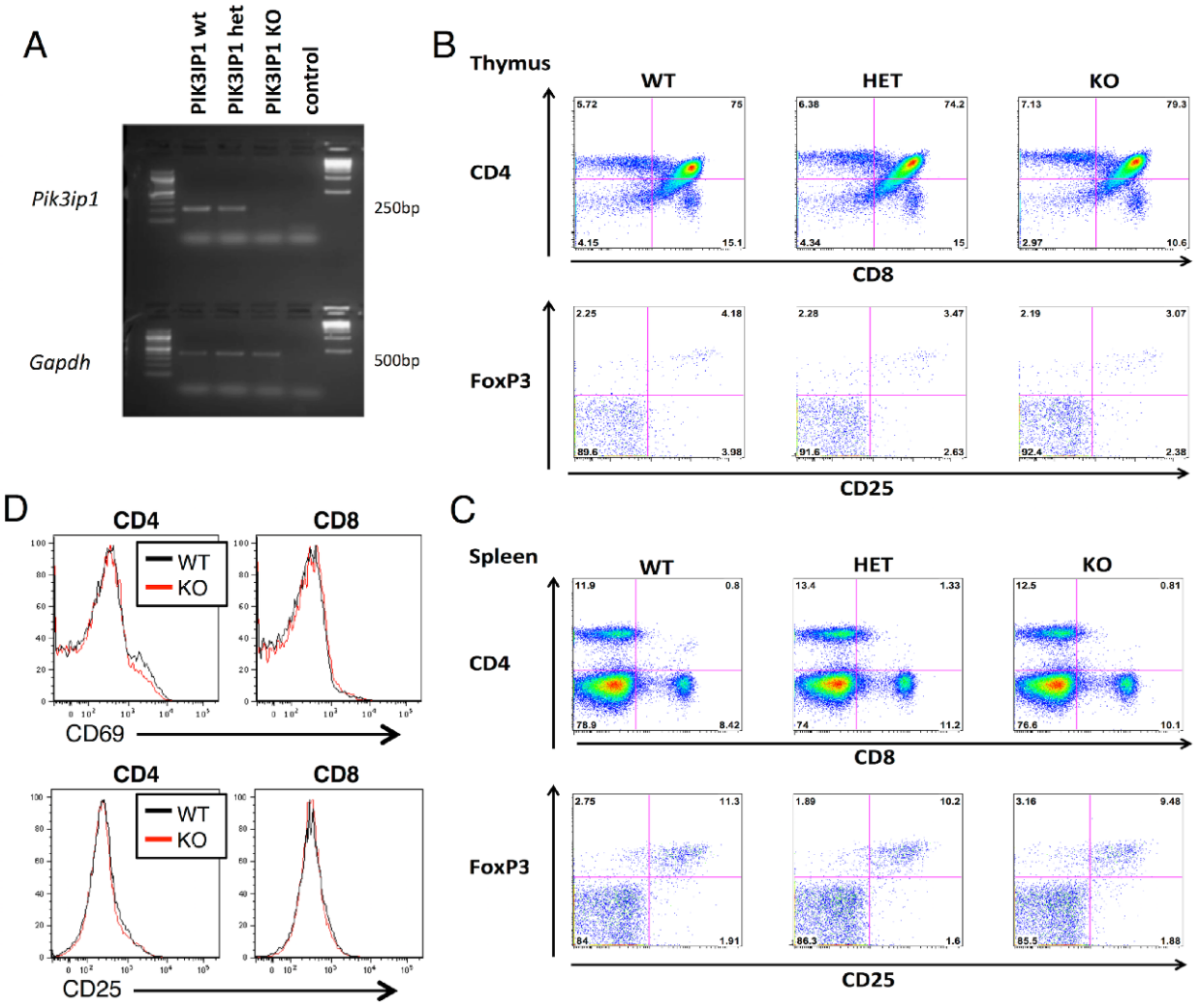

Figure 14 No obvious T cell development defects in CD4-cre conditional TrIP KO mice

A) After confirmation of CD4-Cre and *Pik3ip1* flox by tail snip genotyping, spleen and lymph node cells from naïve mice of indicated genotypes were screened by RT-PCR for the presence of *Pik3ip1* mRNA. B) Characterization of thymocytes and (C) splenocytes from WT, HET and KO mice. (D) Steady-state levels of CD69 (top panels) and CD25 (bottom panels) on splenic CD4+ and CD8+ T cells.

6.3.2 Enhanced T cell activation in the absence of TrIP

Based on data shown in the preceding chapters and previously published findings [91, 95], we predicted that deleting TrIP in primary T cells would lead to enhanced TCR signaling, especially through the PI3K/Akt pathway. We thus stimulated lymphocytes from wild type (WT) and conditionally-deleted TrIP (KO) age-matched mice with α-CD3/CD28 for varying times and evaluated early T cell activation by pS6 and CD69 expression. Following stimulation, TrIP KO T cells showed significantly higher pS6 at later time points (1-4 hrs.) (**Fig. 15A-B**; representative histograms in **Fig. 15C**) These data are consistent with our observation of more robust Akt phosphorylation at T308 and especially S473 in peripheral T cells lacking TrIP (**Fig. 15D-E**). As with ectopic expression of TrIP in D10 T cell (**Fig. 5 F-G**), we measured the effect that deletion of TrIP would have on nuclear exclusion of FoxO1, a direct target of Akt phosphorylation. Using imaging flow cytometry, we noted that even resting, unstimulated, TrIP KO T cells displayed a significant reduction in nuclear FoxO1, compared to WT T cells (**Fig. 15F-G**). Furthermore, while WT T cells displayed a loss of nuclear FoxO1 after anti-CD3/CD28 stimulation, TrIP KO T cells exhibited an even more rapid exclusion of FoxO1 from the nucleus, with an accompanying decrease in total FoxO1 staining, consistent with the lower stability of cytoplasmic FoxO1 [117]. Taken together, these results demonstrate that the loss of TrIP in primary T cells promotes more efficient TCR signaling and early T cell activation, especially through the PI3K/Akt/mTOR signaling pathway.

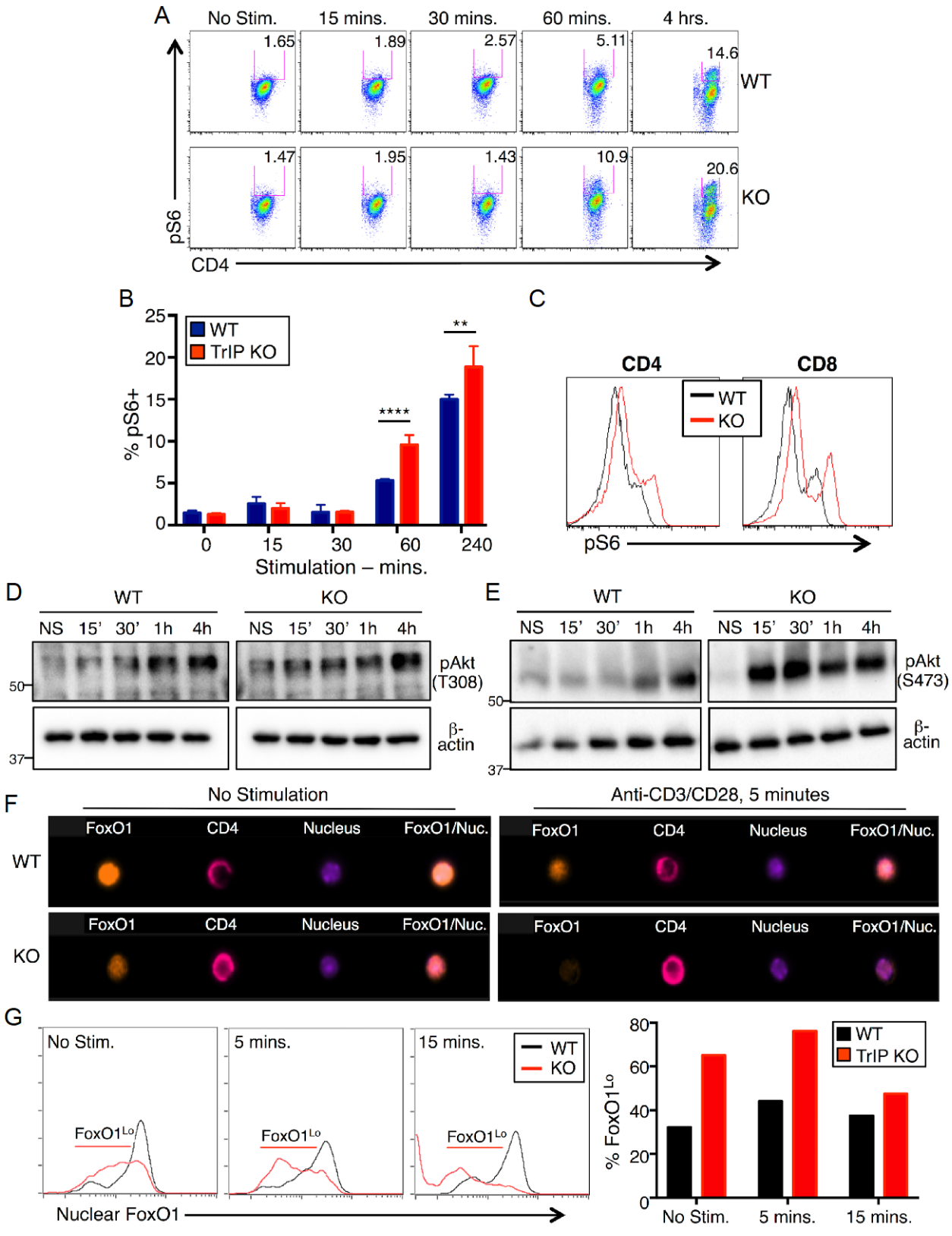
A
No Stim.
15 mins.
30 mins.
60 mins.
4 hrs.
1.65
1.89
2.57
5.11
14.6
WT
1.47
1.95
1.43
10.9
20.6
KO
pS6
CD4
B
WT
TrIP KO
% pS6+
****
**
Stimulation – mins.
C
CD4
CD8
WT
KO
pS6
D
WT
KO
NS 15' 30' 1h 4h
pAkt (T308)
β-actin
E
pAkt (S473)
F
No Stimulation
Anti-CD3/CD28, 5 minutes
FoxO1
CD4
Nucleus
FoxO1/Nuc.
G
No Stim.
5 mins.
15 mins.
FoxO1Lo
Nuclear FoxO1
% FoxO1Lo

Figure 15 Enhanced pAkt and pS6 activation in TrIP-deficient T cells

Splenocytes and lymphocytes were isolated from WT and KO mice and stimulated with anti-CD3/CD28 for the indicated times. (**A**) Flow cytometric analysis of pS6 expression on stimulated $CD4^+$ T cells. (**B**) Quantitation of data shown in panel A. (**C**) Representative histograms of pS6 data corresponding to the four-hour stimulation time point in panel A-B. CD8 data included to show similarity in activation. (**D-E**) T cells were purified from spleen and lymph nodes of WT or TrIP KO mice and stimulated with anti-CD3/CD28 antibodies for the indicated times. Lysates were analyzed by western blot for phospho-Akt (T308-left; S473-right) and β-actin as a loading control. *p* values were calculated using two-way ANOVA with Sidak's multiple comparisons test. *p* values are represented with the following symbols: *0.01-0.05, **0.001-0.01, ***<0.001. Data in panels A-B & D-E are representative of three experiments each. (**F-G**) WT and TrIP KO CD4+ T cells were analyzed for nuclear FoxO1 staining by imaging cytometry. (**F**) Representative images showing FoxO1, CD4 and nuclear (DAPI) staining of resting and stimulated T cells. The yellow scale bar represents 10 μM. (**G**) Left – histograms displaying the magnitude of nuclear FoxO1 in WT vs. TrIP KO T cells, before and after anti-CD3/CD28 stimulation; right – graphical representation of the percentage of cells falling in the nuclear $FoxO1^{Lo}$ gate from the left histograms. Data in panel G represent approximately 1000 CD4+ T cells per condition, from a single experiment, representative of two that were performed.

6.4 DISCUSSION

To probe the function of TrIP in primary T cells, we generated an inducible knockout model which we crossed to CD4-Cre transgenic mice, to delete TrIP in all α/β T cells. T cells from these mice did not exhibit any developmental defects. CD4 and CD8 percentages in the thymus were similar in WT and KO mice. Though we observed a slight difference in Treg numbers, not enough mice were evaluated to make this observation significant. A similar trend was observed in the spleen where single positive CD4 and CD8 percentages were quite similar between the genotypes. Though there were no obvious developmental defects or spontaneous inflammation in TrIP KO mice, this does not rule out the possibility that TrIP may play a role in TCR repertoire selection or T cell homeostasis.

Ex vivo, T cells from these animals did not show upregulation of early activation markers like CD69 or CD25 prior to stimulation. However, KO T cells were hyper-sensitive to stimulation

through the TCR and validated my finding that S6 phosphorylation and FoxO1 exit from the nucleus are relevant downstream readouts for monitoring TrIP activity. The sum of the differences between WT and KO T cells in pAkt, pS6 and FoxO1 nuclear content strongly support previous observation of the physiological relevance of TrIP [94, 142].

7.0 DELETION OF TRIP ENHANCES TH1 CELL INDUCTION AND INHIBITS TREG INDUCTION

7.1 INTRODUCTION

Previous research suggested that higher PI3K signaling may lead to enhanced Th1 potential, while lower levels of PI3K would favor generation of iTreg [94, 143]. Based on my findings, I reasoned that T cell polarization towards a pro-inflammatory phenotype would be enhanced in TrIP KO T cells. To test this theory, I used well established Th differentiation protocols [144-148] and focused on the effect loss of TrIP would have on subsets likely to be involved in an inflammatory response (Th1, Tregs and perhaps Th17).

In order to confirm that any changes observed were due to loss of TrIP regulation of the PI3K pathway, I also carried out Th differentiation in the presence of established PI3K pathway inhibitors of varying substrate specificity. Thereby enabling targeting of the pathway at different stages. During differentiation I used the following inhibitors: the isoform specific PI3Kδ inhibitor, IC87114, to block the predominant p110 catalytic unit in T cells; Akt1/2 kinase inhibitor to obstruct Akt phosphorylation which occurs somewhat early on in the pathway, LY294002 the pan-PI3K inhibitor.

7.2 MATERIALS AND METHODS

Mice. Mice with a floxed *Pik3ip1* gene (Pik3ip1$^{fl/fl}$) were generated by inGenious Targeting Laboratory Inc., using C57BL/6 ES cells. CD4-Cre mice on a C57BL/6 background were originally purchased from Taconic (previously back-crossed for >9 generations to C57BL/6), then maintained by breeding to C57BL/6J mice (Jackson), and were used as WT controls. All control animals were either littermates of KO mice or derived from in-house breeding in the same facility and room. Mice were age-matched within experiments, with approximately equal numbers of male and female animals. Animals were maintained in facilities of the University of Pittsburgh Division of Laboratory Animal Resources. All animal studies were performed in accordance with University of Pittsburgh Institutional Animal Care and Use Committee procedures.

T cell purification and differentiation. Total or CD4+ α/β T cells from spleens and lymph nodes of naïve mice were purified by magnetic separation using T cell isolation kits from Miltenyi Biotec. The purity of the final cell population was >90%. T cells were activated with plate-bound anti-CD3 (clone 145-2C11; Bio X Cell InVivoMab BE0001-1), along with soluble anti-CD28 (clone 37.51 eBioscience #14-0281-85), in complete (RPMI medium supplemented with 10% bovine growth serum, 2 mM L-glutamine, 100 U/ml penicillin, 100 µg/ml streptomycin, 50 µM 2-mercaptoethanol, HEPES and sodium pyruvate). For Th1 differentiation, cells were cultured in the presence of recombinant murine IL-12 (10 ng/ml), anti-IL-4 (10 µg/ml) and recombinant human IL-2 (50 U/ml). For Th17 differentiation, cells were cultured in the presence of recombinant hTGF-β (2.5 ng/ml), recombinant mIL-6 (20 ng/ml), plus anti-IFNγ (10 µg/ml), anti-IL-4 (10 µg/ml) and anti-IL-2 (20 µg/ml) neutralizing antibodies. For iTreg differentiation, cells were cultured in the

presence of anti-IL-4 and anti-IFNγ neutralizing antibodies (10 μg each) plus recombinant hTGFβ2 (10 ng/ml) and recombinant hIL-2 (50 U/ml), with varying concentrations of anti-CD3 (0.25μg/ml, 0.5μg/ml, 1.0μg/ml and 5.0μg/ml) and 1μg/ml anti-CD28. Cells were cultured for 3 days under Th differentiation conditions and then stimulated for 4h with PMA (50 ng/ml) and ionomycin (1.33 μM) in the presence of Golgi Plug (BD biosciences #51-2301KZ). Cells were then harvested and analyzed by flow cytometry.

T helper cell differentiation reagents: Murine IL-12 (Miltenyi Biotec #130-096-707); murine IL-6 (Miltenyi Biotec #130-094-065); recombinant hTGF-β (Sigma SRP3170-5UG); anti-mouse IL-4 clone 11B11(Bio X Cell #BE0045); anti-mIL-2 clone S4B6-1 (Bio X Cell #BE0043); anti-mIFN-γ clone XMG1.2 (Bio X Cell #BE0055).

The following antibodies and dyes were used for flow cytometry: anti-mCD4 Brilliant Violet 510 clone GK1.5 (BioLegend #100449); Ghost Dye Red 780 (TONBO biosciences #13-0865-T100); V450-anti-mFoxp3 clone MF23 (BD Horizon #561293); anti-mouse RORγt-PE (clone Q31-378; BD Biosciences #562607); anti-mouse IL-17A PerCP-Cy5.5 (clone eBio17B7; eBioscience 45-7177-80); anti-mFoxp3 APC (clone FJK-16s; eBioscience 17-5773-82); anti-mTbet eFluor 660 (clone eBio4B10; eBioscience 50-5825-82); anti-m IFN-γ PE-Cy7 (clone XMG1.2; Tonbo Biosciences 60-7311-U025); anti-mouse CD25 FITC (clone PC61.5; Tonbo Biosciences 35-0251-U100).

Flow cytometry. Before staining, cells were washed in staining buffer (1% Bovine Growth Serum-supplemented PBS). For extracellular staining, cells were stained at 4˚C with antibodies re-suspended in staining buffer. For intracellular staining, cells were washed three times to remove excess extracellular staining and then fixed and permeablized with the eBioscience

Foxp3/Transcription factor staining buffer set (#00-5523-00) for transcription factor and cytosol analysis. Fixed and permeablized cells were then stained at 4˚C with antibodies re-suspended in permeablization buffer from the kit.

qPCR. RNA was extracted using the Qiagen RNeasy Mini Kit (#74106) and reverse-transcribed to generate cDNA with the Applied Biosystems High Capacity cDNA Reverse Transcription Kit (#4368813). Quantitative real-time polymerase chain reaction assays were performed with Power SYBR Green PCR Master Mix (Applied Biosystems #4367659) on a Step-One Plus Real Time PCR system. The abundance of TrIP mRNA was normalized to that of mGAPDH as calculated with the $2^{-\Delta\Delta CT}$ method. The following primers were used: forward: 5'-ATGCTGTTGGCTTTGGGTACAC-3'; reverse: 5'-CGGCAGTAGTTGTGGTTGC-3'.

7.3 RESULTS

7.3.1 Deletion of TrIP enhances Th1 T cell polarization and inhibits Treg generation

I isolated naïve $CD4^+$ T cells from WT and KO mice and cultured them with α-CD3/CD28 mAbs for three days under neutral (no polarization), Th0 (suppression of all polarization), Th1, Th17 and iTreg skewing conditions. At the end of culture, cells were re-stimulated with PMA/ionomycin for four hours and then evaluated for Th1 (T-bet and IFN-γ), Th17 (RORγt and IL17a) and iTreg (CD25 and Foxp3) phenotype. Thus, we noted a significant increase in the number of cells producing IFN-γ in TrIP KO T cell cultures, compared to WT cells, especially under Th0 and Th1,

and even iTreg, conditions (**Fig. 16A**). Interestingly, we observed a smaller, but reproducible, decrease in the number of TrIP KO T cells making IL-17a, specifically under Th17 polarization conditions (**Fig. 16B**). More strikingly, we found that TrIP-deficient T cells cultured under iTreg-generating conditions were significantly less efficient at producing $Foxp3^{+}CD25^{+}$ iTreg (**Fig. 16C-D**). This result is consistent with previous findings that PI3K/Akt/mTOR signaling suppresses the generation of iTreg [143]. Interestingly, when we assessed the expression of *Pik3ip1* mRNA after culturing under various Th polarization conditions, we found that *Pik3ip1* was severely down-regulated in Th0 and Th1cells. By contrast, *Pik3ip1* was maintained at a somewhat higher level in iTreg, although still not as high as naïve cells (**Fig. 16E**), consistent with an apparent requirement for weaker PI3K signaling in Treg [149].

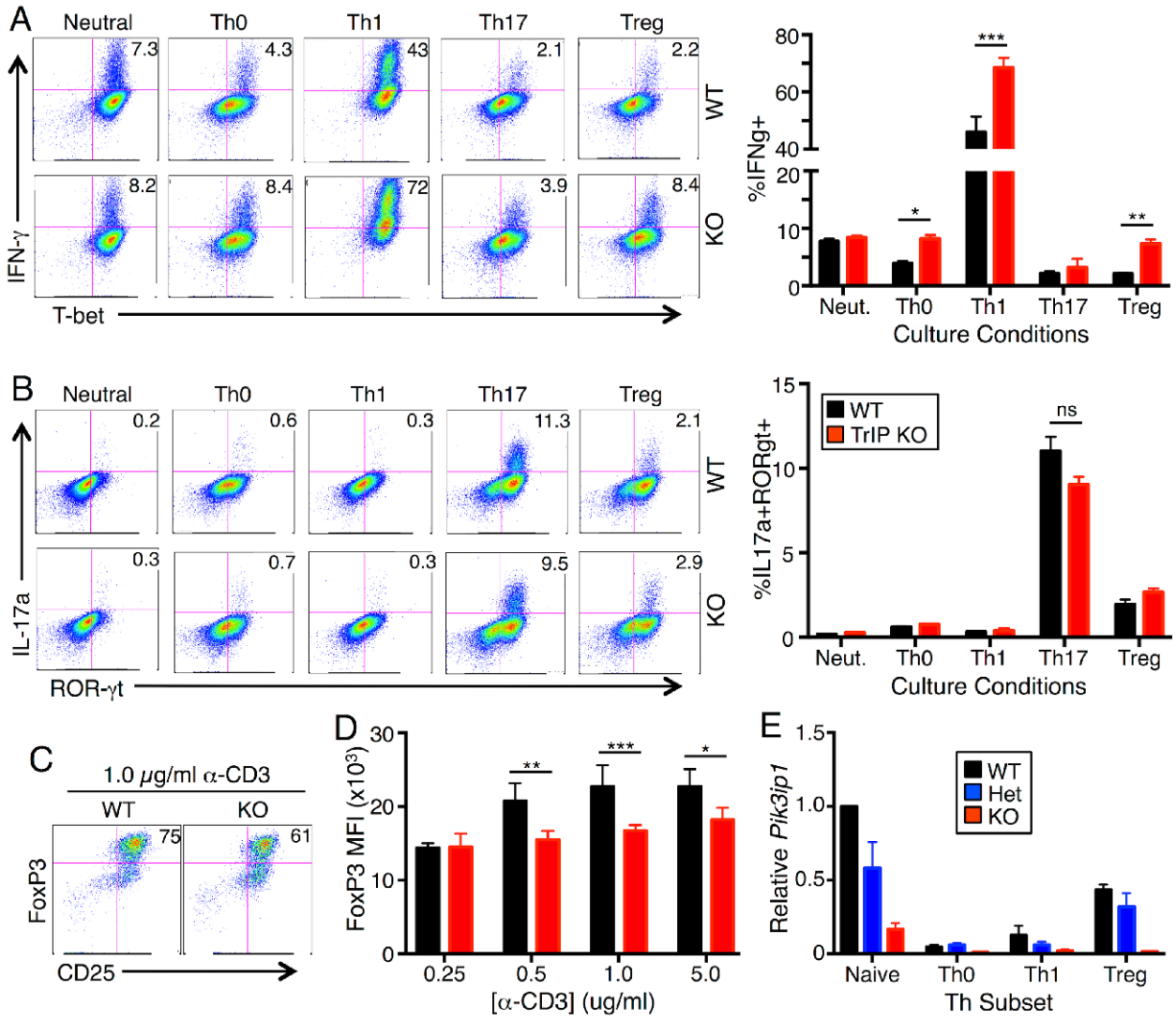

Figure 16 High Th1 and low iTreg differentiation potential in TrIP KO T cells

Naïve T cells from WT and KO mice were cultured under neutral, Th0, Th1, Th17 and iTreg conditions for three days, re-stimulated and analyzed for (**A**) IFNg and T-bet expression, (**B**) IL-17a and RORgt expression, and (**C-D**) Foxp3 and CD25 expression. (**E**) Naïve $CD4^+$ T cells from the indicated mice were stimulated under the indicated conditions and RNA was extracted and analyzed by qPCR for *PIk3ip1* message. Data shown are normalized to naïve WT T cells. *p* values were calculated using two-way ANOVA with Sidak's multiple comparisons test. *p* values are represented with the following symbols: *0.01-0.05, **0.001-0.01, ***<0.001. Data in each panel are representative of at least three experiments.

7.3.2 KO TrIP preference for Th1 polarization is due to enhanced PI3K activity

In order to determine whether the difference in Th1 polarization was actually due to enhanced PI3K activity, we performed the Th1 differentiation assay with the addition of moderate concentrations of PI3K/Akt pathway inhibitors. Specifically, we employed an Akt1/2 inhibitor (Akt*i*-1/2), a pan-PI3K inhibitor (LY294002) and a selective p110δ inhibitor (IC-87114). Cells were stimulated with α-CD3/CD28 as in **Fig. 16** and cultured under Th1 conditions in the presence of varying concentrations of the PI3K inhibitors. At the end of culture, cells were re-stimulated with PMA/Ionomycin and evaluated by flow cytometry for IFN-γ expression. We found that IFN-γ production by KO cells was significantly inhibited by all three inhibitors tested, at concentrations as low as 0.5 μM (**Fig. 17A-B**). Consistent with p110δ being the most prevalent catalytic subunit of PI3K linked to TCR signaling, IC-87114 was the most potent inhibitor at all concentrations. Overall, we observed a reduction of IFN-γ production by both WT and TrIP KO T cells in the presence of inhibitors, but this inhibition was more distinct with the KO cells. These results support the idea that the high IFN-γ production by TrIP KO T cells is due to a loss of TrIP inhibition of PI3K.

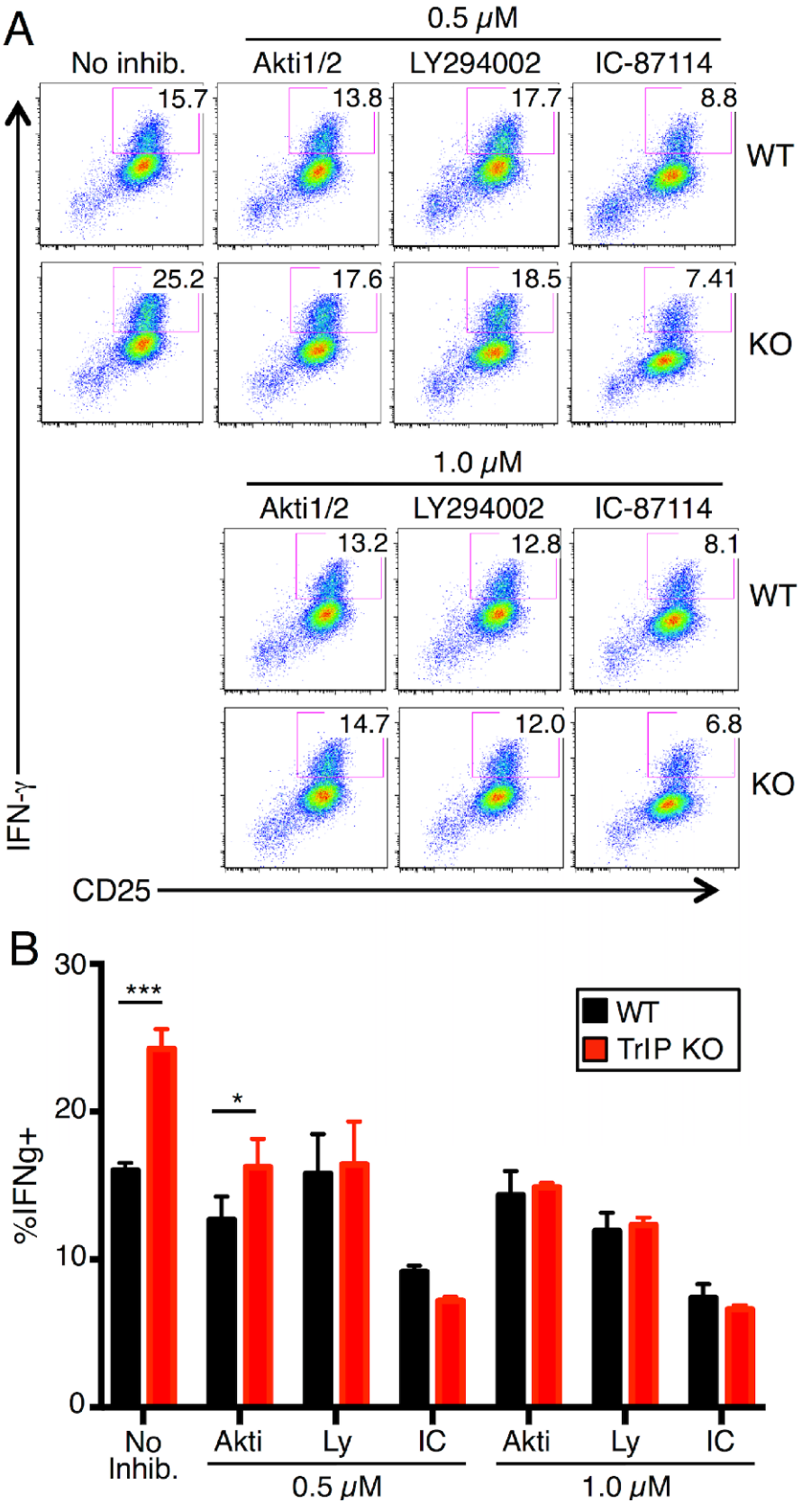
A
0.5 μM
No inhib.
Akti1/2
LY294002
IC-87114
15.7
13.8
17.7
8.8
WT
25.2
17.6
18.5
7.41
KO
1.0 μM
Akti1/2
LY294002
IC-87114
13.2
12.8
8.1
WT
14.7
12.0
6.8
KO
IFN-γ
CD25
B
30
20
10
0
%IFNg+
***
*
WT
TrIP KO
No Inhib.
Akti
Ly
IC
Akti
Ly
IC
0.5 μM
1.0 μM

Figure 17 TrIP KO T cell preference for Th1 polarization is due to enhanced PI3K signaling

(**A**) Naïve T cells from WT and KO mice were cultured under Th1 conditions for three days in the presence of PI3K inhibitors (Akti, LY294002 and IC-87114), re-stimulated with PMA/Ionomycin and analyzed for IFNγ and CD25 expression. (**B**) Quantitation of A. *p* values (comparing WT to KO) were calculated using two-way ANOVA with Sidak's multiple comparisons test. *p* values are represented with the following symbols: *0.01-0.05, **0.001-0.01, ***<0.001. Data in each panel are representative of at least three experiments.

7.4 DISCUSSION

When I differentiated naïve CD4+ T cells from TrIP KO mice, I noted increased production of IFNγ by Th1 cells compared to WT. In fact, across the Th subsets looked at, TrIP KO T cells tended to produce higher amounts of IFNγ (even in Tregs). My use of PI3K pathway inhibitors confirmed that the phenotypes observed here are as a result of unchecked PI3K activity (due to loss of TrIP). While we saw no obvious developmental defects or spontaneous inflammation in mice with T cell-specific TrIP deficiency, these results support the theory that TrIP plays a role in PI3K pathway driven Th subset polarization.

It is curious that Tregs derived from KO mice express higher amounts of IFNγ compared to WT. Even more puzzling is that these mice do generate Tregs, especially since we observe that TrIP is moderately expressed in WT Treg cells. Thus, inferring a role for TrIP in maintenance of multiple Treg subsets [150]. These observations imply that under certain conditions, TrIP can be downregulated in Tregs and that TrIP deficient Tregs are at least functional in the production of inflammatory cytokines. Clues for how such Tregs may arise in a physiological state have come from graft versus host disease transplant studies. While Tregs derived from WT mice prevented disease, those Tregs derived from *Ifnγ*$^{-/-}$ mice did not inhibit GVHD disease progression [151]. In fact, a recent report by Overacre-Delgoffe et al. shows that IFNγ producing Tregs drives loss of

suppressive activity of tumour resident Tregs and creates Treg fragility that can lead to tumour clearance [152]. Future work should evaluate the expression of TrIP in IFNγ producing Tregs in an in vivo setting.

8.0 ENHANCED ACTIVATION AND IN VIVO FUNCTION OF TRIP KO T CELLS

8.1 INTRODUCTION

PI3K dysregulation affects the immune system in terms of response to pathogens, autoimmunity and cancer. While recent research has implicated TrIP as playing a role in tumour suppression [94, 142, 153] no data has been presented on the role of TrIP during infection. Our data shown here strongly supports the theory that high PI3K signaling induces a strong Th1 phenotype and leads to lower Treg induction. This supports the theory that the regulation of PI3K by TrIP could play a role in the immune inflammatory response to certain pathogens.

In responding to invading microbes T cells should undergo activation and rapid proliferation [154]. Thus, I compared early and late activation markers on *in vitro* stimulated WT and KO T cells. I also used the cell proliferation dye eFluor 450 to monitor proliferation of *in vitro* activated cells. We then chose the well established listeria infection model [155] in order to evaluate the *in vivo* functionality of T effector cells from TrIP KO mice.

Listeria monocytogenes is a Gram-positive intracellular bacterial pathogen that causes listeriosis. It is a food-borne human pathogen that can cause severe clinical manifestations such as sepsis and meningitis in immunocompromised individuals, infants, elderly patients and pregnant individuals. It is primarily transmitted via ingestion of contaminated foods whereby the bacterium is able to cross several barriers thereby lodging in the cytosol of cells. In particular, the bacteria

can be found in the spleen and liver of infected hosts as they invade splenic and hapatic macrophages [154]. While the initial response to *L. monocytogenes* infection is via innate immunity [156, 157] early work in the field showed that clearance of an *L. monocytogenes* infection is T cell mediated [158]. Further work has shown that CD8 T cells play a role in eventual clearance and provide long term protective immunity.

Secretion of proinflammatory cytokines such as IFNg and TNFa are important for combating infection of listeria monocytogenes [155, 159, 160]. Early resistance to L. monocytogenes infection has been attributed to CD4 T cells activating macrophages [154]. Based on our data in presented in Figure 15, we therefore hypothesized that our TrIP KO mice would clear the bacteria at a faster rate than the WT mice due to high activation of IFNg potential.

8.2 MATERIALS AND METHODS

Mice. Mice with a floxed *Pik3ip1* gene ($Pik3ip1^{fl/fl}$) were generated by inGenious Targeting Laboratory Inc., using C57BL/6 ES cells. CD4-Cre mice on a C57BL/6 background were originally purchased from Taconic (previously back-crossed for >9 generations to C57BL/6), then maintained by breeding to C57BL/6J mice (Jackson), and were used as WT controls. All control animals were either littermates of KO mice or derived from in-house breeding in the same facility and room. Mice were age-matched within experiments, with approximately equal numbers of male and female animals. Animals were maintained in facilities of the University of Pittsburgh Division of Laboratory Animal Resources. All animal studies were performed in accordance with University of Pittsburgh Institutional Animal Care and Use Committee procedures.

Listeria monocytogenes infection. Control WT (CD4-Cre alone) and Pik3ip1$^{fl/fl}$ x CD4-Cre mice were infected intravenously with 15,000 CFU *L. monocytogenes* in 200µl of PBS. Bacterial titers were quantified by lysing whole livers in PBS, plating of a 1:10 dilution on brain-heart infusion agar plates, and culturing overnight. Cells were stained with the following antibodies and dyes and analyzed by flow cytometry: Ghost Red 780 viability dye (Tonbo Biosciences #13-0865-T100); anti-mCD4 Brilliant Violet 510 (clone GK1.5; BioLegend #100449); anti-mCD8α PE (clone 53-6.7; Tonbo Bioscience 50-0081-U100); anti-mCD62L PerCP-Cy5.5 (clone MEL-14; eBioscience 45-0621-80); anti-mKLRG1 FITC (clone 2F1; Tonbo Biosciences 35-5893-U100); anti-mCD127 PE-Cy7 (clone A7R34; Tonbo Biosciences 60-1271-U025); anti-mCD44 violetFluor 450 (clone IM7; Tonbo Biosciences 75-0441-U025). All Ab staining was performed at 4˚C in PBS containing 1% Bovine Growth Serum and 0.1% sodium azide. GP33 tetramers were provided as APC fluorophore-conjugated tetramers by the NIH tetramer core facility and used for identification of gp33-specific CD8$^+$ and CD4$^+$ T cells.

T cell proliferation. CD4 T cells from spleens of naïve mice were purified by magnetic separation using the Miltenyi Biotec naïve CD4 T cell isolation kit (#130-104-453). The purity of the final cell population was >90%. Prior to activation, T cells were labeled with cell proliferation dye efluor 450 (eBioscience #65-0842) following the manufacturer's protocol. T cells were then activated with plate-bound anti-CD3 (clone 145-2C11; Bio X Cell InVivoMab BE0001-1) in complete RPMI medium (supplemented with 10% bovine growth serum, 2 mM L-glutamine, 100 U/ml penicillin, 100 µg/ml streptomycin, 50 µM 2-mercaptoethanol, HEPES and sodium pyruvate) in the presence or absence of 1 µg/ml anti-CD28 (clone 37.51 eBioscience #14-0281-85). Cells were then cultured for 3 or 5 days before harvesting and analysis by flow cytometry.

Flow cytometry. Before staining, cells were washed in staining buffer (1% Bovine Growth Serum-supplemented PBS). For extracellular staining, cells were stained at 4˚C with antibodies re-suspended in staining buffer. For intracellular staining, cells were washed three times to remove excess extracellular staining and then fixed and permeablized with either the eBioscience Foxp3/Transcription factor staining buffer set (#00-5523-00) or the BD Biosciences cytofix/perm kit (#554714) for transcription factor and cytosol analysis, respectively. Fixed and permeablized cells were then stained at 4˚C with antibodies re-suspended in permeablization buffer from the respective kits.

8.3 RESULTS

8.3.1 TrIP KO T cells upregulate activation markers and proliferate at a higher rate than control.

I returned to the question of how TrIP regulates early T cell activation and whether this translates to downstream effects on proliferation and pathogen clearance. Thus, naïve T cells from $TrIP^{fl/fl}$ x CD4-Cre mice were purified from spleen and lymph node and stimulated with anti-CD3 +/- anti-CD28. One of the earliest cell-surface changes after T cell activation is upregulation of CD69, a sensitive marker of TCR signaling that plays a role in delaying trafficking of nascently activated T cells out of the lymph node [161]. Thus, we noted that TrIP-deficient T cells upregulated CD69 more robustly than did WT T cells (**Fig. 18A**). A somewhat later event is the upregulation of CD25, which is a component of the high-affinity IL-2 receptor. We noted higher expression of CD25 in

TrIP-deficient T cells at both days three and five after stimulation (**Fig. 18B**), specifically on cells stimulated with anti-CD3 alone, which is intriguing because CD25 is a known target of CD28 co-stimulation [162]. Importantly, basal expression of both CD69 and CD25 was identical in naive TrIP KO vs. WT T cells (**Fig. 14D**). I did note a slight, but reproducible, decrease in basal levels of CD62L on naïve CD8+ T cells lacking TrIP, which was eventually normalized over the course of initial T cell activation (**Fig. 18C**). I also collected supernatants from stimulated T cells and measured secretion of IL-2 by ELISA. Thus, I observed significantly more IL-2 production from TrIP-deficient T cells, compared with WT cells, with or without CD28 co-stimulation (**Fig. 18D**).

The PI3K pathway plays a major role in triggering T cell response to antigen via a number of processes, including proliferation. The effects on early activation discussed above, especially the increases in CD25 and IL-2, suggested that TrIP loss might also impact T cell proliferation. Naïve T cells were isolated from WT and KO mice, stained with cell trace violet and cultured on anti-CD3 coated plates in the presence or absence of anti-CD28. Cells were analyzed for proliferation at days three and five after stimulation. I found that at both time points, KO T cells had proliferated to a greater extent than WT T cells, after stimulation with either anti-CD3 alone or anti-CD3/CD28 (**Fig. 18E-F**). These findings further support the model that TrIP restricts T cell activation.

8.3.2 TrIP KO mice are less susceptible to *L. monocytogenes* infection

To explore the role of TrIP function *in vivo,* we infected mice with *Listeria monocytogenes*, a disease model that requires effective $CD8^+$ and Th1 T cell responses for clearance of pathogen and generation of immune memory [154, 163]. We infected mice with a relatively high dose (15,000 CFU) of *L. monocytogenes* , as we hypothesized that TrIP KO mice would be able to clear the

infection more efficiently, based on the *in vitro* data detailed above. Thus, we observed significantly lower bacterial load from the livers of TrIP KO mice, compared to WT mice, at day four after infection (**Fig. 18G**). Thus, the enhanced sensitivity of TrIP KO T cells described above does indeed translate to more robust *in vivo* activity of these cells in response to an intracellular bacterial infection.

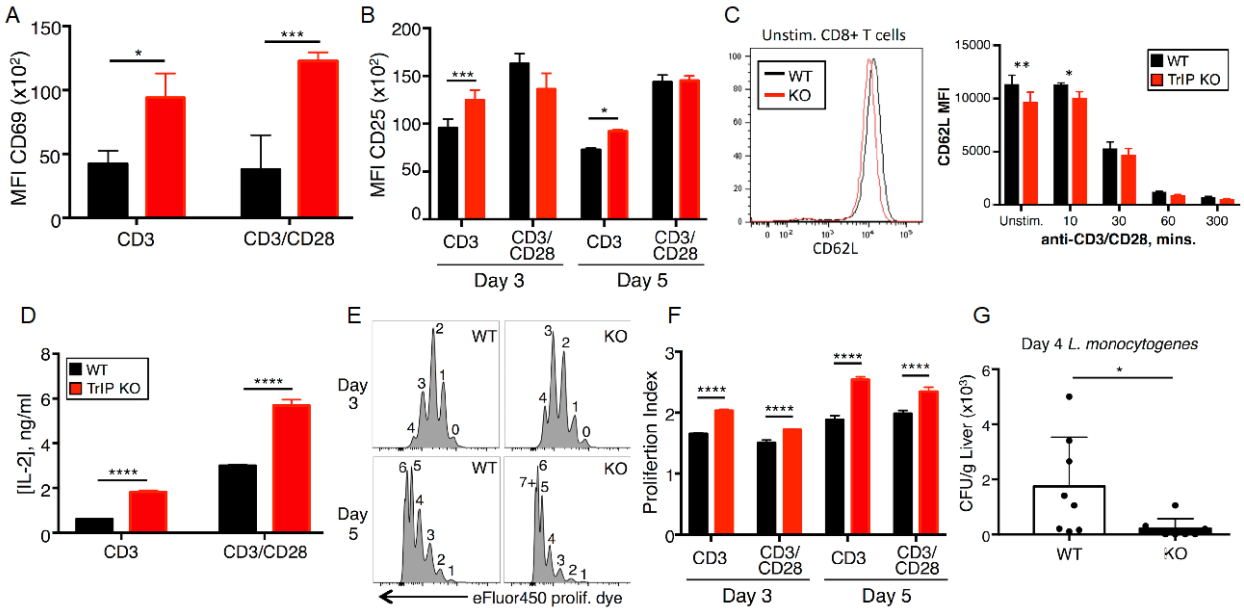

Figure 18 TrIP KO T cells display increased proliferation and activation and T cell specific TrIP KO mice are less susceptible to L. monocytogenes infection

(**A-B**) WT or TrIP naïve T cells were stimulated as indicated for 24 hours (A) or 3-5 days (B), then analyzed by flow cytometry for expression of CD69 (A) or CD25 (B). (**C**) Steady-state and stimulation-dependent CD62L expression on splenic CD8+ T cells. (**D**) WT or TrIP KO T cells were stimulated for three days and supernatants were analyzed by ELISA for IL-2. (**E-F**) WT or TrIP KO CD8+ T cells were labeled with eFluor450 cell proliferation dye and stimulated with anti-CD3 +/- anti-CD28 mAb for the indicated times. Representative flow cytometry histograms for anti-CD3 stimulation are shown in panel E. Compiled data from triplicate wells are shown in panel F**.** (**G**) Liver extracts from WT (CD4-Cre only) and TrIP KO mice infected with *L. monocytogenes* were obtained four days after infection and plated to measure bacterial burden. *p* values in panels A-D and F (WT vs. KO) were calculated using two-way ANOVA with Sidak's multiple comparisons test; in panel G, a two-tailed unpaired t test was used. *p* values are represented with the following symbols: *0.01-0.05, **0.001-0.01, ***<0.001.

8.4 DISCUSSION

The high PI3K activity, induction of early activation markers as well as the tendency of the TrIP KO T cells to differentiate into pro-inflammatory Th1 cells suggested that these cells would be readily activated for response to an infection. Adhesion molecules such as CD62L are constitutively expressed on naïve cells and allow these cells to migrate into secondary lymphoid organs [164, 165]. Upon immune activation, CD62L is rapidly downregulated in order for the now, T effector cells, to home to sites of inflammation [166]. CD62L expression has been shown to be subject to PI3K signaling in two ways. First, shedding of CD62L occurs via cleavage which begins after TCR activation [167, 168]. The factors that govern cleavage, such as ADAM 17 are controlled by PI3K activity [169]. Secondly, KLF2, the transcription factor that regulates CD62L expression, is downregulated upon TCR activation (also via the PI3K pathway) [169]. Thus, my observation that CD62L exhibited a lower degree of expression, at the naïve state suggests that the TrIP KO T cells are "poised" for activity when compared to the WT T cells. The high rate of proliferation observed in vitro supports this theory.

Previous work by others has shown that *L. monocytogenes* replicates for three days after infection of mice [170]. Here we observed that by day four, TrIP knockout mice had cleared the infection, compared to wild type mice that still had significant bacterial burden. Based on the typical immune response to *L. monocytogenes* infection [154, 170], clearance of bacteria correlates with the peak of the immune response. Taken together, our results suggest that with the increased T cell signaling in the absence of TrIP, CD8 T cells from KO mice were acutely activated, leading

to more rapid expansion of responding cells. Thus, due to this faster rate of expansion of effector cells, KO mice cleared bacteria faster.

9.0 CONCLUSION

Overall, our results reveal TrIP as a potential target for modulating immune responses under conditions of infection, cancer or autoimmunity. In the former settings, reducing the TrIP inhibitory pathway could promote more effective clearance of pathogens or tumors. Conversely, increasing TrIP activity or expression may be an effective strategy for combating pathological immune responses such as autoimmune diseases.

9.1 SUMMARY AND FUTURE DIRECTIONS

9.1.1 Importance of the Kringle and p85-like domains

The discovery by DeFrances et al which showed that TrIP interacts with and inhibits PI3K activity, followed by the subsequent findings by the same group and others, that TrIP acts as a tumour suppressor has alerted the field of tumour immunology to a new avenue of cancer therapy. While DeFrances et al highlighted the importance of the p85-like domain as relevant to PI3K binding and inhibition, it was still unclear what the function of the kringle domain at the extracellular region of the protein was and how its function coordinated with the p85-like domain in the overall inhibitory function of TrIP with respect to PI3K.

Here I show that both the kringle and p85-like domains are necessary for TrIP inhibition of PI3K. I reiterate the findings of the DeFrances group and show that in T cells, the p85-like domain interacts with the prevalent catalytic subunit of PI3K, p110δ. Through mutation of either the kringle or the p85-like domain, I show that in either instance, PI3K inhibition is nullified on TrIP. By substituting the kringle domain for hCD8 and leaving the p85-like domain intact, I was able to crosslink TrIP with a monoclonal anti-hCD8. This crosslinking led to the inhibition of TCR activation. In the absence of anti-hCD8 crosslinking, TCR activation was observed to progress similarly to controls. These results, indirectly suggested that the role of the kringle domain on TrIP involves interaction with ligands or other TrIP molecules leading to a possible increase in p110δ binding. By differentially tagging TrIP with a flag tag or a myc tag, I was able to observe co-immunoprecipitation of the myc tagged full length TrIP by the flag tagged full length TrIP. Thus showing that, TrIP molecules expressed on the surface of cells interact with each other and this interaction indeed leads to an increase in the binding affinity of the p85-like domain for p110δ. The proposed model is shown below (Fig. 19).

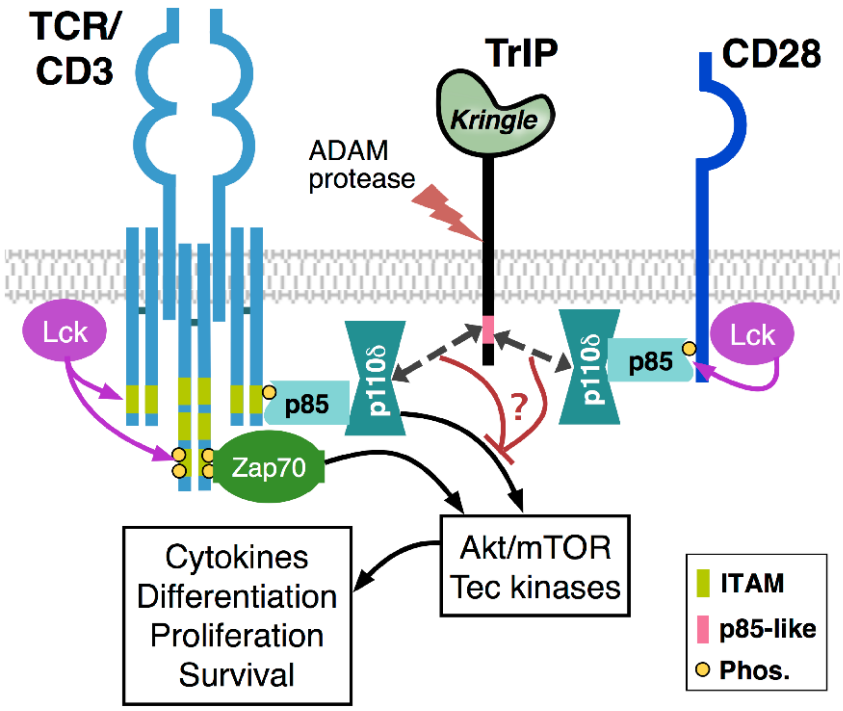

Figure 19 Model for the regulation and function of TrIP during T cell activation

The latter finding however does not rule out the possibility of there being other species or modes of interaction with the kringle domain. Especially as my studies on T cell activation by antigen primed antigen presenting cells (APC) showed that the kringle domain is lost in order for T cell activation to progress. I have found that the loss of the kringle domain during T cell activation is probably due to proteolytic cleavage which may involve interaction with another cell surface protein. In fact, I have data suggesting that at least one type of proteolytic enzyme capable of cleaving TrIP is expressed on the T cell itself. This is because in experiments with anti-CD3/CD28 stimulation (that is, without antigen primed APCs), TrIP loss on the T cell was observed after TCR activation. Interestingly in both APC-Ag and antibody stimulation experiments, TCR activation only proceeded after TrIP loss. My experiments have implicated the metalloproteinases, ADAM10 and ADAM 17 as T cell based regulators of TrIP. Using an inhibitor

specific for both ADAM proteins, I was able to prevent loss of TrIP after TCR activation. Overall, these data further highlights the importance of TrIP to PI3K regulation.

9.1.2 Future directions in evaluation of the TrIP domains

Throughout the course of this project, the lack of a suitable antibody for the detection of TrIP has been a significant challenge. An antibody would greatly help to detect TrIP at steady state, during T cell activation and in concert with would be binding partners in both cell line and primary T cells. An antibody would also help ascertain the protein expression profile of TrIP in a variety of cells. Presently, our best knowledge of the range of cellular expression of TrIP comes from the on-line gene expression database- BioGPS [171, 172]. While antibodies which recognize TrIP have been used in western blot assays [91], new lots of those antibodies have proven to be less effective at binding TrIP in my hands. Our lab has recently set out to design a recombinant mouse TrIP protein with binary objectives. The first being to be used as an immunogen in rodents so as to generate antibodies against the extracellular region of mouse TrIP. The second objective is to use the recombinant protein to detect possible ligands of TrIP.

We have termed this recombinant protein- EctoPIK3IP1 or EctoTrIP. EctoTrIP was created using the plasmid, pFuse-hIgG1-Fc2. This plasmid is a member of the family of plasmids developed by InvivoGen to facilitate the construction of Fc-fusion proteins [173]. In particular for our needs, this plasmid features a) IL2ss- the IL-2 signal sequence to allow secretion of the protein. B) human IgG1-Fc with flexible CH2 and CH3 domains. The human IgG1-Fc would potentially allow the use of the fusion protein as a primary binder against TrIP ligands that recognize TrIP kringle domain. I successfully cloned and expressed this protein (Fig20A) and we have started generating monoclonal antibodies through an agreement with Rockland antibodies and assays

[174] (Fig 20C-D). Initially, antibodies obtained were of an IgM isotype. While these IgM antibodies recognized TrIP, all clones exhibited relatively low binding affinity for TrIP (Fig 20C). A second round of antibody generation with Rockland has yielded several IgG antibodies that have, in early tests, shown relatively high affinity for TrIP (Fig 20D).

Testing our theory of the mechanism of TrIP regulation of PI3K would be possible with an antibody against TrIP. Using imaging flow cytometry, we could visualize TrIP oligomerization and loss before and after TCR activation or synapse formation.

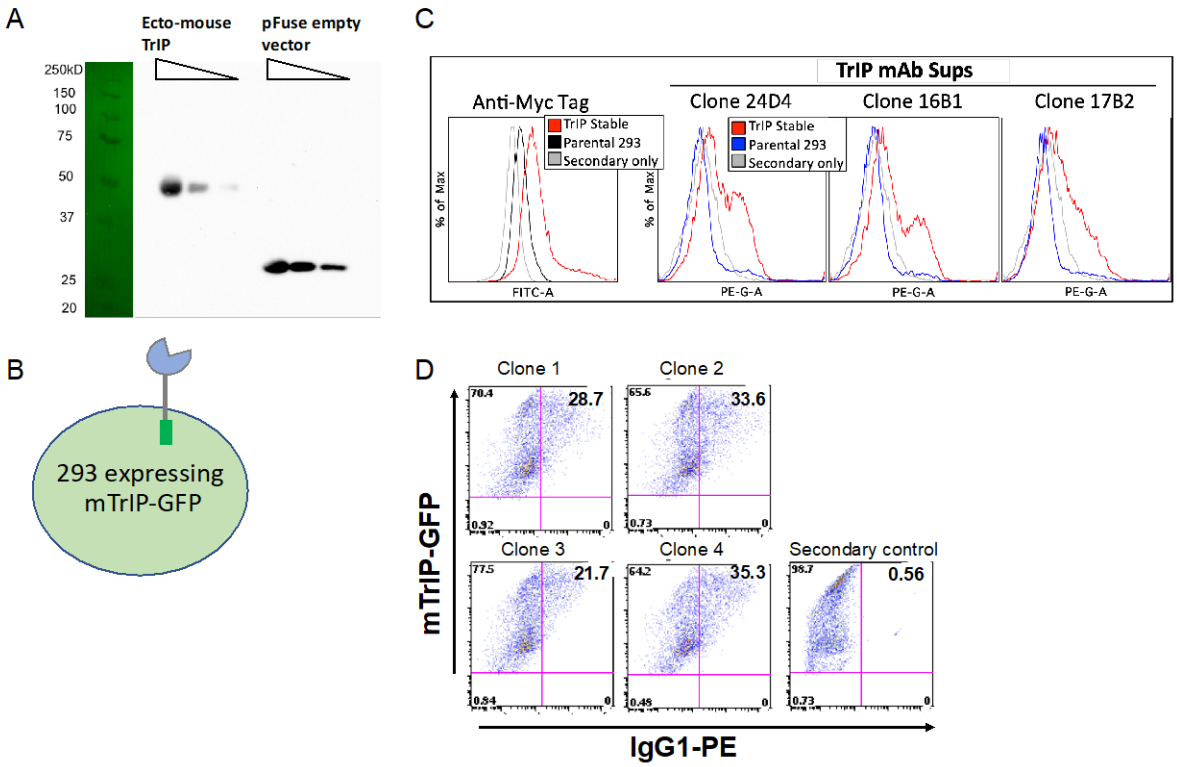

Figure 20 Generation of antibodies directed at mouse TrIP

(**A**)Production of TrIP-Ig fusion protein. Supernatants obtained from transfected 293 cells were separated from solution using Protein A beads. After elution, supernatants were serially diluted (1:3), run on a 10% reducing gel and detected with Protein A HRP. Ecto-mouse TrIP expected size is 42.85kD. pFuse Empty vector Fc protein expected size is 27kD. (**B**) Schematic of 293 cells transfected with mTrIP-GFP. GFP is located intracellularly and acts as a marker for TrIP in the assay. (**C-D**) IgM (**C**) and IgG (**D**) monoclonal antibody supernatants obtained from hybridomas were used to stain 293 cells transfected with mTrIP-GFP. Hybridomas were generated by using Ecto-mouse TrIP as an immunogen in rats.

Apart from TrIP itself, there may be other ligands that can bind to TrIP, especially via the kringle domain. In previous studies, Crabtree and colleagues identified TrIP in the media of a breast cancer cell line, MCF7. They carried out a phage screen and identified a protein they termed CRKR (calcineurin regulated kringle domain protein receptor) that recognized TrIP [175]. This protein was later termed TremL6 (Triggering receptor expressed on myeloid cells like 6). TremL6 is a 33kDa protein with an IgV extracellular domain (Fig 21A). Data from Biogps suggests that TremL6 is significantly expressed on macrophages [171, 172]. In preliminary experiments, I expressed TremL6 on 293 cells and used the EctoTrIP fusion protein to test for binding with TremL6 (Fig 21B). I did observe significant binding to TremL6 expressing cells compared to control transfected 293 cells (Fig 21D). These results highlight the possibility that there could be other ligands that recognize TrIP via the kringle domain. Further experiments in the Kane lab will look at the potential effects of TremL6 binding to TrIP in a T cell line.

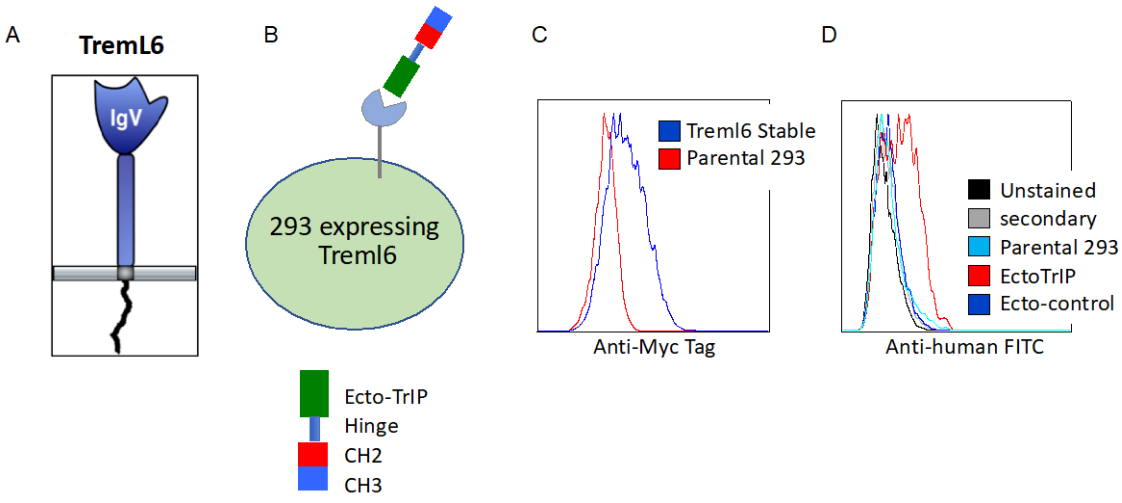

Figure 21 Binding of TrIP Fusion protein to TremL6

(**A**) Schematic of TremL6. A 33kDa transmembrane protein with an extracellular IgV domain. (**B**) 293 cells were transfected with Myc-tagged TremL6. (**C**) TremL6 expression on transfected 293 cells was detected using anti-myc antibody (clone 9B11). (**D**) Parental and TremL6 expressing 293 cells were stained with EctoTrIP. EctoTrIP staining was detected using anti-human Fc-FITC antibody.

In our evaluation of flag tagged Δkringle-TrIP and Δp85-like-TrIP, unlike WT-TrIP, in the absence of either domain during TCR activation, the flag tag was still intact. While this highlighted the importance of each domain to the function of TrIP, it has confounded us as to how TrIP is downregulated. What we know is that it occurs upon TCR activation and either or both ADAM10/17 play a role in regulating TrIP expression. Due to there being no cleavage of the flag tag observed with Δp85-like-TrIP, we cannot rule out endocytic or proteasomal degradation pathways in TrIP regulation. A possible future direction would entail cloning a none cleavable TrIP variant (resistance to cleavage can be confirmed by an ADAM10/17 assay) and observing for extracellular loss. The effects such a non-cleavable TrIP clone would have on T cell activation and effector functions would also be of interest. Especially with regards accumulation of p110δ on non-cleavable TrIP after activation.

As of now we have only tested the Δp85-like-TrIP and Δkringle-TrIP variants in D10 cell lines. It would be interesting to see what effects these mutants would have as T cell specific transgenes in a mouse. This bears physiological relevance since TrIP has been identified as a tumour suppressor [94, 176] and mouse models have been valuable in cancer studies [30, 177]. A potential clinical manifestation could be as a result of a loss of function mutation on one of the two domains of TrIP.

9.1.3 Summary of TrIP KO mice data

Following up on their *in vitro* studies on TrIP, the DeFrances lab has shown that TrIP is indeed a tumour suppressor. Mice specific for the TrIP transgene in the liver showed reduction of PI3K

activity in the form of reduced PIP3 production and phosphorylation of Akt [94]. When these mice were crossed onto a spontaneous hepatocellular carcinoma background, incidence of liver tumours were significantly reduced. Others have since shown that increasing tumour growth is associated with transcriptional downregulation of TrIP in a range of human cancers [176]. Thus, highlighting the relevance of a mouse model to our studies.

Here, our lab has generated a mouse with TrIP specifically deleted in T cells. In evaluating these mice, I found no obvious T cell developmental defects. Similar percentages of CD4 and CD8 T cells were observed in thymic and spleen compartments. In addition, these KO mice did not show any adverse autoimmune conditions or spontaneous tumour growth.

Activation of T cells from these mice however yielded results that correlated with my in vitro studies. Upon TCR activation, TrIP KO mice expressed higher levels of phosphorylated Akt and S6 and exhibited earlier exit of FoxO1 from the nucleus when compared to WT. This translated into high levels of CD69 activation (a costimulatory molecule that leads to high proliferation) [178]. Indeed, when proliferation was evaluated, I found that KO T cells did proliferate faster than WT cells. This high activation and proliferation potential translated into higher levels of pro-inflammatory T cells. My Th subset differentiation experiments showed that KO T cells tended to produce significantly higher percentages of active Th1 cells as evidenced by secretion of IFNγ. In contrast, these same cells produced less Tregs. Interestingly, Tregs produced by KO T cells also secreted a high amout of IFNγ (though IFNγ from KO Tregs was much less compared to that produced by KO Th1 cells). Based on this latter finding, I used the well-established listeria mouse model to evaluate TrIP KO mice. I found that these mice were less susceptible to *L. monocytogenes* and were able to clear the infection by day four. This was in stark contrast to infected WT mice that still had significant levels of the pathogen in their liver by day four.

It is important to note that I did observe slightly lower levels of CD62L in unstimulated KO T cells. Given the role of CD62L in restriction of naïve T cells to secondary lymphoid compartments and findings that show CD62L expression is controlled by PI3K activity, my observation implies that KO T cells, due to higher levels of PI3K, appear to be more "poised" for effector status. The initial response to listeria is through the innate immune system and the pathogen usually replicates for three days. Clearance of the bacteria has been shown to correlate with the peak of the immune response. The model for "poised" effector status is thus supported by the early clearance of the pathogen in KO mice.

9.1.4 Future directions with the TrIP KO mouse model

A more complete characterization of TrIP KO mice is underway. The slight but consistent differences in CD62L expression that was observed between KO and WT T cells suggests that loss of TrIP affects at least one of the pathways for CD62L regulation (shedding or transcription). RNA sequencing of steady state and stimulated T cell samples could enable us identify any changes in transcription that may affect KLF2 (the factor responsible for CD62L upregulation) [179]. Comparing the TCR repertoire of conventional and regulatory T cells from WT and KO would also be of interest. As previously mentioned, though we do not notice any developmental defects, it is possible that subtle differences in the T cell selection process can occur due to signaling differences. This possibility is heightened by our observation that *in vitro* derived Tregs from KO mice secreted significantly higher amounts of IFNγ compared to WT.

The CD8 T cells implicated in mediating clearance of *L. monocytogenes* can be divided into two types based on MHC class restrictions: MHC class Ia and MHC class Ib or H2-M3 [154]. The H2-M3 restricted CD8 T cells have been found to expand early on during the infection. These

cells produce IFNg and are cytolytic [180]. As our data shows that the loss of TrIP affects functions in both CD4 and CD8 T cells, it is possible that H2-M3 restricted CD8 T cells in KO mice respond earlier and begin clearance of the bacteria compared to WT mice. It has also been shown that although class Ia restricted cells respond later than H2-M3 restricted CD8 T cells, the class Ia CTLs have a significantly higher response to secondary *L. monocytogenes* infection compared to H2-M3 restricted CTLs [180, 181]. It would be interesting to evaluate if these findings translate in our present model. Whereby class Ia restricted CTLs in KO mice would mount a significantly higher secondary response compared to WT counterparts.

Studies have also shown that CD4 T cells are required for efficient response to L. monocytogenes infection in mice [158, 182, 183]. Infected macrophages secrete IL-2 which leads to the expansion and differentiation of Th1 T cells. The Th1 cells then secrete IFNg which activates the macrophages and leads to early anti-bacterial functions [182]. A potential future direction would be to evaluate the activity of macrophages in TrIP KO mice compared to those in WT mice after infection with *L. monocytogenes*. Based on the high potential for Th1 differentiation in KO mice, I expect that macrophages would be activated earlier and/or to a higher degree in KO mice compared to WT counterparts. This could be why early clearance of the bacteria is observed.

Finally, our data support the notion that TrIP is a viable target for therapeutic research. Our use of the hCD8-TrIP construct suggests a way TrIP could be employed as a chimeric antigen receptor to inhibit errant PI3K signaling and some of our collaborators have begun to clone CAR molecules based on this theory. Data from biogps [171, 172] shows a high expression of TrIP in Mast cells. Researchers are still uncovering how degranulation and cytokine release by mast cells can be better regulated in cases of severe allergies. Given that the PI3K pathway plays a major role

in mast cell function [184-186], studying TrIP in the context of Mast cells is another avenue we are looking at.

APPENDIX

I would like to thank the following people: Dr. Ann Piccirillo and Dr. Louise D'Cruz for assistance with the Listeria experiments. Dr. Amanda Poholek for her guidance with the Th differentiation experiments and Dr. Shunsuke Kataoka for his assistance with the Imaging Flow Cytometry analysis of FoxO1.

BIBLIOGRAPHY

1. Cantrell, D., *T cell antigen receptor signal transduction pathways.* Annu Rev Immunol, 1996. **14**: p. 259-74.

2. Rincon, M., *MAP-kinase signaling pathways in T cells.* Curr Opin Immunol, 2001. **13**(3): p. 339-45.

3. Bommhardt, U., et al., *Activation of the extracellular signal-related kinase/mitogen-activated protein kinase pathway discriminates CD4 versus CD8 lineage commitment in the thymus.* J Immunol, 1999. **163**(2): p. 715-22.

4. Sharp, L.L. and S.M. Hedrick, *Commitment to the CD4 lineage mediated by extracellular signal-related kinase mitogen-activated protein kinase and lck signaling.* J Immunol, 1999. **163**(12): p. 6598-605.

5. Sharp, L.L., et al., *The influence of the MAPK pathway on T cell lineage commitment.* Immunity, 1997. **7**(5): p. 609-18.

6. Rincon, M., et al., *The JNK pathway regulates the In vivo deletion of immature CD4(+)CD8(+) thymocytes.* J Exp Med, 1998. **188**(10): p. 1817-30.

7. Rao, A., *NF-ATp: a transcription factor required for the co-ordinate induction of several cytokine genes.* Immunol Today, 1994. **15**(6): p. 274-81.

8. Schreiber, S.L. and G.R. Crabtree, *The mechanism of action of cyclosporin A and FK506.* Immunol Today, 1992. **13**(4): p. 136-42.

9. Cantley, L.C., *The phosphoinositide 3-kinase pathway.* Science, 2002. **296**(5573): p. 1655-7.

10. Engelman, J.A., *Targeting PI3K signalling in cancer: opportunities, challenges and limitations.* Nat Rev Cancer, 2009. **9**(8): p. 550-62.

11. Fruman, D.A., *The role of class I phosphoinositide 3-kinase in T-cell function and autoimmunity.* Biochem Soc Trans, 2007. **35**(Pt 2): p. 177-80.

12. Stark, A.K., et al., *PI3K inhibitors in inflammation, autoimmunity and cancer.* Curr Opin Pharmacol, 2015. **23**: p. 82-91.

13. Engelman, J.A., J. Luo, and L.C. Cantley, *The evolution of phosphatidylinositol 3-kinases as regulators of growth and metabolism.* Nat Rev Genet, 2006. **7**(8): p. 606-19.

14. Suire, S., et al., *p84, a new Gbetagamma-activated regulatory subunit of the type IB phosphoinositide 3-kinase p110gamma.* Curr Biol, 2005. **15**(6): p. 566-70.

15. Voigt, P., M.B. Dorner, and M. Schaefer, *Characterization of p87PIKAP, a novel regulatory subunit of phosphoinositide 3-kinase gamma that is highly expressed in heart and interacts with PDE3B.* J Biol Chem, 2006. **281**(15): p. 9977-86.

16. Liu, P., et al., *Targeting the phosphoinositide 3-kinase pathway in cancer.* Nat Rev Drug Discov, 2009. **8**(8): p. 627-44.

17. Franco, I., et al., *PI3K class II alpha controls spatially restricted endosomal PtdIns3P and Rab11 activation to promote primary cilium function.* Dev Cell, 2014. **28**(6): p. 647-58.

18. Mountford, J.K., et al., *The class II PI 3-kinase, PI3KC2alpha, links platelet internal membrane structure to shear-dependent adhesive function.* Nat Commun, 2015. **6**: p. 6535.

19. Yoshioka, K., et al., *Endothelial PI3K-C2alpha, a class II PI3K, has an essential role in angiogenesis and vascular barrier function.* Nat Med, 2012. **18**(10): p. 1560-9.

20. Braccini, L., et al., *PI3K-C2gamma is a Rab5 effector selectively controlling endosomal Akt2 activation downstream of insulin signalling.* Nat Commun, 2015. **6**: p. 7400.

21. Jaber, N. and W.X. Zong, *Class III PI3K Vps34: essential roles in autophagy, endocytosis, and heart and liver function.* Ann N Y Acad Sci, 2013. **1280**: p. 48-51.

22. Fruman, D.A. and G. Bismuth, *Fine tuning the immune response with PI3K.* Immunol Rev, 2009. **228**(1): p. 253-72.

23. Matheu, M.P., et al., *Class IA phosphoinositide 3-kinase modulates basal lymphocyte motility in the lymph node.* J Immunol, 2007. **179**(4): p. 2261-9.

24. Shiroki, F., et al., *The p85alpha regulatory subunit of class IA phosphoinositide 3-kinase regulates beta-selection in thymocyte development.* J Immunol, 2007. **178**(3): p. 1349-56.

25. Gillham, H., et al., *Intracellular movement of green fluorescent protein-tagged phosphatidylinositol 3-kinase in response to growth factor receptor signaling.* J Cell Biol, 1999. **146**(4): p. 869-80.

26. Yu, J., et al., *Regulation of the p85/p110 phosphatidylinositol 3'-kinase: stabilization and inhibition of the p110alpha catalytic subunit by the p85 regulatory subunit.* Mol Cell Biol, 1998. **18**(3): p. 1379-87.

27. Burbach, B.J., et al., *T-cell receptor signaling to integrins.* Immunol Rev, 2007. **218**: p. 65-81.

28. Chen, L. and D.B. Flies, *Molecular mechanisms of T cell co-stimulation and co-inhibition.* Nat Rev Immunol, 2013. **13**(4): p. 227-42.

29. Fresno Vara, J.A., et al., *PI3K/Akt signalling pathway and cancer.* Cancer Treat Rev, 2004. **30**(2): p. 193-204.

30. Sansal, I. and W.R. Sellers, *The biology and clinical relevance of the PTEN tumor suppressor pathway.* J Clin Oncol, 2004. **22**(14): p. 2954-63.

31. Li, J., et al., *PTEN, a putative protein tyrosine phosphatase gene mutated in human brain, breast, and prostate cancer.* Science, 1997. **275**(5308): p. 1943-7.

32. Li, D.M. and H. Sun, *TEP1, encoded by a candidate tumor suppressor locus, is a novel protein tyrosine phosphatase regulated by transforming growth factor beta.* Cancer Res, 1997. **57**(11): p. 2124-9.

33. Maehama, T. and J.E. Dixon, *The tumor suppressor, PTEN/MMAC1, dephosphorylates the lipid second messenger, phosphatidylinositol 3,4,5-trisphosphate.* J Biol Chem, 1998. **273**(22): p. 13375-8.

34. Lee, H.J. and J.J. Zheng, *PDZ domains and their binding partners: structure, specificity, and modification.* Cell Commun Signal, 2010. **8**: p. 8.

35. Hsu, F. and Y. Mao, *The structure of phosphoinositide phosphatases: Insights into substrate specificity and catalysis.* Biochim Biophys Acta, 2015. **1851**(6): p. 698-710.

36. Simpson, L. and R. Parsons, *PTEN: life as a tumor suppressor.* Exp Cell Res, 2001. **264**(1): p. 29-41.

37. Liu, X., et al., *Distinct roles for PTEN in prevention of T cell lymphoma and autoimmunity in mice.* J Clin Invest, 2010. **120**(7): p. 2497-507.

38. Dillon, L.M. and T.W. Miller, *Therapeutic targeting of cancers with loss of PTEN function.* Curr Drug Targets, 2014. **15**(1): p. 65-79.

39. Lorenz, U., *SHP-1 and SHP-2 in T cells: two phosphatases functioning at many levels.* Immunol Rev, 2009. **228**(1): p. 342-59.

40. Rohrschneider, L.R., et al., *Structure, function, and biology of SHIP proteins.* Genes Dev, 2000. **14**(5): p. 505-20.

41. Backers, K., et al., *The termination of PI3K signalling by SHIP1 and SHIP2 inositol 5-phosphatases.* Adv Enzyme Regul, 2003. **43**: p. 15-28.

42. Choi, Y., et al., *PTEN, but not SHIP and SHIP2, suppresses the PI3K/Akt pathway and induces growth inhibition and apoptosis of myeloma cells.* Oncogene, 2002. **21**(34): p. 5289-300.

43. Norris, F.A., R.C. Atkins, and P.W. Majerus, *The cDNA cloning and characterization of inositol polyphosphate 4-phosphatase type II. Evidence for conserved alternative splicing in the 4-phosphatase family.* J Biol Chem, 1997. **272**(38): p. 23859-64.

44. Norris, F.A., V. Auethavekiat, and P.W. Majerus, *The isolation and characterization of cDNA encoding human and rat brain inositol polyphosphate 4-phosphatase.* J Biol Chem, 1995. **270**(27): p. 16128-33.

45. Gewinner, C., et al., *Evidence that inositol polyphosphate 4-phosphatase type II is a tumor suppressor that inhibits PI3K signaling.* Cancer Cell, 2009. **16**(2): p. 115-25.

46. Fruman, D.A., et al., *Impaired B cell development and proliferation in absence of phosphoinositide 3-kinase p85alpha.* Science, 1999. **283**(5400): p. 393-7.

47. Suzuki, H., et al., *Xid-like immunodeficiency in mice with disruption of the p85alpha subunit of phosphoinositide 3-kinase.* Science, 1999. **283**(5400): p. 390-2.

48. Juntilla, M.M. and G.A. Koretzky, *Critical roles of the PI3K/Akt signaling pathway in T cell development.* Immunol Lett, 2008. **116**(2): p. 104-10.

49. Okkenhaug, K., et al., *Impaired B and T cell antigen receptor signaling in p110delta PI 3-kinase mutant mice.* Science, 2002. **297**(5583): p. 1031-4.

50. Di Cristofano, A., et al., *Pten is essential for embryonic development and tumour suppression.* Nat Genet, 1998. **19**(4): p. 348-55.

51. Suzuki, A., et al., *High cancer susceptibility and embryonic lethality associated with mutation of the PTEN tumor suppressor gene in mice.* Curr Biol, 1998. **8**(21): p. 1169-78.

52. Ciofani, M. and J.C. Zuniga-Pflucker, *Notch promotes survival of pre-T cells at the beta-selection checkpoint by regulating cellular metabolism.* Nat Immunol, 2005. **6**(9): p. 881-8.

53. Cantrell, D.A., *Phosphoinositide 3-kinase signalling pathways.* J Cell Sci, 2001. **114**(Pt 8): p. 1439-45.

54. Jones, R.G., et al., *Protein kinase B regulates T lymphocyte survival, nuclear factor kappaB activation, and Bcl-X(L) levels in vivo.* J Exp Med, 2000. **191**(10): p. 1721-34.

55. Na, S.Y., et al., *Constitutively active protein kinase B enhances Lck and Erk activities and influences thymocyte selection and activation.* J Immunol, 2003. **171**(3): p. 1285-96.

56. Rathmell, J.C., et al., *Activated Akt promotes increased resting T cell size, CD28-independent T cell growth, and development of autoimmunity and lymphoma.* Eur J Immunol, 2003. **33**(8): p. 2223-32.

57. Hinton, H.J., D.R. Alessi, and D.A. Cantrell, *The serine kinase phosphoinositide-dependent kinase 1 (PDK1) regulates T cell development.* Nat Immunol, 2004. **5**(5): p. 539-45.

58. Lucas, C.L., et al., *Dominant-activating germline mutations in the gene encoding the PI(3)K catalytic subunit p110delta result in T cell senescence and human immunodeficiency.* Nat Immunol, 2014. **15**(1): p. 88-97.

59. Pirola, L., et al., *Activation loop sequences confer substrate specificity to phosphoinositide 3-kinase alpha (PI3Kalpha). Functions of lipid kinase-deficient PI3Kalpha in signaling.* J Biol Chem, 2001. **276**(24): p. 21544-54.

60. Okkenhaug, K., et al., *The p110delta isoform of phosphoinositide 3-kinase controls clonal expansion and differentiation of Th cells.* J Immunol, 2006. **177**(8): p. 5122-8.

61. Soond, D.R., et al., *PI3K p110delta regulates T-cell cytokine production during primary and secondary immune responses in mice and humans.* Blood, 2010. **115**(11): p. 2203-13.

62. Gamper, C.J. and J.D. Powell, *All PI3Kinase signaling is not mTOR: dissecting mTOR-dependent and independent signaling pathways in T cells.* Front Immunol, 2012. **3**: p. 312.

63. Battaglia, M., A. Stabilini, and M.G. Roncarolo, *Rapamycin selectively expands CD4+CD25+FoxP3+ regulatory T cells.* Blood, 2005. **105**(12): p. 4743-8.

64. Delgoffe, G.M., et al., *The mTOR kinase differentially regulates effector and regulatory T cell lineage commitment.* Immunity, 2009. **30**(6): p. 832-44.

65. Miskov-Zivanov, N., et al., *The duration of T cell stimulation is a critical determinant of cell fate and plasticity.* Sci Signal, 2013. **6**(300): p. ra97.

66. Vivanco, I. and C.L. Sawyers, *The phosphatidylinositol 3-Kinase AKT pathway in human cancer.* Nat Rev Cancer, 2002. **2**(7): p. 489-501.

67. Dienstmann, R., et al., *Picking the point of inhibition: a comparative review of PI3K/AKT/mTOR pathway inhibitors.* Mol Cancer Ther, 2014. **13**(5): p. 1021-31.

68. Carnero, A. and J.M. Paramio, *The PTEN/PI3K/AKT Pathway in vivo, Cancer Mouse Models.* Front Oncol, 2014. **4**: p. 252.

69. Samuels, Y., et al., *High frequency of mutations of the PIK3CA gene in human cancers.* Science, 2004. **304**(5670): p. 554.

70. LoPiccolo, J., et al., *Targeting the PI3K/Akt/mTOR pathway: effective combinations and clinical considerations.* Drug Resist Updat, 2008. **11**(1-2): p. 32-50.

71. Suzuki, A., et al., *T cell-specific loss of Pten leads to defects in central and peripheral tolerance.* Immunity, 2001. **14**(5): p. 523-34.

72. Borlado, L.R., et al., *Increased phosphoinositide 3-kinase activity induces a lymphoproliferative disorder and contributes to tumor generation in vivo.* FASEB J, 2000. **14**(7): p. 895-903.

73. Kim, M.V., et al., *The transcription factor Foxo1 controls central-memory CD8+ T cell responses to infection.* Immunity, 2013. **39**(2): p. 286-97.

74. Lucas, C.L., et al., *PI3Kdelta and primary immunodeficiencies.* Nat Rev Immunol, 2016. **16**(11): p. 702-714.

75. Deau, M.C., et al., *A human immunodeficiency caused by mutations in the PIK3R1 gene.* J Clin Invest, 2014. **124**(9): p. 3923-8.

76. Lucas, C.L., et al., *Heterozygous splice mutation in PIK3R1 causes human immunodeficiency with lymphoproliferation due to dominant activation of PI3K.* J Exp Med, 2014. **211**(13): p. 2537-47.

77. Conley, M.E., et al., *Agammaglobulinemia and absent B lineage cells in a patient lacking the p85alpha subunit of PI3K.* J Exp Med, 2012. **209**(3): p. 463-70.

78. Li, J., S.G. Kim, and J. Blenis, *Rapamycin: one drug, many effects.* Cell Metab, 2014. **19**(3): p. 373-9.

79. Rae, W., et al., *Precision treatment with sirolimus in a case of activated phosphoinositide 3-kinase delta syndrome.* Clin Immunol, 2016. **171**: p. 38-40.

80. Okkenhaug, K., M. Graupera, and B. Vanhaesebroeck, *Targeting PI3K in Cancer: Impact on Tumor Cells, Their Protective Stroma, Angiogenesis, and Immunotherapy.* Cancer Discov, 2016. **6**(10): p. 1090-1105.

81. Coulter, T.I., et al., *Clinical spectrum and features of activated phosphoinositide 3-kinase delta syndrome: A large patient cohort study.* J Allergy Clin Immunol, 2017. **139**(2): p. 597-606 e4.

82. Elkaim, E., et al., *Clinical and immunologic phenotype associated with activated phosphoinositide 3-kinase delta syndrome 2: A cohort study.* J Allergy Clin Immunol, 2016. **138**(1): p. 210-218 e9.

83. Berns, K., et al., *A functional genetic approach identifies the PI3K pathway as a major determinant of trastuzumab resistance in breast cancer.* Cancer Cell, 2007. **12**(4): p. 395-402.

84. Bianco, R., et al., *Loss of PTEN/MMAC1/TEP in EGF receptor-expressing tumor cells counteracts the antitumor action of EGFR tyrosine kinase inhibitors.* Oncogene, 2003. **22**(18): p. 2812-22.

85. Engelman, J.A., et al., *ErbB-3 mediates phosphoinositide 3-kinase activity in gefitinib-sensitive non-small cell lung cancer cell lines.* Proc Natl Acad Sci U S A, 2005. **102**(10): p. 3788-93.

86. Mellinghoff, I.K., et al., *Molecular determinants of the response of glioblastomas to EGFR kinase inhibitors.* N Engl J Med, 2005. **353**(19): p. 2012-24.

87. Moulder, S.L., et al., *Epidermal growth factor receptor (HER1) tyrosine kinase inhibitor ZD1839 (Iressa) inhibits HER2/neu (erbB2)-overexpressing breast cancer cells in vitro and in vivo.* Cancer Res, 2001. **61**(24): p. 8887-95.

88. Yakes, F.M., et al., *Herceptin-induced inhibition of phosphatidylinositol-3 kinase and Akt Is required for antibody-mediated effects on p27, cyclin D1, and antitumor action.* Cancer Res, 2002. **62**(14): p. 4132-41.

89. Juric, D., et al., *Convergent loss of PTEN leads to clinical resistance to a PI(3)Kalpha inhibitor.* Nature, 2015. **518**(7538): p. 240-4.

90. Brown, K.K. and A. Toker, *The phosphoinositide 3-kinase pathway and therapy resistance in cancer.* F1000Prime Rep, 2015. **7**: p. 13.

91. Zhu, Z., et al., *PI3K is negatively regulated by PIK3IP1, a novel p110 interacting protein.* Biochem Biophys Res Commun, 2007. **358**(1): p. 66-72.

92. Amzel, L.M., et al., *Structural comparisons of class I phosphoinositide 3-kinases.* Nat Rev Cancer, 2008. **8**(9): p. 665-9.

93. Yu, J., C. Wjasow, and J.M. Backer, *Regulation of the p85/p110alpha phosphatidylinositol 3'-kinase. Distinct roles for the n-terminal and c-terminal SH2 domains.* J Biol Chem, 1998. **273**(46): p. 30199-203.

94. He, X., et al., *PIK3IP1, a negative regulator of PI3K, suppresses the development of hepatocellular carcinoma.* Cancer Res, 2008. **68**(14): p. 5591-8.

95. DeFrances, M.C., et al., *Inhibition of T-cell activation by PIK3IP1.* Eur J Immunol, 2012. **42**(10): p. 2754-9.

96. Lee, C.H., et al., *Engineering of a human kringle domain into agonistic and antagonistic binding proteins functioning in vitro and in vivo.* Proc Natl Acad Sci U S A, 2010. **107**(21): p. 9567-71.

97. Marti, D.N., J. Schaller, and M. Llinas, *Solution structure and dynamics of the plasminogen kringle 2-AMCHA complex: 3(1)-helix in homologous domains.* Biochemistry, 1999. **38**(48): p. 15741-55.

98. Christen, M.T., et al., *Human plasminogen kringle 3: solution structure, functional insights, phylogenetic landscape.* Biochemistry, 2010. **49**(33): p. 7131-50.

99. Ikeo, K., K. Takahashi, and T. Gojobori, *Evolutionary origin of numerous kringles in human and simian apolipoprotein(a).* FEBS Lett, 1991. **287**(1-2): p. 146-8.

100. Menhart, N., et al., *Roles of individual kringle domains in the functioning of positive and negative effectors of human plasminogen activation.* Biochemistry, 1995. **34**(5): p. 1482-8.

101. Patthy, L., et al., *Kringles: modules specialized for protein binding. Homology of the gelatin-binding region of fibronectin with the kringle structures of proteases.* FEBS Lett, 1984. **171**(1): p. 131-6.

102. McMullen, B.A. and K. Fujikawa, *Amino acid sequence of the heavy chain of human alpha-factor XIIa (activated Hageman factor).* J Biol Chem, 1985. **260**(9): p. 5328-41.

103. Lacroix, R., et al., *Activation of plasminogen into plasmin at the surface of endothelial microparticles: a mechanism that modulates angiogenic properties of endothelial progenitor cells in vitro.* Blood, 2007. **110**(7): p. 2432-9.

104. Lijnen, H.R., *Elements of the fibrinolytic system.* Ann N Y Acad Sci, 2001. **936**: p. 226-36.

105. Castellino, F.J. and S.G. McCance, *The kringle domains of human plasminogen.* Ciba Found Symp, 1997. **212**: p. 46-60; discussion 60-5.

106. Kwak, S.H., et al., *The kringle domain of urokinase-type plasminogen activator potentiates LPS-induced neutrophil activation through interaction with {alpha}V{beta}3 integrins.* J Leukoc Biol, 2005. **78**(4): p. 937-45.

107. Byeon, I.J., et al., *Ligand binding to the tissue-type plasminogen activator kringle 2 domain: structural characterization by 1H-NMR.* Biochemistry, 1995. **34**(9): p. 2739-50.

108. Uche, U.U., et al., *PIK3IP1/TrIP restricts activation of T cells through inhibition of PI3K/Akt.* J Exp Med, 2018. **215**(12): p. 3165-3179.

109. Paigen, B., et al., *Variation in susceptibility to atherosclerosis among inbred strains of mice.* Atherosclerosis, 1985. **57**(1): p. 65-73.

110. Ojeda, G., et al., *A hyperreactive variant of a CD4+ T cell line is activated by syngeneic antigen presenting cells in the absence of antigen.* Cell Immunol, 1995. **164**(2): p. 265-78.

111. Kaye, J., et al., *Both a monoclonal antibody and antisera specific for determinants unique to individual cloned helper T cell lines can substitute for antigen and antigen-presenting cells in the activation of T cells.* J Exp Med, 1983. **158**(3): p. 836-56.

112. Medema, R.H., et al., *AFX-like Forkhead transcription factors mediate cell-cycle regulation by Ras and PKB through p27kip1.* Nature, 2000. **404**(6779): p. 782-7.

113. Tang, T.T. and L.A. Lasky, *The forkhead transcription factor FOXO4 induces the down-regulation of hypoxia-inducible factor 1 alpha by a von Hippel-Lindau protein-independent mechanism.* J Biol Chem, 2003. **278**(32): p. 30125-35.

114. Urbich, C., et al., *FOXO-dependent expression of the proapoptotic protein Bim: pivotal role for apoptosis signaling in endothelial progenitor cells.* FASEB J, 2005. **19**(8): p. 974-6.

115. Cheng, J., K.S. Hamilton, and L.P. Kane, *Phosphorylation of Carma1, but not Bcl10, by Akt regulates TCR/CD28-mediated NF-kappaB induction and cytokine production.* Mol Immunol, 2014. **59**(1): p. 110-6.

116. Kane, L.P., M.N. Mollenauer, and A. Weiss, *A proline-rich motif in the C terminus of Akt contributes to its localization in the immunological synapse.* J Immunol, 2004. **172**(9): p. 5441-9.

117. Hedrick, S.M., et al., *FOXO transcription factors throughout T cell biology.* Nat Rev Immunol, 2012. **12**(9): p. 649-61.

118. Mikels, A., Y. Minami, and R. Nusse, *Ror2 receptor requires tyrosine kinase activity to mediate Wnt5A signaling.* J Biol Chem, 2009. **284**(44): p. 30167-76.

119. Ji, W.R., et al., *Characterization of kringle domains of angiostatin as antagonists of endothelial cell migration, an important process in angiogenesis.* FASEB J, 1998. **12**(15): p. 1731-8.

120. Nishimura, H., et al., *Developmentally regulated expression of the PD-1 protein on the surface of double-negative (CD4-CD8-) thymocytes.* Int Immunol, 1996. **8**(5): p. 773-80.

121. Wang, J., et al., *PD-1 deficiency results in the development of fatal myocarditis in MRL mice.* Int Immunol, 2010. **22**(6): p. 443-52.

122. Bardhan, K., T. Anagnostou, and V.A. Boussiotis, *The PD1:PD-L1/2 Pathway from Discovery to Clinical Implementation.* Front Immunol, 2016. **7**: p. 550.

123. Parry, R.V., et al., *CTLA-4 and PD-1 receptors inhibit T-cell activation by distinct mechanisms.* Mol Cell Biol, 2005. **25**(21): p. 9543-53.

124. Patsoukis, N., et al., *Selective effects of PD-1 on Akt and Ras pathways regulate molecular components of the cell cycle and inhibit T cell proliferation.* Sci Signal, 2012. **5**(230): p. ra46.

125. Shin, H. and E.J. Wherry, *CD8 T cell dysfunction during chronic viral infection.* Curr Opin Immunol, 2007. **19**(4): p. 408-15.

126. Goldberg, M.V. and C.G. Drake, *LAG-3 in Cancer Immunotherapy.* Curr Top Microbiol Immunol, 2011. **344**: p. 269-78.

127. Li, N., et al., *Metalloproteases regulate T-cell proliferation and effector function via LAG-3.* EMBO J, 2007. **26**(2): p. 494-504.

128. Hawse, W.F., et al., *Cutting Edge: Differential Regulation of PTEN by TCR, Akt, and FoxO1 Controls CD4+ T Cell Fate Decisions.* J Immunol, 2015. **194**(10): p. 4615-9.

129. Newton, R.H. and L.A. Turka, *Regulation of T cell homeostasis and responses by pten.* Front Immunol, 2012. **3**: p. 151.

130. Haughton, G., et al., *The CH series of murine B cell lymphomas: neoplastic analogues of Ly-1+ normal B cells.* Immunol Rev, 1986. **93**: p. 35-51.

131. Irving, B.A. and A. Weiss, *The cytoplasmic domain of the T cell receptor zeta chain is sufficient to couple to receptor-associated signal transduction pathways.* Cell, 1991. **64**(5): p. 891-901.

132. Li, N., et al., *Biochemical analysis of the regulatory T cell protein lymphocyte activation gene-3 (LAG-3; CD223).* J Immunol, 2004. **173**(11): p. 6806-12.

133. Clayton, K.L., et al., *Soluble T cell immunoglobulin mucin domain 3 is shed from CD8+ T cells by the sheddase ADAM10, is increased in plasma during untreated HIV infection, and correlates with HIV disease progression.* J Virol, 2015. **89**(7): p. 3723-36.

134. Thery, C. and C.D. Stern, *Roles of kringle domain-containing serine proteases in epithelial-mesenchymal transitions during embryonic development.* Acta Anat (Basel), 1996. **156**(3): p. 162-72.

135. Cao, Y., R. Cao, and N. Veitonmaki, *Kringle structures and antiangiogenesis.* Curr Med Chem Anticancer Agents, 2002. **2**(6): p. 667-81.

136. Tolbert, W.D., et al., *Structural basis for agonism and antagonism of hepatocyte growth factor.* Proc Natl Acad Sci U S A, 2010. **107**(30): p. 13264-9.

137. Dhand, R., et al., *PI 3-kinase: structural and functional analysis of intersubunit interactions.* EMBO J, 1994. **13**(3): p. 511-21.

138. Klippel, A., et al., *A region of the 85-kilodalton (kDa) subunit of phosphatidylinositol 3-kinase binds the 110-kDa catalytic subunit in vivo.* Mol Cell Biol, 1993. **13**(9): p. 5560-6.

139. Okkenhaug, K. and B. Vanhaesebroeck, *PI3K-signalling in B- and T-cells: insights from gene-targeted mice.* Biochem Soc Trans, 2003. **31**(Pt 1): p. 270-4.

140. Okkenhaug, K., *Signaling by the phosphoinositide 3-kinase family in immune cells.* Annu Rev Immunol, 2013. **31**: p. 675-704.

141. Okkenhaug, K. and D.A. Fruman, *PI3Ks in lymphocyte signaling and development.* Curr Top Microbiol Immunol, 2010. **346**: p. 57-85.

142. Wong, C.C., et al., *Inactivating CUX1 mutations promote tumorigenesis.* Nat Genet, 2014. **46**(1): p. 33-8.

143. Sauer, S., et al., *T cell receptor signaling controls Foxp3 expression via PI3K, Akt, and mTOR.* Proc Natl Acad Sci U S A, 2008. **105**(22): p. 7797-802.

144. Ivanov, II, et al., *The orphan nuclear receptor RORgammat directs the differentiation program of proinflammatory IL-17+ T helper cells.* Cell, 2006. **126**(6): p. 1121-33.

145. McGeachy, M.J., et al., *TGF-beta and IL-6 drive the production of IL-17 and IL-10 by T cells and restrain T(H)-17 cell-mediated pathology.* Nat Immunol, 2007. **8**(12): p. 1390-7.

146. McGeachy, M.J. and D.J. Cua, *T cells doing it for themselves: TGF-beta regulation of Th1 and Th17 cells.* Immunity, 2007. **26**(5): p. 547-9.

147. Szabo, S.J., et al., *A novel transcription factor, T-bet, directs Th1 lineage commitment.* Cell, 2000. **100**(6): p. 655-69.

148. Yang, J., et al., *Induction of interferon-gamma production in Th1 CD4+ T cells: evidence for two distinct pathways for promoter activation.* Eur J Immunol, 1999. **29**(2): p. 548-55.

149. Huynh, A., R. Zhang, and L.A. Turka, *Signals and pathways controlling regulatory T cells.* Immunol Rev, 2014. **258**(1): p. 117-31.

150. Zhang, H., et al., *Subsets of regulatory T cells and their roles in allergy.* J Transl Med, 2014. **12**: p. 125.

151. Koenecke, C., et al., *IFN-gamma production by allogeneic Foxp3+ regulatory T cells is essential for preventing experimental graft-versus-host disease.* J Immunol, 2012. **189**(6): p. 2890-6.

152. Overacre-Delgoffe, A.E., et al., *Interferon-gamma Drives Treg Fragility to Promote Anti-tumor Immunity.* Cell, 2017. **169**(6): p. 1130-1141 e11.

153. Gilbert, D.C., et al., *Minimum regions of genomic imbalance in stage I testicular embryonal carcinoma and association of 22q loss with relapse.* Genes Chromosomes Cancer, 2011. **50**(3): p. 186-95.

154. Pamer, E.G., *Immune responses to Listeria monocytogenes.* Nat Rev Immunol, 2004. **4**(10): p. 812-23.

155. Edelson, B.T. and E.R. Unanue, *Immunity to Listeria infection.* Curr Opin Immunol, 2000. **12**(4): p. 425-31.

156. Bancroft, G.J., R.D. Schreiber, and E.R. Unanue, *Natural immunity: a T-cell-independent pathway of macrophage activation, defined in the scid mouse.* Immunol Rev, 1991. **124**: p. 5-24.

157. Nickol, A.D. and P.F. Bonventre, *Anomalous high native resistance to athymic mice to bacterial pathogens.* Infect Immun, 1977. **18**(3): p. 636-45.

158. Ladel, C.H., et al., *Studies with MHC-deficient knock-out mice reveal impact of both MHC I- and MHC II-dependent T cell responses on Listeria monocytogenes infection.* J Immunol, 1994. **153**(7): p. 3116-22.

159. Lochner, M., et al., *Decreased susceptibility of mice to infection with Listeria monocytogenes in the absence of interleukin-18.* Infect Immun, 2008. **76**(9): p. 3881-90.

160. Khan, S.H. and V.P. Badovinac, *Listeria monocytogenes: a model pathogen to study antigen-specific memory CD8 T cell responses.* Semin Immunopathol, 2015. **37**(3): p. 301-10.

161. Shiow, L.R., et al., *CD69 acts downstream of interferon-alpha/beta to inhibit S1P1 and lymphocyte egress from lymphoid organs.* Nature, 2006. **440**(7083): p. 540-4.

162. Cerdan, C., et al., *Prolonged IL-2 receptor alpha/CD25 expression after T cell activation via the adhesion molecules CD2 and CD28. Demonstration of combined transcriptional and post-transcriptional regulation.* J Immunol, 1992. **149**(7): p. 2255-61.

163. Lara-Tejero, M. and E.G. Pamer, *T cell responses to Listeria monocytogenes.* Curr Opin Microbiol, 2004. **7**(1): p. 45-50.

164. Arbones, M.L., et al., *Lymphocyte homing and leukocyte rolling and migration are impaired in L-selectin-deficient mice.* Immunity, 1994. **1**(4): p. 247-60.

165. Galkina, E., et al., *T lymphocyte rolling and recruitment into peripheral lymph nodes is regulated by a saturable density of L-selectin (CD62L).* Eur J Immunol, 2007. **37**(5): p. 1243-53.

166. Weninger, W., et al., *Migratory properties of naive, effector, and memory CD8(+) T cells.* J Exp Med, 2001. **194**(7): p. 953-66.

167. Venturi, G.M., et al., *Leukocyte migration is regulated by L-selectin endoproteolytic release.* Immunity, 2003. **19**(5): p. 713-24.

168. Galkina, E., et al., *L-selectin shedding does not regulate constitutive T cell trafficking but controls the migration pathways of antigen-activated T lymphocytes.* J Exp Med, 2003. **198**(9): p. 1323-35.

169. Sinclair, L.V., et al., *Phosphatidylinositol-3-OH kinase and nutrient-sensing mTOR pathways control T lymphocyte trafficking.* Nat Immunol, 2008. **9**(5): p. 513-21.

170. Wong, P. and E.G. Pamer, *Feedback regulation of pathogen-specific T cell priming.* Immunity, 2003. **18**(4): p. 499-511.

171. Wu, C., et al., *BioGPS: building your own mash-up of gene annotations and expression profiles.* Nucleic Acids Res, 2016. **44**(D1): p. D313-6.

172. Wu, C., et al., *BioGPS: an extensible and customizable portal for querying and organizing gene annotation resources.* Genome Biol, 2009. **10**(11): p. R130.

173. Invivogen. *pFUSE-hIgG1-Fc2*. Available from: https://www.invivogen.com/sites/default/files/invivogen/old/PDF/pFUSE_hIgG1_Fc2_TDS.pdf

.

174. Rockland, *Rockland antibodies & assays.*

175. Crabtree, G. and K. Corbit, *Use of CRKD as a breast cancer marker and cancer therapy target*. 2006, Google Patents.

176. Wong, C.C., et al., *Inactivating CUX1 mutations promote tumorigenesis.* 2014. **46**(1): p. 33-8.

177. Fruman, D.A., et al., *The PI3K Pathway in Human Disease.* Cell, 2017. **170**(4): p. 605-635.

178. Ziegler, S.F., F. Ramsdell, and M.R. Alderson, *The activation antigen CD69.* Stem Cells, 1994. **12**(5): p. 456-65.

179. Bai, A., et al., *Kruppel-like factor 2 controls T cell trafficking by activating L-selectin (CD62L) and sphingosine-1-phosphate receptor 1 transcription.* J Immunol, 2007. **178**(12): p. 7632-9.

180. Kerksiek, K.M., et al., *H2-M3-restricted T cells in bacterial infection: rapid primary but diminished memory responses.* J Exp Med, 1999. **190**(2): p. 195-204.

181. Seaman, M.S., C.R. Wang, and J. Forman, *MHC class Ib-restricted CTL provide protection against primary and secondary Listeria monocytogenes infection.* J Immunol, 2000. **165**(9): p. 5192-201.

182. Campbell, D.J. and N. Shastri, *Bacterial surface proteins recognized by CD4+ T cells during murine infection with Listeria monocytogenes.* J Immunol, 1998. **161**(5): p. 2339-47.

183. Kaufmann, S.H. and C.H. Ladel, *Role of T cell subsets in immunity against intracellular bacteria: experimental infections of knock-out mice with Listeria monocytogenes and Mycobacterium bovis BCG.* Immunobiology, 1994. **191**(4-5): p. 509-19.

184. Kim, M.S., et al., *Activation and function of the mTORC1 pathway in mast cells.* J Immunol, 2008. **180**(7): p. 4586-95.

185. Okayama, Y., et al., *Comparison of Fc epsilon RI- and Fc gamma RI-mediated degranulation and TNF-alpha synthesis in human mast cells: selective utilization of phosphatidylinositol-3-kinase for Fc gamma RI-induced degranulation.* Eur J Immunol, 2003. **33**(5): p. 1450-9.

186. Kim, M.S., M. Radinger, and A.M. Gilfillan, *The multiple roles of phosphoinositide 3-kinase in mast cell biology.* Trends Immunol, 2008. **29**(10): p. 493-501.